INVESTIGATION OF THE EFFECTS OF RUTIN AND SOME OTHER SIMILAR PLANT COMPONENTS ON ANALGESIA RELATED NEURONAL ELECTROPHYSIOLOGICAL PARAMETERS IN PRIMARY CELL CULTURE

Abderaouf BOUBEKKA

MASTER OF SCIENCE THESIS

Supervisor: Prof. Dr. Yusuf OZTURK

Eskişehir

Anadolu University

Graduate School of Health Sciences

June 2021

JÜRİ VE ENSTİTÜ ONAYI

ÖZET

RUTİN VE BENZERİ BAZI BİTKİSEL KOMPONENTLERİN ANALJEZİ İLİŞKİLİ NÖRONAL ELEKTROFİZYOLOJİK PARAMETRELER ÜZERİNE ETKİLERİNİN PRİMER HÜCRE KÜLTÜRÜNDE İNCELENMESİ

Abderaouf BOUBEKKA

Farmakoloji Anabilim Dalı

Anadolu Üniversitesi, Sağlık Bilimleri Enstitüsü, Haziran 2021

Danışman: Prof. Dr. Yusuf ÖZTÜRK

Analjezik etkilere sahip polifenolik fitokimyasallar, ağrı yönetiminde bir ilgi alanı oluşturmaktadır. Literatürde klorojenik asit, rutin ve hesperidinin ağrı ve ilgili mekanizmalar / süreçler üzerindeki etkileri üzerine birçok çalışma bulunmaktadır. Bu alanda gelecek vaat eden biyoaktif maddeler olan bu test maddelerinin dorsal kök gangliyon nöronları düzeyinde, yani periferik düzeyde, akım-voltaj eğrisi ve aksiyon potansiyeli parametreleri üzerinden etkilerini incelemek için henüz bir çalışma yapılmamıştır. Bu tezde, 1 µM, 10 µM ve 100 µM konsantrasyonlardaki uygulamalara ve hem voltaj-clamp hem de akım-clamp modunda yapılan kayıtlar ile bu parametreler araştırılmıştır. Her hücreden ilaç uygulama öncesinde alınan kayıtlarla kontrol verileri alınmıştır. Test edilen üç kimyasalın hepsinin aksiyon potansiyeli ateşleme ve hiperpolarizasyon sonrası potansiyellerin eşiğini etkilediği ve A tipi potasyum akım yoğunluklarını ve potasyumun maksimum iletkenliğini azalttığı gözlenmiştir. Elde edilen bu sonuçlar bu maddelerin nöronal uyarılabilirlik ve analjezinin indüksiyonu üzerine olumlu etkileri olduğunu düşündürmektedir.

Test edilen fitokimyasalların tek kanal üzerine etkilerinin mekanizmaları ile ilişkili, gözlemlenen etkilerin daha kapsamlı bir şekilde anlaşılması için single channel patch clamp metodu ile ileride yapılacak incelemeler gereklidir.

Anahtar Sözcükler: Patch Clamp, Rutin, Hesperidin, Klorojenik asit, Arka kök ganglionu.

ABSTRACT

INVESTIGATION OF THE EFFECTS OF RUTIN AND SOME OTHER SIMILAR PLANT COMPONENTS ON ANALGESIA RELATED NEURONAL ELECTROPHYSIOLOGICAL PARAMETERS IN PRIMARY CELL CULTURE

Abderaouf BOUBEKKA

Department of Pharmacology

Anadolu University, Graduate School of Health Sciences, June 2021

Supervisor: Prof. Dr. Yusuf OZTURK

Polyphenolic phytochemicals with analgesic effects are generating an area of interest in pain management. There are many studies in the literature on the effects of chlorogenic acid, routine and hesperidin on pain and related mechanisms / processes. No study has yet been carried out to examine the effects of these test substances, which are promising bioactive substances in this field, on dorsal root ganglion neurons, in other words at the peripheral level, through the current-voltage curve and action potential parameters. In this thesis, these parameters were investigated via getting recordings performed both in voltage-clamp and current-clamp mode, using each cell as an auto control for the recordings, for the concentrations at concentration of 1 µM, 10 µM and 100 µM. Results obtained provided that all the three tested chemicals have been found to affect the threshold of action potential firing and after-hyperpolarization potentials and reduce type A potassium current densities and maximum conductance of potassium, which suggest a possible beneficial effect on neuronal excitability and induction of analgesia.

As for the mechanisms by which these chemicals affect these cells at the single channels, future examination at single channel level is required for more exhaustive understanding of the observed effects.

Keywords: Patch Clamp, Rutin, Hesperidin, Chlorogenic Acid, Dorsal root ganglia.

ACKNOWLEDGEMENTS

June 2021

I would like to express my gratitude to Prof. Dr. Yusuf OZTURK for being my mentor and leading my journey in my master's studies, for the time he devoted to providing me with the tools essential to the conduct of this research and for giving me the opportunity to be a part of the first team that worked in the electrophysiology laboratory which is the first one among pharmacology departments of pharmacy faculties in Turkey and to conduct this thesis work which is the first thesis from the mentioned laboratory.

I am extremely thankful to Dr. Feyza ALYU for being there at the entire thesis process, offering invaluable assistance, insights, guidance and limitless help.

I would like to thank Dr. Yusuf OLGAR for the priceless advices and insights he offered, his advices helped us surpass an important part of the difficulties we faced in through this journey.

My sincere thanks go to Prof. Dr. Nilgun OZTURK, for all the valuable contributions she offered. I express my limitless thanks to Prof.Dr. Ramazan BAL for his priceless contributions and all the insights he offered.

I would like to recognize the invaluable assistance of Prof. Dr Alexander ZHOLOS for the thorough guidance, support and teaching he offered, for which I am greatly thankful.

My endless gratitude goes to Dr. Wafaa DERBALE, for all the help and support she generously offered and her invaluable contribution in initiating my master's journey.

To colleagues and friends Ahmed and Ilham for the everything they did to help accomplish this work and all the thing we have been through together I am indefinitely thankful.

Most importantly, I am grateful for my family's unconditional, unequivocal, and loving support. To my mother, her endless love, encouragement and prayers gave me strength at all moment. I express my Deepest thanks to my siblings especially my sister Dr. Ahlam, who keep me grounded, remind me of what is important in life, and is always supportive of my adventures.

17/06/2021

STATEMENT OF COMPLIANCE WITH ETHICAL PRINCIPLES AND RULES

I hereby truthfully declare that this thesis is an original work prepared by me; that I have behaved in accordance with the scientific ethical principles and rules throughout the stages of preparation, data collection, analysis and presentation of my work; that I have cited the sources of the data and information that could be obtained within the scope of this study, and included these sources in the references section; and that this study has been scanned for plagiarism with "scientific plagiarism detection program" used by Anadolu University, and that "it does not have any plagiarism" whatsoever. I also declare that if any inconsistency appears concerning my work, I consent to all moral and legal consequences**.**

TABLE OF CONTENTS

Page

JÜRI VE ENSTİTÜ ONAYI ii
ÖZET iii
ABSTRACT iv
ACKNOWLEDGEMENTS v
STATEMENT OF COMPLIANCE WITH ETHICAL PRINCIPLES AND RULES vi
LIST OF FIGURES x
LIST OF TABLES xiii
LIST OF SYMBOLS AND ABBREVIATIONS xv
1. INTRODUCTION 1
1.1. Statement of The Problem 1
1.2. Purpose of the Study and Objective 1
1.3. Statement of Research Hypothesis and Rationale for Hypothesis 3
2. REVIEW OF THE LITERATURE 4
2.1. Basic Scientific Knowledge of Pain 4
2.1.1. Nature of pain 4
2.1.2. Physiology of pain 4
2.2. Types of Pain 8
2.2.1. Transient acute pain 8
2.2.2. Chronic Pain 8
2.3. Primary Afferent Neurons 9
2.4. Ion Channels Present in DRG Neurons 10
2.4.1. The TRPV1 channel 10
2.4.2. Kv Channels 11
2.4.3. Ca_v channels 14
2.4.4. Na_v channels 15
2.4.5. HCN channels 16

Page

2.5. Electrical Phenomena in Cells 17

2.5.1. Electrical properties of the neuronal membrane 17

2.5.2. Ionic mechanisms at origin of the resting membrane potential 19

2.6. The Patch Clamp Technique 21

2.6.1. General principle 22

2.7. Test Chemicals Used in The Study 24

2.7.1. Rutin 24

2.7.2. Hesperidin 27

2.7.3. CGA 29

3. MATERIALS AND METHODS 32

3.1. Experimental Animals 32

3.2. Chemicals 32

3.3. Apparatus 33

3.4. Dissection of DRG and Primary DRG Cells Culture 33

3.5. Solutions Used for Patch-Clamp Recordings 35

3.5.1. Current clamp recordings 35

3.5.2. Voltage clamp recordings 35

3.6. Application of the patch-clamp technique 36

3.6.1. Voltage-clamp recordings 37

3.6.2. Current-clamp recordings 38

3.7. Statistical Analysis 38

4. RESULTS 39

4.1. K^+ Current Results 39

4.1.1. Rutin 39

4.1.2. Hesperidin 44

4.1.3. CGA 49

Page

4.2. AP Results 55

4.2.1. Rutin 55

4.2.2. Hesperidin 59

4.2.3. CGA 63

5. GENERAL DISCUSSION, CONCLUSIONS, RECOMMENDATIONS 67

5.1. General Discussion 67

5.2. Conclusions 70

5.3. Recommendations 70

REFERENCES 72

APPENDICE I

APPENDICE II

CURRICULUM VITAE

LIST OF FIGURES

Page

Figure 2.1. Spinothalamic tract of pain and temperature for the body [31]..... 6
Figure 2.2. Protective withdrawal reflex response against painful stimulus [8] 7
Figure 2.3. Cell-attached patch-clamp configuration [31] 22
Figure 2.4. Whole cell patch-clamp configuration [31] 23
Figure 2.5. Inside-out patch-clamp configuration [31] 23
Figure 2.6. Outside-out patch-clamp configuration [31] 24
Figure 2.7. Molecular structure of Rutin..... 25
Figure 2.8. Molecular structure of hesperidin [153] 28
Figure 2.9. Chemical structure of CGA (5-caffeoylquinic acid, 5CQA) [170] 29
Figure 3.1. Electrophysiology rig 37
Figure 4.1. K^+ currents densities recorded from control cell and K^+ currents densities after application of 1 µM dose of rutin..... 39
Figure 4.2. Graphic representation of mean values ± SEM IV relationship from control cell and after application of 1 µM of rutin. 39
Figure 4.3. K^+ channels conductance in relation to membrane potential and from control DRG cells and after application of 1 µM of rutin. 40
Figure 4.4. K^+ currents densities recorded from control cell and K^+ currents densities after application of 10 µM dose of rutin..... 40
Figure 4.5. Graphic representation of mean values ± SEM of IV relationship from control cell and after application of 10 µM of rutin 41
Figure 4.6. K^+ channels conductance in relation to membrane potential and from control cells and after application of 10 µM 41
Figure 4.7. K^+ currents densities recorded from control cell after application of 100 µM dose of rutin. 42
Figure 4.8 Graphic representation of mean values ± SEM of IV relation from control cell and after application of 100 µM of rutin 42
Figure 4.9. K^+ channels conductance in relation to membrane potential and from control cells and after application of 100 µM 43
Figure 4.10. Dose related effect of rutin on relative K^+ current 43
Figure 4.11. K^+ currents densities recorded from control cell and after application of 1 µM dose of hesperidin..... 44

Page

Figure 4.12. Graphic representation of mean values ± SEM of IV relation from control cell and after application of 1 µM of hesperidin 44
Figure 4.13. K^+ channels conductance in relation to membrane potential and from control cells and after application of 1 µM of hesperidin 45
Figure 4.14. K^+ currents densities recorded from control cell and after application of 10 µM dose of hesperidin..... 45
Figure 4.15. Graphic representation of mean values ± SEM of IV relation from control cell and after application of 10 µM of hesperidin. 46
Figure 4.16. K^+ channels conductance in relation to membrane potential and from control cells and after application of 10 µM of hesperidin. 46
Figure 4.17. K^+ currents densities recorded from control cell and after application of 100 µM dose of hesperidin..... 47
Figure 4.18. Graphic representation of mean values ± SEM of IV relation from control cell and after application of 100 µM of hesperidin. 47
Figure 4.19. K^+ channels conductance in relation to membrane potential and from control cells and after application of 100 µM of hesperidin. 48
Figure 4.20. Dose related effect of hesperidin on relative K^+ current 48
Figure 4.21. K^+ currents densities recorded from control cell and after application of 1 µM dose of CGA..... 49
Figure 4.22. Graphic representation of mean values ± SEM of the IV relation from control cell and after application of 1 µM of CGA 49
Figure 4.23. K^+ channels conductance in relation to membrane potential and from control DRG cells and after application of 1 µM of CGA. 50
Figure 4.24. K^+ currents densities recorded from control cell and after application of 10 µM dose of CGA..... 51
Figure 4.25. Graphic representation of mean values ± SEM of IV relation from control cell and after application of 10 µM of CGA 51
Figure 4.26. K^+ channels conductance in relation to membrane potential and from control DRG cells and after application of 10 µM of CGA 52
Figure 4.27. K^+ currents densities recorded from control cell and after application of 100 µM dose of CGA..... 52

Page

Figure 4.28. Graphic representation of mean values ± SEM of IV relation from control cell and after application of 100 µM of CGA 53

Figure 4.29. K^+ channels conductance in relation to membrane potential and from control DRG cells and after application of 100 µM of CGA 53

Figure 4.30. Dose related effect of CGA on relative K^+ current..... 54

Figure 4.31. Control recording of elicited AP before (A) and after application of rutin at 1 µM dose (B). 55

Figure 4.32. Recording of elicited AP before (A) and after application of rutin at 10 µM dose (B)..... 56

Figure 4.33. Recording of elicited AP before (A) and after application of 100 µM of rutin (B). 57

Figure 4.34. Recording of elicited before (A) and after application 1 µM of hesperidin (B). 59

Figure 4.35. Recording of elicited AP before (A) and after application of hesperidin at 100 µM dose (B)..... 61

Figure 4.36. Recording of elicited AP before (A) and after application of CGA at 1 µM dose (B)..... 63

Figure 4.37. Recording of elicited AP before (A) and after application of CGA at 10 µM dose (B 64

LIST OF TABLES

Page

Table 3.1. List of chemicals utilized 32
Table 3.2. List of used apparatus..... 33
Table 3.3. Pipette solution for AP recordings 35
Table 3.4 Bath solution for AP recordings..... 35
Table 3.5. Pipette solution for currents recordings 36
Table 3.6. Pipette solution for currents recordings 36
Table 4.1. AP parameters measured from DRG cells before application of 1 µM of rutin 55
Table 4.2. AP parameters measured from DRG cells After application of 1 µM of rutin and statistical analysis of the variation observed. 56
Table 4.3. AP parameters measured from DRG cells before application of 10 µM of rutin..... 56
Table 4.4. AP parameters measured from DRG cells After application of 10 µM of rutin and statistical analysis of the variation observed. 57
Table 4.5. AP parameters measured from DRG cells before application of 100 µM of rutin..... 57
Table 4.6. AP parameters measured from DRG cells After application of 100 µM of rutin and statistical analysis of the variation observed. 58
Table 4.7. AP parameters measured from DRG cells before application of 1 µM of hesperidin 59
Table 4.8. AP parameters measured from DRG cells After application of 1 µM of hesperidin and statistical analysis of the variation observed. 60
Table 4.9. AP parameters measured from DRG cells before application of 10 µM of hesperidin..... 60
Table 4.10. AP parameters measured from DRG cells After application of 10 µM of hesperidin and statistical analysis of the variation observed. 61
Table 4.11. AP parameters measured from DRG cells before application of 100 µM of hesperidin..... 62
Table 4.12. AP parameters measured from DRG cells After application of 100 µM of Hesperidin and statistical analysis of the variation observed 62

Page

Table 4.13. AP parameters measured from DRG cells before application of 1 µM of CGA..... 63

Table 4.14. AP parameters measured from DRG cells After application of 1 µM of CGA and statistical analysis of the variation observed. 64

Table 4.15. AP parameters measured from DRG cells before application of 10 µM of CGA..... 65

Table 4.16. AP parameters measured from DRG cells After application of 10 µM of CGA and statistical analysis of the variation observed 65

Table 4.17. AP parameters measured from DRG cells before application of 100 µM of CGA..... 65

Table 4.18. AP parameters measured from DRG cells After application of 100 µM of CGA and statistical analysis of the variation observed. 66

LIST OF SYMBOLS AND ABBREVIATIONS

AHP : After Hyper Polarization

AP : Action Potential

ATP : Adenosine Triphosphate

C_{av} : Voltage-gated Ca^{2+} channels

CGA : Chlorogenic Acid

Cm : Membrane Capacitance

CNS : Central Nervous System

DMEM : Dulbecco's Modified Eagle's Medium

DMSO : Dimethyl Sulfoxide

DRG : Dorsal Root Ganglia

EGTA : Ethylene Glycol TetraAcetic Acid

F : Faraday Constant

FBS : Fetal Bovine Serum

G : Conductance

GABA : Gamma-Aminobutyric Acid

G_{ion} : Membrane Ionic Conductance

HCN : Hyperpolarization-activated cyclic nucleotide-gated cation channels

HEPES : 4-(2-hydroxyethyl)-1-piperazineethanesulfonic acid

HVA : High Voltage Activated Channels

IASP : International Association for the Study of Pain

IL : Interleukin

IPA : Integrated Patch Amplifier

IV : Current-Voltage

Kv : Voltage-Gated K^+ Channel

LR : Longitudinal Resistance

mRNA : Messenger RNA

n : Sample Size

N_{av} : Voltage-Gated Na^+ Channels

N_{ion} : Total number of channels of the ionic species in the membrane

NMDA : N-methyl-D-aspartate

NQS : Not Quite Significant

NS : Not Significant

p	: p-value
PBS	: Phosphate Buffered Saline
PNS	: Peripheral Nervous System
Q	: Charge Carried by The Conducting Elements
R	: Resistance
Rm	: Membrane Resistance
S	: Significant
S.E.M.	: Standard Error of The Mean
T	: Temperature in Kelvin
TRP	: Transient Receptor Potential
TRPV1	: Transient Receptor Potential Vanilloid 1
TTX	: Tetrodotoxin
TTX-R	: TTX-resistant
TTX-S	: TTX-sensitive
$V_{1/2}$	: Potential of Half Activation
VS	: Very Significant
z	: Ion Charge

1. INTRODUCTION

Within the scope of this master's thesis, the effects of plant components: rutin [1], hesperidin [2] and chlorogenic acid (CGA) [3]; on analgesia related neuronal electrophysiological parameters in primary cell culture have been investigated using *in vitro* electrophysiological experiments.

1.1. Statement of The Problem

Pain is defined according to the International Association for the Study of Pain (IASP) as "An unpleasant sensory and emotional experience associated with actual or potential tissue damage, or described in terms of such damage", where pain is a subjective experience that is influenced by different factors, pain should be distinguished from nociception [4, 5].

In one hand pain and nociception is there playing the role of an alarm system that detects and notify about damage, abnormal disturbance and other events that may impair normal physiological functioning of the body [6]. On the other hand, the excess of pain and nociception may affect the person's quality of life as a result of hospital visits and reduced productivity [7].

Effective pain treatment improves quality of life, reduces physical discomfort, promotes earlier mobilization and return to work, decreases the number of visits to the hospital or doctor's office, reduces the length of hospital stays and therefore reduces health costs [8]

Providing more *in vitro* evidence about the positive effects of the substances on pain that already proven to have *in vivo* benefits in treatment of pain will provide more certainty and open more horizons to go further on clinical and pharmacological research to develop new treatments for pain based on these substances.

1.2. Purpose of the Study and Objective

Antihyperalgesic effects of CGA, a bioactive polyphenol [9, 10], its anti-inflammatory, antipyretic and analgesic effects [11, 12] have been shown in many studies. Bearing a similar structure, hesperidin have also been shown to provide antihyperalgesic effects at peripheral and central levels [13], positive effects on neuropathic pain [14], anti-inflammatory and analgesic effects mediated by transient receptor potential (TRP) channels and a reducing effects on oxidative stress leading to the antioxidant effects [15]. There are many studies on pain-related effects of this phytochemical in neuropathic pain,

for instance showing its activity on the P2X3 receptor [16]. Another bioactive substance with structural similarities with the previous ones is rutin. The amendatory effects of rutin on neuropathic pain [17, 18], its antinociceptive effects [19], related to its antioxidant-mediated healing effects on peripheral neuropathy [20] have been brought to the literature.

So far, a study in which the electrophysiological effects of these substances at the peripheral level evaluated in terms of pain, based on the action potential (AP) and the current-voltage (IV) curve, has not been carried out yet. It is important to clarify the mechanisms of the effects of these substances for their possible use in treatment of pain.

Pain significantly reduces the quality of life [21]. Determining effective pharmacological agents in pain transmission process is of great clinical importance. This study to be carried out on dorsal root ganglion (DRG) neurons will present preclinical data on the peripheral aspect of pain related to routine, hesperidin and CGA, whose effects have been examined from various aspects and presented to the literature [22].

DRG neurons carry nociceptors that create pain perception and are active through ion channels. These ganglia are considered as new potential therapeutic targets in neuropathic pain [22]. Changes in these neurons affect pain transmission and change the pain threshold. In the neuropathic pain model, there are studies in which substances have an effect on AP or potassium (K^+) and similar currents in DRG neurons by electrophysiological methods.

Analgesic effects are associated with the change of parameters and/of various currents such as AP and K^+ current in DRG neurons [23]. In this study, the effects of test chemicals on AP parameters and current-voltage (IV) curves on DRG neurons were investigated. According to the voltage range in which the differences occur, the effects of the test substances on the IV curve show which currents and in what direction it changes them. There is no study in the literature that examines the electrophysiological effects of the substances to be tested in this study on DRG neurons in the periphery in terms of AP and IV and compares these effects with each other. The fact that CGA exhibited ion channel-related effects on neurons [12, 24, 25], with the pain-related effects of it and similar pharmacological agents affecting electrophysiological processes at the DRG level suggests that it may be related. Therefore, in this mechanistic study, it is planned to illuminate the possible ion channels affected by the test substances by the patch clamp method.

When their effects on the AP are examined, a prediction about which channels they affect will be obtained and further studies will be designed accordingly. Thanks to the comparative analysis, it is aimed to draw attention to which of these similar test substances is the most active in both pain-related new drug development studies and clinical applications.

1.3. Statement of Research Hypothesis and Rationale for Hypothesis

Polyphenols, whose analgesic effects have been demonstrated in various studies and whose possible mechanisms of action will be examined electrophysiologically from the peripheral perspective, are promising in this field in the light of previous data.

There are many studies in the literature on the effects of CGA, routine and hesperidin on pain and related mechanisms/processes. No study has yet been carried out to examine the effects of these test substances, which may be promising bioactive substances in this field, on DRG at the peripheral level through the IV curve and AP parameters.

Investigation of the effects of these substances on DRG neurons, which are indicated as a potential new target in neuropathic pain, will provide valuable data to the literature and guide further studies. After evaluating the IV curve and AP, it will be possible to work on these channels separately by getting an idea about which channels they affect.

Treatment with herbal-based solutions is a field of interest and a health practice today. Demonstrating the effects of plant-based bioactive substances with detailed scientific studies will provide guiding data on the use of these substances in treatment. Also, more effective treatment solutions are needed for pain conditions that greatly affect the patient's quality of life.

2. REVIEW OF THE LITERATURE

Pain is a perception experienced by all human, more or less intense, and despite that pain is the main reason for seeking healthcare, its etiology remains poorly understood [26]. Pain is purely subjective. A person does not feel the same pain stimuli the same way with another person, and two painful events do not seem to trigger the same response or sensation in the same person [5]. Even though pain relief is a fundamental human right as it is written in many texts, pain continues to be a major public health problem [27].

Despite of the discomfort and impairment inflicted by pain, it is still a biological necessity, it serves as a warning call for escape or withdrawal and helps to assess the state of health, but in some cases regardless of the fulfillment of the beneficial role of pain, it persists, and there it becomes a threat. The goals of medicine are to preserve and restore health and alleviate suffering and pain, and for this it is essential to understand the mechanisms of pain [6].

2.1. Basic Scientific Knowledge of Pain

Pain has always been an important part of human experience [27]. For a long time, pain was only considered as a symptom of an illness or disorder. However, it is regarded today as a disease in itself [5, 28].

2.1.1. Nature of pain

The pain experience is at the same time subjective and complex as it involves physical, emotional and cognitive components, where the painful stimulus could be physical and/or mental in nature.[5, 29, 30].

2.1.2. Physiology of pain

There are four physiological processes of nociceptive (normal) pain: transduction, transmission, perception and modulation [31, 32]. Knowing each of them, helps to identify the factors responsible for the pain, the accompanying symptoms, and the rationale for choosing certain treatments.

Thermal, chemical or mechanical stimuli usually cause pain. The energy of these stimuli is converted into electrical energy, a phenomenon called transduction [8].

Transduction begins at the periphery when an algogenic stimulus sends an influx into a specific peripheral sensory nerve fiber (nociceptor) and triggers an AP [8, 31].

Therein the end of transduction, the transmission of painful stimuli begins. Cellular damage caused by thermal, mechanical or chemical stimuli results in the release of

excitatory neurotransmitters such as prostaglandins, bradykinin, K^+, histamine or substance P [32]. These pain provoking substances surround the pain fibers by bathing in the extracellular fluid, spreading the pain message and inducing an inflammatory response. Pathways responsible for pain originate in DRG, the specialized pain fibers enter the medulla at the posterior horn and follow one of the different pathways that end in the gray matter of the spinal cord [31].

In the posterior horn, the release of substance P allows the trans synaptic transmission of the signal from the peripheral nerve fibers afferent (sensory) to the nerve fibers of the spinothalamic bundle which pass on the opposite side [33].

Nerve impulses resulting from painful stimuli follow the path of afferent peripheral nerve fibers (sensory) [8, 32]. The signal leading to perception of innocuous mechanical stimuli is relatively fast and transported via myelinated axons. On the other hand, nociception signal is relatively slow, transported via lightly myelinated or unmyelinated axons falling under myelinated A delta group with a conductance velocity of 5 to 30 m/s, and unmyelinated C fibers with velocity less than 2 m/s [34]. A fibers send sharp, precisely localized and distinct sensations which locate the origin of the pain and determine its intensity while The C fibers relate poorly localized stimuli, giving a burning sensation which persist longer [8, 32, 34].

Pain and temperature information are transported to higher centers via the anterolateral system, the painful influxes go up along the spinal cord following the spinothalamic tract (Figure 2.1.). Once the painful impulses have passed through the spinal cord, the thalamus transmits the information to higher centers in the brain: reticulate formation, limbic system, somatosensory cortex and associative cortex [34]. As soon as a painful stimulus reaches the cerebral cortex, the brain qualitatively interprets the pain and processes the information from its past experience, knowledge, and cultural associations of pain perception [5, 35]. Perception is the moment when awareness of the presence pain starts. The somatosensory cortex identifies the location and intensity of pain, while the associative cortex, primarily the limbic system, determines how pain is experienced [34].

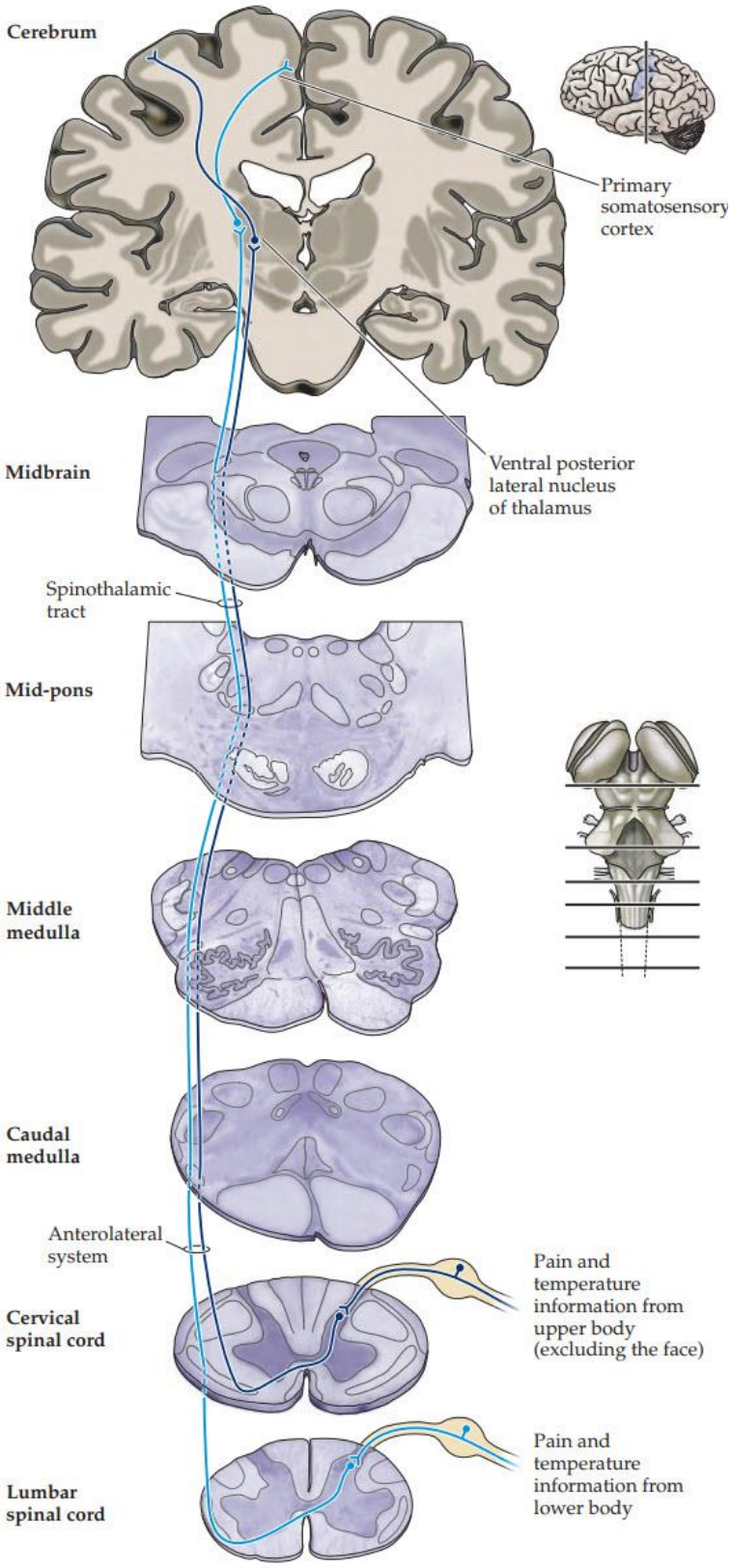

Figure 2.1. *Spinothalamic tract of pain and temperature for the body [31]*

Awareness of pain triggers a complex reaction. Psychological and cognitive factors interfere with neurophysiological factors during the process of pain perception, the reaction to pain is the physiological and behavioral responses that occur after the subject perceives pain [34].

Response to acute painful stimuli is mediated by activation of α-amino-3-hydroxy-5-methyl-4-isoxazolepropionic acid receptor of dorsal horn neurons [36]. N-methyl-D-aspartate (NMDA) receptors are involved in the perception of pain and the magnesium ion (Mg^{2+}) blocks them physiologically [36]. After the brain percepts pain, there is a release of inhibitory neurotransmitters, such as endogenous opioids (endorphins and enkephalins), serotonin, norepinephrine, and gamma-aminobutyric acid (GABA), the action of these inhibitory neurotransmitters is to prevent the transmission of pain and generate an analgesic effect. This inhibition of painful impulses is the fourth phase of the nociceptive process and is called modulation [32, 34].

A protective withdrawal reflex response (Figure 2.2.) also occurs with the perception of pain A-delta fibers send sensory impulses to the spinal cord where they are transmitted to medullary motor neurons. The motor impulses start, thanks to a reflex arc supported by efferent nerve fibers (motor), towards a peripheral muscle close to the site of the stimulation, thus bypassing the brain, the contraction of the muscle results in a protective removal from the source of the pain [37, 38].

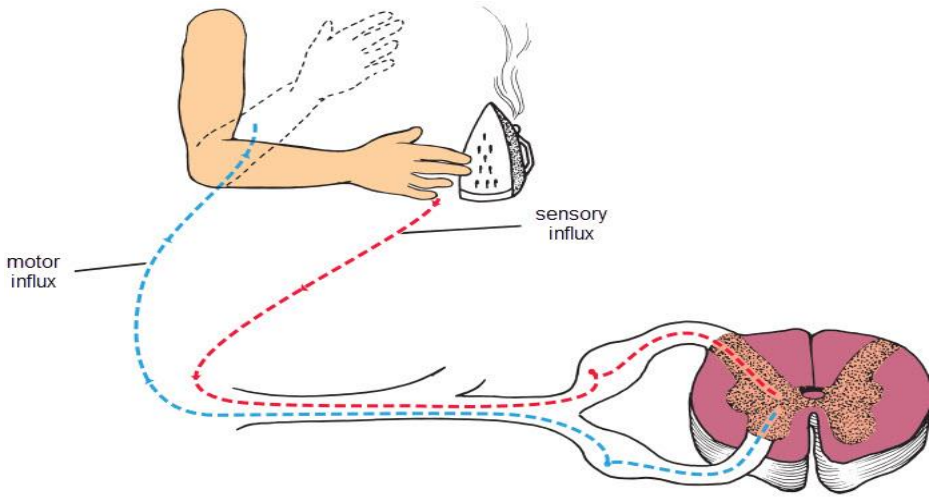

Figure 2.2. *Protective withdrawal reflex response against painful stimulus [8]*

2.2. Types of Pain

Pain is classified according to its duration (acute or chronic) or according to the underlying pathology (for example, cancer or neuropathy) [39]. Nociceptive pain includes somatic pain (musculoskeletal) and visceral pain (internal organs), while neuropathic pain results from an abnormality or damage to nerves specializing in the transmission of pain [40, 41].

2.2.1. Transient acute pain

Acute pain has an identifiable cause, short-lived, corresponds to tissue damage and has limited emotional response. It eventually goes away with or without treatment after the injured area has healed. The goal of acute pain is to protect the body against damage [40, 41].

2.2.2. Chronic Pain

In contrast to acute pain, chronic pain is not protective and therefore has no purpose [42]. It lasts longer, sometimes of an unknown cause, and results in great impairment of life quality. chronic pain can be of different origins such as cancer, polyarthritis, myo-aponeurotic pain, low back pain headache and peripheral neuropathy [30]. It could be divided into three broad categories: The first one is pain resulting of disease or damage to a tissue an example of this type is osteoarthritis. The second category contains diseases and impairments or damage to the somatosensory system that leads to pain such as neuropathic pain, the third one contains a mixture of both mechanisms where nociceptive coexist with neuropathic pain [33, 40].

2.2.2.1. *Chronic episodic pain*

Pain that occasionally occurs over an extended period of time is an episodic pain. Painful episodes could last a few hours, days, or weeks. This include, for example migraine or the pain of sickle cell anemia [43, 44].

2.2.2.2. *Chronic cancer pain*

Not all cancer patients experience pain, some of them experience acute and/or chronic pain where it could be of the nociceptive and/or neuropathic type. Cancer pain is usually due to tumor progression, invasive procedures, toxicity of treatments, physical limitations and infection. It is felt at the exact site of the tumor, or at a distance from it, also called referred pain [45, 46].

2.2.2.3. *Chronic idiopathic pain*

Chronic idiopathic pain is a chronic pain without an identifiable physical or psychological cause, or it is a pain that is perceived as excessive to be caused by an existing organic pathology [47].

2.2.2.4. *Neuropathic pain*

Neuropathic pain is defined by IASP as "pain caused by a lesion or disease of the somatosensory nervous system" [39]. The inappropriate response of the nervous system to damage can lead to spontaneous generation of pain it is divided following the cite of lesion to central and peripheral, Treatments for neuropathic pain are non-specific and often insufficiently effective [39, 41].

Central neuropathic pain results from and injury the central nervous system (CNS) and it is different form allodynia and hyperalgesia [48]. Neuropathic pain could result from as alcohol (toxic mechanism), diabetes (ischemic mechanism), traumatic (injury of the spinal cord) [49].

2.3. Primary Afferent Neurons

DRG is a complex of many ganglia where the cell bodies of the primary afferent neurons' clusters. APs are generated in response to stimuli and transported from the periphery to the neurons' dorsal horn where glutamate will be released, or directly from DRG neurons which can also generate Aps [50], the pattern of firing generated by DRGs gives information about location, duration and intensity of the stimuli [51].

Each type of sensory modalities is represented in a different DRG neurons, so that afferent neurons with different functions are represented by the DRGs [52], but in general while classifying DRGs this diversity is not taken in consideration, instead of that the velocity of conduction (measured in m/s: slow < 1; medium: 1-8; fast: 9-60) and cell size (represented by diameter or capacitance: Small :10-30 μm or < 70 pF; Medium: 31-40 μm or 71-90 pF; Large: 41-60 μm or > 90 pF) are used [50]. Other classifications attempts such as immunoreactivity (IR) based [52] and the one based on the AP's shape [50] have been proposed.

Primary afferents are nociceptors triggered by noxious external stimuli (chemical, mechanical, thermal, etc) [53]. Based on the type of the stimuli, the pathway also changes. There are DRG neurons responsive only to one type and others respond to different types at the same time. Transducer proteins of different types are expressed in these neurons

and are responsible of this difference in responsiveness [54]. This difference in responsiveness makes it difficult to determine the function of neurons solely on the base of stimuli responses.

One of the reasons why DRGs are considered as pain transmitters is their expression of transient receptor potential vanilloid 1 (TRPV1) channels which are capsaicin responsive and activated by heat (>43 °C) [55]. There are other many channels that are also accepted as the reasons for DRGs to be considered as pain transmitters.

2.4. Ion Channels Present in DRG Neurons

Electrophysiological characteristics of sensory systems are studied using cultures of dissociated DRG neurons, these neurons present different types of channels that are involved in the process of generation and transduction of pain signaling.

2.4.1. The TRPV1 channel

As a vanilloid compound active ingredient in peppers of the capsicum family, capsaicin has been shown to produce a sensation of heat and pain *in vivo* [56], and depolarizes nociceptors and increases the concentration of free cytosolic Ca^{2+} *in vitro* [57]. These properties allowed the cloning of a heat-activated channel, the capsaicin receptor ion channel or TRPV1 [58].

TRPV1 is a member of the superfamily of TRP ion channels which contains more than 20 members, the TRPV subfamily is formed of 6 members TRPV1/TRPV2, TRPV3, TRPV4, TRPV5/TRPV6. They are tetrameric complexes which contain three to five ankyrin residues in their terminal amino domain for the attachment of cell membrane [59]. They are cation channels that play a critical role in a wide range of functions ranging from the sensorial physiology to hearing and male fertility [60]. Expressed in a heterologous system (cell lines, Xenopus oocyte) and in the absence of capsaicin, from 42°C TRPV1 generates a non-selective inward cationic current with preference to Ca^{2+} (Ionic permeability of Ca^{2+}/ Ionic permeability of $Na^{+} \sim 9$). The intensity of this current increases with temperature below 50 °C [58, 61].

In mice for which the gene that codes for TRPV1 was knocked-out, a decrease in thermosensitivity from 43°C and which is heightened around 50 °C has been observed. This results in a decrease in the currents induced by these temperatures on the cultured neurons [62]. TRPV1 is therefore a channel involved in thermo-nociception, but it is not the only one responsible for this function because, neuropathic thermal hyperalgesia

remains intact in mice where the gene coding for TRPV1 was knocked-out [62], also the despite fact that the currents induced are similar, a study has suggested that there may be a segregation between the maximum responses to capsaicin and to heat on cultured sensory neurons [63]. In addition to that it has been found that some sensory neurons are sensitive to capsaicin and insensitive to heat [63]. Moreover, TRPV1 seems to be involved in other types of pain. this channel is potentiated by certain inflammatory mediators, Nerve Growth Factor, ATP, and bradykinin in the spinal ganglia [64–66] The expression of TRPV1 is upregulated under inflammatory conditions, as such, it is considered to be an integrator of inflammatory pain [67].

DRG neurons express TRPV1, TRPV2, TRPV3 and TRPV4. The TRPV1 is largely known and studied, the influx of Ca^{2+} into DRG neurons cause a depolarization and a series of APs is induced, DRG neurons are sensitive to capsaicin as it is used to prove the presence of TRPV1 channels although other receptors are sensitive to capsaicin as well [68].

In addition to TRPV1 channels, other members of the TRP family such as TRPA1 and TRPC6 are present in the DRG neurons [69].

2.4.2. Kv Channels

Voltage-gated K^+ channels (Kv) channels are tetramers of α subunits, capable of forming homo or heterotetramers [70]. These channels are characterized by their dependence on potential; hence, their name is Kv. An α subunit of a Kv channel contains 6 transmembrane helixes S1 to S6 including the S4 segment that contain positively charged residues such as lysines or arginines, this segment represents the major component of the potential sensor of the channel. Site-directed mutagenesis studies coupled with voltage-clamp fluorometry fluorescence measurements and crystallographic studies have shown that the movement of these charges during a change in membrane potential induces a structural rearrangement of the S5 and S6 domains leading to opening of the pore domain (P) of the channel which is formed by S5 and S6 [71, 72].

Kv is involved in pain perception phenomena. These K^+ channels are potassium-selective transmembrane ionic pores constitutively open at rest and playing central functions in the control of neuronal excitability. At rest, these channels bring the membrane potential close -90mV which is the equilibrium potential of K^+ (-50 to -60mV in spinal ganglion sensory neurons) and therefore reduce neuronal hyperexcitability. They

have a major role in the regulation of membrane resting potential, the duration of APs, membrane resistance and the release of neurotransmitters [73].

The mainly expressed Kv channels found in DRGs are Kv1.4, Kv3.4, Kv4.1, and Kv4.3 [74]. In addition to that, the presence of other A-type Kv channels, Kv1.1-1.6, Kv2.2, Kv3.4, Kv4.2, Kv4s, Kv7.2-7.5, Kir6.2, KCa1, KCa2 and other types of K^+ channels have been establish in DRGs of mammalians, with noticeable variations in the expression of Kv1.2, Kv 1.4 and Kv 2.2 in models of neuropathic pain [74–82].

The channels Kv1.4 and Kv4s are sensitive to low voltages with the first recovers slowly and the later recovers fast and it is responsible for the hyperpolarizing voltage in the steady state. On the other hand, Kv3.4 channel needs high voltage to be activated [74].

Members of the KCNQ (K^+ Channel responsible for long QT syndrome) channel family, also known as Kv7 channels and their subtypes (Kv7.1-7.5) are found in different cells from different organs, their subunits are abundantly found in the pancreas, kidney, heart, the inner ear, CNS and peripheral nervous system (PNS) as well as their presence in the DRG neurons, their role in these tissue is related to membrane excitability hence their utility in studies direct to understand the mechanism of membrane excitability and treat related disorders [80, 83].

In neurons, Kv7 channels are slowly activated and are therefore involved in the hyperpolarization phase called AHP (After Hyper Polarization). that comes after the AP.

The importance of Kv7 channels in the brain and heart has been highlighted thanks to the phenotypes and pathologies caused by their mutations. In the heart, Kv7.1 is primarily recognized for its involvement in congenital long QT syndrome, an inherited heart disease characterized by prolongation of the QT interval and a high risk of arrhythmias. This channel has also been found in the inner ear where it is involved in some forms of deafness [70].

The slow activation of the Kv7 channels and their tendency for driving outward current are the reasons that these channels are called *delayed rectifier*. First discovered in bullfrog sympathetic ganglia, the M-current, also detected in rat DRGs, is believed to be correlated to Kv7 [80, 84]. This current appears not to inactivate, a feature that can be used to identify and isolate the Kv7 currents among other currents generated by other channels in the cell by applying an inactivation protocol. The detection of currents generated by these channels can also be performed using pharmacological agents such as

retigabine or the less potent flupirtine, that modulate the action of Kv7 channels. In the study of Kv7 currents inhibitors, linopirdine and its analogue XE991 were used [80].

2.4.2.1. *Functions of A-Type Kv Channel Subtypes in DRG Neurons*

2.4.2.1.1. *Kv1.4*

These channels are present in the axons and cell bodies [85]. They are specifically inhibited by 4-aminopyridine [81] and modulated by Ca^{2+}. The inactivation of Kv1.4 is fast [86]. In physiological conditions the role of this channel in controlling AP properties in DRGs is not fully understood, nevertheless evidence shown indicates it's probable involvement in controlling firing frequency and the latency of APs [81]. On the other hand, the role of Kv1.4 channels in DRGs models of pain is well established. In diabetic neuropathic pain, chronic axon constriction injury, pancreatitis, inflammatory bowel disease and temporomandibular joint pain models, a downregulation in the expression of the channel and drop in the current produced by Kv1.4 have been illustrated [74].

2.4.2.1.2. *Kv3.4*

These channels are expressed in the axon, presynaptic terminals and especially cell bodies of small DRG neurons [87, 88]. They are high voltage activated and hypersensitive to tetraethylammonium [89]. The slow inactivation of Kv3.4 channels is due to the relatively lengthy processes such as oxidation and phosphorylation of the N-terminal inactivation domain [90].

Kv3.4 channels have been found to be involved in the regulation of the duration of AP through modulation of the repolarization of the nociceptor and this is supported by abundance of Kv3 currents in the repolarizing phase during nociceptor AP [74, 91].

A substantial effect of the decrease of Kv3.4 channel expression or activity and attenuation of its current on slowing the AP repolarization and nociceptor excitability has been clearly shown [88].

2.4.2.1.3. *Kv4.1, Kv4.2, and Kv4.3*

These channels are expressed in the cell bodies of small and large DRG cells with predominance of Kv4.3 in small sized cells. Their functioning is modulated by phosphorylation [76, 88, 92]. Dysfunction of the Kv4 channels has been related to chronic pain and it manifests as both a reduction of expression of mRNA and the currents produced by these types of channels which leads to depolarization of the membrane potential and increases the excitability of the cells [88, 93, 94]. The role of Kv4 channels present in DRG neurons in mechanical allodynia is proven [95].

2.4.3. Ca_v channels

Voltage-gated Ca^{2+} channels (Ca_v), regulated by voltage changes in the plasma membrane form the main way of entry of Ca^{2+} into excitable cells [96]. These channels are closed upon hyperpolarization and open upon depolarization of the plasma membrane. Ca_v are divided into 2 major classes based on their activation threshold: high voltage activated channels (HVA) which include L-type ('Long lasting' or $Ca_v1.1$-1.4), -P/Q ('Purkinje/granule cells' or $Ca_v2.1$), -N ("Neither T or L' or $Ca_v2.2$) and -R ('Resistant' or $Ca_v2.3$) channels and low voltage activated channels represented by fast activated and inactivated T-type channels ($Ca_v3.1$-3.3).

Ca_v are made up of a ductal subunit α1 - which forms the pore through which the Ca^{2+} ions circulate - different depending on the type of the channels, subunits β, α2, δ and γ are associated with this α1 subunit [96]. They are involved in the assembly, targeting and anchoring of the channels in the membrane and are responsible for modulating the biophysical parameters of Ca_v. In neurons, Ca_v perform several functions such as integrating incoming electrical signals at the level of dendrites as well as the regulation of neurotransmitters release. Genetic mutations induced changes in these channels can cause many pathologies such as epilepsy, migraines, ataxia, myopathies, etc.

A depolarizing step to -50 mV will activate T-type current which is generally seen between -70 to -40 mV in DRG neurons. The transient T-type currents is deactivated by applying a holding potential of -60 to the cells [97], or by pharmacological blockers such as dihydropyridines (nifedipine or nimodipine). On the contrary, HVA are insensitive to dihydropyridines.

$Ca_v1.2$-1.3; $Ca_v2.1$-2.3 and $Ca_v3.1$- 3.3 types of Ca_v channels have been found to be expressed in DRG neurons [98]. At presynaptic terminals of DRG neurons N-type channels represent the majority of Ca_v expressed there and are believed to be involved in the release of neurotransmitters. On the other hand, T-type channels are abundantly found in the cell bodies, the activation of this type of Ca_v may lower the APs threshold and contribute to spontaneous pain [99].

Ca_v channels are regulated by a variety of coupled metabotropic receptors such as G protein-coupled receptors which regulate N-Type Ca_v and the Activation of $GABA_B$ receptor that inhibits those channels on rat's DRG neurons, the inhibition of this type of channels leads to suppression of N-Type Ca_v currents and the alleviation of pain through the inhibition of excitatory neurotransmitters release. As such the involvement of Ca_v

channels in the phenomena of pain made them a target for different studies of the effects of different pharmacological agents such as ziconotide and gabapentin on pain modulation [99–101].

2.4.4. Na_v channels

Voltage-gated Na^+ channels (Na_v) play a major role in the initiation and propagation of the AP since they are responsible for the initial phase of membrane depolarization. They are found in neurons and electrically excitable cells and also expressed at lower levels in non-excitable cells [102].

Na_v channels are a multimeric complexes composed of an alpha subunit of approximately 260 kDa associated with one or two beta subunits of 30 to 40kDa (heterodimeric or heterotrimeric complexes) [102].

The alpha subunit is a transmembrane protein of approximately 2000 amino acids that contains four homologous but not identical domains (DI-DIV), each composed of six transmembrane segments (S1-S6). The four domains join together at the membrane level to form a central pore [102].

The four isoforms of the beta subunit consist of a single transmembrane segment, with a large glycosylated extracellular domain comprising an immunoglobulin like part and a small C-terminal intracellular domain [103].

Since the alpha subunit is enough by itself for the functionality of the channel, the beta subunits essentially regulate the activity of these channels. They exert a control of the changes of conformations of the channel (modulate the kinetics and the voltage necessary for the activation of the channel), regulate the level of expression of the alpha subunit in the plasma membrane. They also play a role in the interaction with the cytoskeleton, the extracellular matrix and other cell adhesion molecules [104].

In mammalian cells, nine voltage-gated Na^+ channel isoforms belonging to a single family (Na_v1) have been characterized. Encoded by 9 different genes, these isoforms are distinguished by their biophysical properties and by their tissue distribution. These isoforms can be classified either by their localization or by their sensitivity to tetrodotoxin (TTX) [102].

Classification of Na_v channels is based generally on the reaction of the channel to TTX (found in the venom of the puffer fish), those channels are divides into two groups: TTX-resistant (TTX-R) channels and TTX-sensitive (TTX-S) channels.

The isoforms $Na_v1.1$, $Na_v1.2$, $Na_v1.3$, $Na_v1.4$, $Na_v1.6$ and $Na_v1.7$ are said to be TTX-sensitive (the toxin blocks the activity of the channel and the entry of Na^+ into the cell). $Na_v1.1$, $Na_v1.2$, $Na_v1.3$, and $Na_v1.6$ are mainly found at the neuronal level in the CNS, $Na_v1.7$ is found in the PNS and $Na_v1.4$ is found in skeletal muscles [102].

On the other hand, $Na_v1.5$, $Na_v1.8$, $Na_v1.9$ are said to be TTX-resistant (the presence of the neurotoxin does not prevent the activity of the channel and the entry of Na^+ ions into the cell). $Na_v1.8$ and $Na_v1.9$ are expressed in the PNS (especially in the DRGs). $Na_v1.5$ is found in heart muscle and is also found in embryonic skeletal muscle [102].

It should be noted that although these isoforms have a main localization, their distribution in the organism is wide and they can be localized in many other tissues at lower expression levels.

A related 10th Na^+ channel (Na_x) is expressed in the heart, uterus, smooth muscles, astrocytes, and neurons of the hypothalamus and PNS system. Despite about 50% match in their amino acid sequences, it is possible that it is not highly Na^+ selective or fully voltage dependent [105].

Rat DRG neurons express both TTX-R and TTX-S channels, with the first type deactivates relatively slowly form an activation between – 35 to – 25 mV. And later deactivates and activates rapidly in the range of - 50 to - 40 mV [106, 107]. Large DRGs cells bodies express only TTX-S channels while small DRGs express both types with the generation of AP in these neurons involves in big part $Na_v1.8$ channels [108].

The involvement of Na_v channels in pain mechanisms is extensively studied and their role in neuropathic pain models is well established.

2.4.5. HCN channels

Hyperpolarization-activated cyclic nucleotide-gated cation channels (HCN) are cation channels activated by hyperpolarization (~ -50mV). They play an important role during repolarization phase following AP by induction of a depolarizing current, an important activity that facilitate the generation of a new AP [109].

HCN channels are modulated by cyclic nucleotides like cAMP and cGMP which increase the probability of activation of the HCN channels via shifting the threshold of activation towards more positive potentials.

The HCN channel family is formed of 4 members (4 isoforms) HCN1-4, each functional HCN channel is made up of 4 subunits that each contain 6 transmembrane

domains S1-6, as well as cyclic nucleotide-binding domain (CNBD) composed of 8 β strands surrounded by 4 α helices for the reception of the cAMP [110]. It is the S4 transmembrane domain, which is voltage sensitive in all 4 isoforms, the S5 and S6 segments constitute the P domain which allows the conduction and the selectivity of the ions [111].

These channels participate in the pacemaker activity found in heart cells and neurons, they cause the cell to depolarize and do not or very little inactivate. The current generated by these channels (sometimes called I_f or I_h) is present at the resting potential of neurons and in fact participates in the establishment of this potential. Activates between -120 mV and -60 mV and have a reversal membrane potential of -30 mV these channels are permeable to Na^+ and K^+ [112].

It is also involved in cardiac rhythmicity by playing a role in controlling the frequency of APs. These channels are also involved in neuropathic pain of traumatic and chemical origin during cancer treatments [113].

HCN4 channels are the least expressed in rat DRG neurons which express all isoforms of HCN channels with difference in the channel isoform abundance depending on the neuron's diameter as HCN1 and HCN2 represent the largest part in larger neurons, and HCN3 in the smaller ones, with difference also in the amplitude of currents elicited were small and medium sized DRG neurons elicit more I_h currents than larger ones [114]

A clear increase in I_h currents was found in chronic and neuropathic pain models [115]. On the other hand, the diminution of I_h currents amplitude was related to analgesia [116].

2.5. Electrical Phenomena in Cells

2.5.1. Electrical properties of the neuronal membrane

The neuronal membrane is made up of a lipid bilayer into which proteins are inserted, this lipid bilayer separates the intracellular compartment from the extracellular compartment. Membrane proteins are electrically charged molecules and, like any charge-carrying element, can conduct electric current. This property can be schematized by a conductance by a resistance (inverse of the conductance: $R = 1 / G$) which is an opposition to the flow of current [117, 118].

The electrical circuit equivalent to the neuronal membrane thus corresponds until then to that of a current generator (battery) of 60 mV whose positive pole is oriented

towards the extracellular compartment and the negative pole towards the interior of the cell supplying a membrane resistance (Rm) [117, 118].

The value of this Rm, which is a direct function of the quantity of proteins included in a portion of the membrane, is very variable: from 102 to 104 W. cm^2; these values correspond to conductances ($G = 1 / R$) varying from 10^{-4} to 10^{-2} Siemens / cm^2 [117, 118].

Conversely, the lipid bilayer consists of non-conductive phospholipids, giving the membrane capacitive properties, which can be represented by a capacitor (two conductive elements separated by an insulator) of membrane capacitance (Cm) [117, 118].

This capacitor does not modify the value of the potential difference but plays the role of a "reservoir" of charges, which absorbs the instantaneous variations of the potential difference between the two faces of the membrane.

The separation of the positive and negative charges carried by the capacitor induces a potential difference between the two conducting elements such that:

$$V\ (Volts) = Q\ (Coulombs) / Cm\ (Farads) \qquad (2.1)$$

Where Q is the charge carried by the conducting elements. The value of the Cm varies little from one membrane element to another; it is on average 1 µF / cm^2 [117, 118].

The two media, intra- and extracellular, are not perfect conductors. They have a resistance to the passage of electric current, which can be represented schematically by a longitudinal resistance LR.

These electrical properties of the neuronal membrane have functional consequences.

If we consider the resistive properties of the neuronal membrane (transverse resistance R_m), the injection of a current I through this membrane (transmembrane current I_m) reveals, at the terminals of this membrane, a voltage V_m such then:

$$Vm = Rm\ x\ Im \text{ (Ohm's law) [117, 118]} \qquad (2.2)$$

In reality, if the variation of the current is fast, the variation of the membrane potential follows an exponential curve, due to the capacitive properties (C_m) of the membrane. The transverse resistance R_m and the C_m combine their effects to determine

the evolution over time of the installation of the voltage V_m at the terminals of the membrane [118].

The product $Rm.Cm$ is the time constant of the circuit (t). This product indicates, in seconds, the time required for the voltage across the membrane to reach 63.2% of its maximum value [118].

By its structure, the neuronal membrane is a poor conductor. An electrical stimulation of this membrane is deformed as in a resistive-capacitive system ($Rm - Cm$), and propagates only over short distances linked to the diameters of the fibers (R_L) [117, 118].

2.5.2. Ionic mechanisms at origin of the resting membrane potential

In all cells, the distribution of ions on either side of the membrane is uneven. The main free ions encountered are Na^+, K^+, Ca^{2+} and Cl^- ions. The distribution of ions on each other of a plasma membrane follows two major principles: electroneutrality and osmotic balance [118, 119].

Ionic solutions of intra and extracellular medium must be electrically neutral. They must each contain as many anions as cations. This is the principle of electroneutrality [118, 119].

The number of particles in solution located on each side of the membrane must be the same, regardless of the charge of these particles. It is the osmotic balance. Indeed, if the osmotic pressure of the two media is not equal, water movements will occur (from the least concentrated medium to the most concentrated medium) which will modify the cell volume.

The existence of a concentration gradient on one side of a permeable membrane to this ion leads to the formation of an electric gradient which leads to the movement of this ion. The ionic flux born from a concentration gradient is self-limited by the electric field that it generates [118].

Since the bilipid layer is impermeable to ions, passive movements of ions only occur at the level of specialized transmembrane proteins: channel proteins whose three-dimensional structure delimits an aqueous pore through which certain ions pass selectively. They themselves ensure the passage of ions through the membrane - they are also called ion channels [118, 119].

For the K^+ ion for example, as long as the two chemical and electrical gradients are different, i.e., the electrochemical gradient is not zero, there is passage of K^+ ions through the plasma membrane, that is to say a K^+ ionic current. This leads to an equilibrium where the chemical gradient and the electrical gradient are equal and opposite, ie a zero electrochemical gradient, hence a zero ionic current.

At equilibrium, the value of the electric gradient is called the equilibrium potential of the K^+ ion, E_{K+}

The equilibrium potential of an ion depends only on the nature of the ion and the concentrations on either side of the membrane, it is defined by Nernst equation [117, 118]:

$$Eion = \frac{R.T}{z.F}.Ln\frac{[ion]ext}{[ion]int} \quad (2.3)$$

$R = universal\ gas\ constant$

$T = temperature\ in\ Kelvin$

$z = ion\ charge$

$F = Faraday\ constant$

2.5.2.1. *The electrochemical gradient: $Vm - Eion$*

To cross the membrane, an ion is subjected to an electrochemical gradient or driving force" which is expressed by the difference between the membrane potential (V_m) of the cell and the equilibrium potential of the considered ion (E_{ion}).The net flux of an ionic species through its own channels is proportional to this electrochemical gradient [118, 119].

For the K^+ ion and a resting membrane potential of -60 mV: $EK = -87\ mV$

$$Vm - EK = -60 - (-87) = +27\ mV \quad (2.4)$$

Which gives a net outward ion flux, as by convention, the net flux is positive when a cation tends to leave the cell and is negative when the cation tends to enter it.

2.5.2.2. *Membrane ionic conductance*

Electrical conductance (expressed in Siemens, S) measures the ease with which a current move between two points: it is the inverse of resistance (expressed in ohms, Ω). In the case of an ion channel, conductance characterizes the ease with which ions pass through the aqueous pore of the protein channel [117, 118].

The conductance of the entire membrane of a cell for an ion (membrane ionic conductance), G_{ion}, is proportional to the elementary conductance of an ion channel: G_{ion}, but also to the total number of channels of the ionic species considered in the membrane: N_{ion} and the probability p0 for these channels to be in the open state [118, 119]:

$$Gion = Gion . Nion . p0 \quad (2.5)$$

The G_{ion} value can vary from 10 to 200 pS (1 Pico Siemens, pS = 10^{-12} Siemens) depending on the type of ion channel. Taking in consideration that most ionic channels are not perfectly selective: the measurement of G_{ion} therefore depends on the experimental conditions and, in particular, on the presence of other ions [119].

2.5.2.3. *Ionic currents*

The intensity of the currents measured in electrophysiology. (I_{ion}, expressed in Amps: Coulombs.sec-1) flowing through an ion channel or elementary ion current is equal to [119]:

Membrane ionic current: $(Iion) = Gion\,(Vm - Eion)$

which is only the transposition of Ohm's law ($V = R.I$ therefore $I = G.V$) to an electrochemical gradient.

The resting membrane potential is a result of the permeability of the plasma membrane to several ion at the same time, in addition to that, the active transport mechanisms (Na^+/ K^+/ATPase pump) which make it possible to maintain constant concentrations of K^+ and Na^+ ions on either side of the membrane, the equilibrium potentials of the K^+ (E_K) and Na^+ (E_{Na}) ions therefore remain constant. The membrane potential (V_m), which will be established, is therefore intermediate between the equilibrium potentials of the two ions, E_K (-87 mV) and E_{Na} (+60 mV) [118, 119].

The membrane potential of the cell (V_m) will reach a stable state when the net flux of charges (K^+ & Na^+) passing through the membrane is zero, that is, in terms of ionic currents, when $INa + IK = 0$ [118, 119].

2.6. The Patch Clamp Technique

The cell membrane behaves like a circuit with a capacitor and a resistor placed in parallel, to measure them we most often use the technique of imposed potential (voltage clamp).

In 1976, the so-called patch-clamp method, "patch" for a very small part of neuronal membrane, was developed by Erwin Neher and Bert Sakmann [120]. this method revolutionized the study of ionic currents by recording the processes in action in a single channel.

2.6.1. General principle

A pipette containing a conductive solution is positioned on the cell membrane comprising the ion channels. The pipette is connected to an amplifier that either imposes potentials and measures currents (voltage clamp) or imposes currents and measures potentials (current clamp). The currents measured on a single channel are very low (of the order of 10^{-12} ampere or picoampere). Leaks must therefore be avoided [31, 121].

By applying a slight suction, the membrane sticks tightly to the pipette and forms a seal so the ions which pass through the channel when it is opened necessarily pass through the pipette and create a measurable current thanks to the amplifier [121].

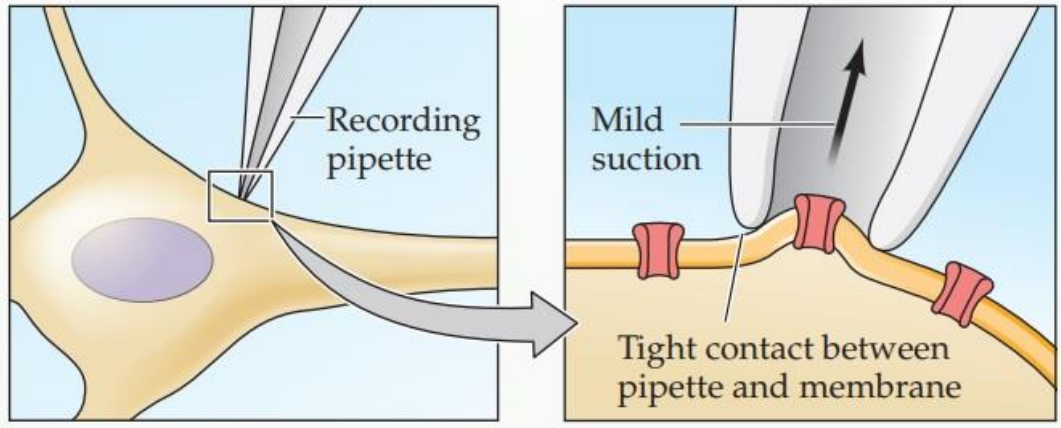

Figure 2.3. *Cell-attached patch-clamp configuration [31]*

This method is called cell-attached patch-clamp, in which the cell membrane is kept unbroken [31].

This configuration is used in cases where channel activity requires intracytoplasmic factor, or binding with cytoskeletal proteins. Other configurations are possible depending on the strength of the suction.

2.6.1.1. *Whole-cell patch*

The whole cell patch clamp is obtained by applying strong suction to the membrane, which causes it to tear. The pipette is in contact with the entire cell cytoplasm and therefore allows measurements of global potentials and currents. This method also allows substances to be injected into the cytoplasm for experiments [31, 121, 122].

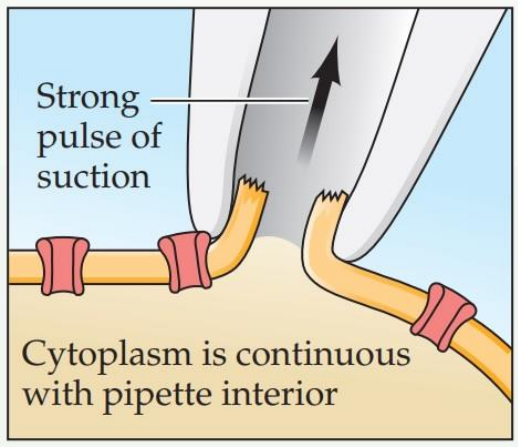

Figure 2.4. *Whole cell patch-clamp configuration [31]*

The other patch-clamp configurations (inside-out and outside-out) are used to measure the currents flowing through a single channel (single-channel recordings). These configurations are established by tearing off the small membrane part sealed on the pipette, which isolate it form the rest of the cell that is no longer involved [31, 121].

2.6.1.2. ***The inside-out patch configuration***

This configuration is gotten from the cell-attached patch. A portion of the membrane is aspirated and taken away from the cell, the intracellular face of which is therefore is located outside the pipette. In this configuration it is also possible to change the composition of the medium which is in contact with the intracellular face which is facing the outside and to study the intracellular modulations of this channel by different molecules [31, 121].

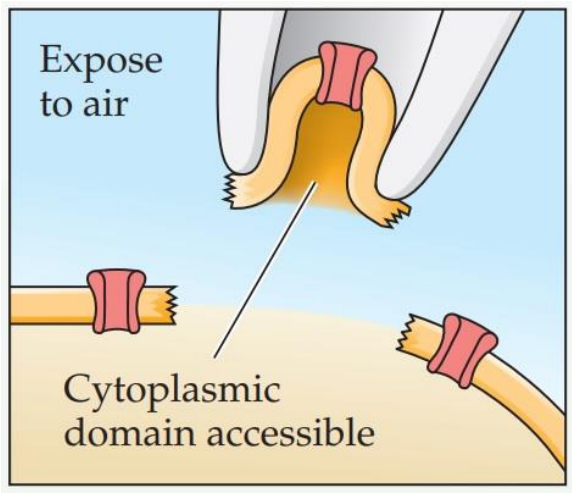

Figure 2.5. *Inside-out patch-clamp configuration [31]*

2.6.1.3. *The outside-out patch configuration*

Starting from the whole cell patch configuration, A part of the membrane is aspirated and taken away, the part of the membrane taken away will solder and the extracellular face of which is therefore located outside the pipette.

It is then possible to study the extracellular modulations of this channel, and in particular the action of neurotransmitters on the channels activated by ligand binding, such as the nicotinic acetylcholine receptor or the $GABA_A$ receptors [31].

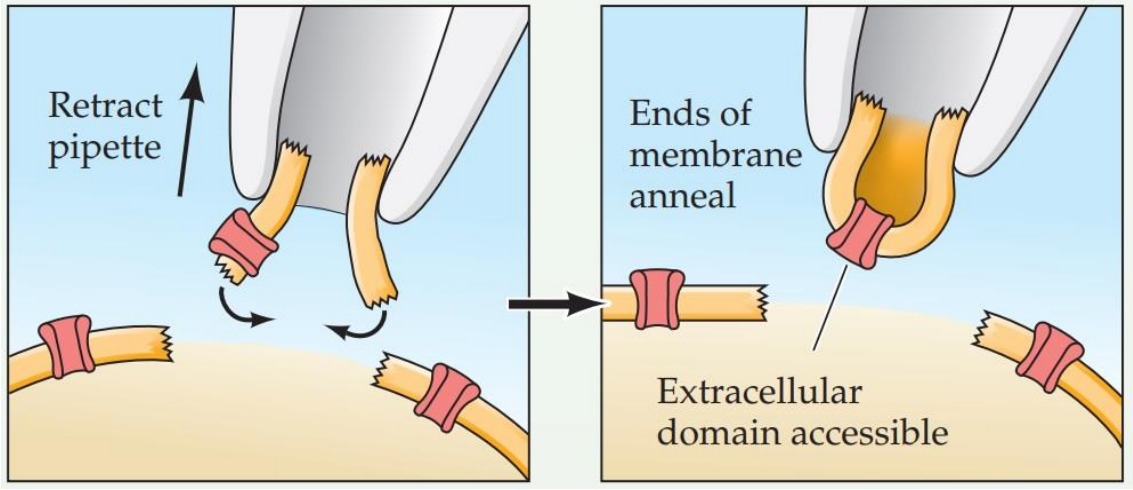

Figure 2.6. *Outside-out patch-clamp configuration [31]*

2.7. Test Chemicals Used in The Study

2.7.1. Rutin

Rutin is a flavonoid that is found in abundance in nature. It is one of the most interesting phytochemicals due to its numerous properties; It is mostly found in plants' leaves in a heterosidic form. There are approximately 180 quercetin heterosides present in nature, with rutin being one of the most common [123, 124]

The onion (*Allium cepa*) was identified as the food with the highest concentration of rutin. asparagus, Green beans, broccoli, apple, lettuce, tomatoes are also among the foods richest in rutin [125].

The term “flavonoids” designates a wide range of compounds belonging to the family of polyphenols. Flavonoids are almost universal pigments found in the plant world. They are, for some, responsible for the color of flowers and fruits. Flavonoids are mainly present in plants in the form of heteroside (or glycoside), that is to say a molecule born

from the condensation between an ose (sugar), and a non-carbohydrate substance called "aglycone" or "genin".

The heterosidic forms of flavonoids are water soluble and accumulate in vacuoles and depending on the species, concentrate in the epidermis of the leaves or are distributed between the epidermis and the mesophyll.

Rutin (also called rutoside) is a heteroside of quercetin, a flavonol. Quercetin is therefore the aglycone of rutin, it is linked to rutinose, that is to say a disaccharide (sugar made up of two oses) [126].

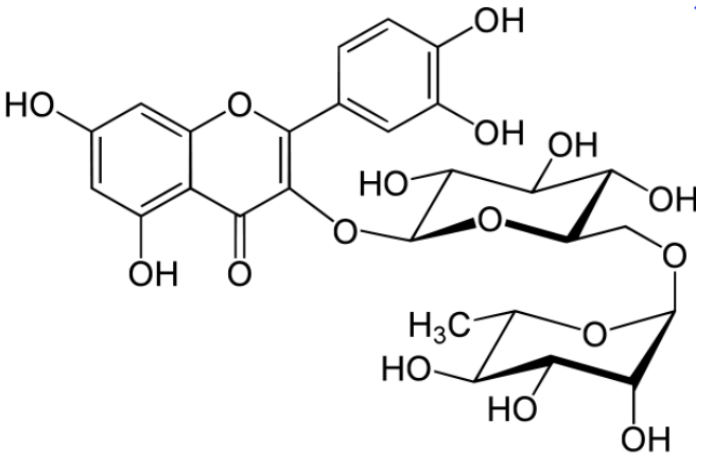

Figure 2.7. *Molecular structure of Rutin*

Rutin's strong antioxidant effects have led to a broad variety of pharmacological applications.

Rutin is commonly used as an antimicrobial, antifungal, and antiallergenic agent and its pharmacological properties for the treatment of multiple chronic disorders such as cancer, diabetes, hypertension, and hypercholesterolemia have been shown in recent studies [127].

2.7.1.1. *Antioxidant activity*

Flavonoids' antioxidant function is linked to their ability to scavenge free radicals and is determined by their molecular structure. The potent antioxidant property of rutin, especially as a free radical scavenger, is largely responsible for most of its biological activities, such as anti-inflammatory, anti-microbial, anti-tumor, and anti-asthma [128].

Rutin demonstrated concentration-dependent strong antioxidant ability against a variety antioxidant systems *in vitro*, and its ability to scavenge or neutralize free radicals was documented [129].

2.7.1.2. *Antimicrobial activity*

Rutin showed significant antimicrobial activity in hydrogel formulation [130]. Furthermore, a high antibacterial activity of rutin was demonstrated against *Pseudomonas aeruginosa* and *Klebsiella pneumoniae* [131], it also have antiviral activity against herpes simplex virus, respiratory syncytial virus, poliovirus, and Sindbis virus [132]. Rutin also have potent antimicrobial and antifungal activity against isolated strains of *A. baumannii, S. aureus*, and *C. krusei* [133].

2.7.1.3. *Anti-inflammatory activity*

Rutin's anti-inflammatory activity is explained by the inhibition of several main enzymes involved in the inflammatory response. Rutin has several beneficial effects in the management of inflammatory bowel disease (IBD) [134] and reduces cytokine levels [135]. In rats, rutin has been shown to reduce ROS-induced oxidative stress and inflammation by targeting COX-2, p38-MAPK, i-NOS, NFκB, IL-6 and TNF-α [136].

Rutin's anti-inflammatory effects have also been shown to help minimize brain damage and enhance neurologic dysfunctions [137]. In human endothelial cells, rutin inhibited HMGB1 release and suppressed HMGB1-dependent inflammatory responses [138].

2.7.1.4. *Anticancer activity*

Rutin has been shown to have anticancer properties *in vitro* and *in vivo* in several trials, it causes cell cycle arrest and trigger apoptosis in a variety of human cancer cell lines [139] and it has been proven to have anti-carcinogenic and protective effects in a dose-dependent manner [140], as well as antiangiogenic [141] and anti-neuroblastoma properties [142]. And inhibitory properties on human lung and colon cancer cells [143].

2.7.1.5. *Antidiabetic activity*

The antioxidant activities and anti-inflammatory properties of rutin reduced blood glucose levels in STZ-induced diabetic rats, inducing a protective effect against diabetic complications [144].

As compared to diabetic control rats, rutin offered important defense against diabetes-related oxidative stress, avoided cardiac degeneration, and enhanced ECG parameters [145].

2.7.1.6. *Antiallergic activity*

Rutin had an anti-allergic inflammatory effect on immunoglobulin E-mediated mast cell activation suppression levels of chemokines (ICAM-1 and MIP-2) in a sample, suggesting its protective activity against allergic rhinitis [146, 147]. Furthermore, rutin has been discovered to suppress AD and ACD, stipulating that rutin could be used to cure allergic skin diseases [148].

2.7.1.7. *Other biological activities*

Rutin can protect from oxidative stress caused by Aβ, and may have therapeutic potential in the treatment of Alzheimer's disease [149]. By reducing capillary permeability and fragility, it can help to maintain normal blood vessel conditions [150]. Furthermore, it has been shown that rutin intake can protect from Parkinson's disease like neurological disorders [151].

2.7.2. Hesperidin

Hesperidin is a flavonoid extracted from the species *Rutaceae aurantieae*, Orange and other citrus fruit such as *Citrus aurantium*, *C. sinensis*, *C. unshiu* peels represent a main source of this substance. Apart from citrus fruits, hesperidin can also be found in a variety of other plants, such as Legumes, Birch and Honeysuckle [152].

The biological effects of hesperidin are numerous, whose main physiological property is its anti-inflammatory activity which was related to its action on signaling pathways, particularly the nuclear factor κβ pathway [153]. Evidence have shown that hesperidin can modulate the capacity of the synthesis of prostaglandins and the expression pathways of the COX 2 gene in RAW 264.7 cells by inhibition Lipopolysaccharide induced inflammation, which supports the anti-inflammatory activity of Hesperidin [154, 155].

Hesperidin's function in neuropathic pain was investigated, and the findings revealed that it inhibits P2X3 receptor-mediated nociceptive transmission in DRG neurons, as a result of which mechanical and thermal hyperalgesia in chronic constriction injury was reduced in rats [156]. In another study, the protective role of hesperidin was investigated using rat model of partial sciatic nerve ligation, as a result hesperidin was found to reduce in a dose dependent manner mechanical and thermal hyperalgesia, mechanical allodynia and down regulate TNF-α, IL-6 and IL-1β [157].

Furthermore, it was discovered that hesperidin helps to improve spinal cord injury by lowering IL-1β and TNF-α levels and reducing the number of caspase 3 apoptotic cells through its anti-inflammatory, anti-oxidant, and anti-apoptotic effects [158].

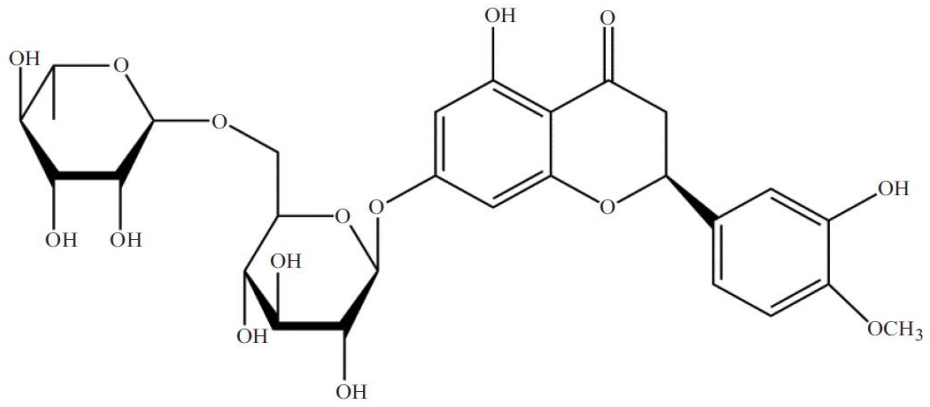

Figure 2.8. *Molecular structure of hesperidin* [153]

Hesperidin's antioxidant potential was investigated, and it was discovered that this flavonoid has a high capacity for sequestering reactive oxygen species including the hydroxyl radical and superoxide. Furthermore, this flavonoid promotes nitric oxide sequestration as well as the prevention of damage caused by hydrogen peroxide, such as lipid peroxidation in RBC cell membranes [159].

Hesperidin's neuroprotective activities, and its activity of sequestering reactive species and inhibiting lipid peroxidation as a way to prevent oxidative stress is a property of interest in several researches [160].

Neuroprotective activity of hesperidin has been tested and proven in animal and cell models of Parkinson's Disease [158, 159]. In animal models, hesperidin at a dosage of 50 mg/kg was shown to have the greatest neuroprotective potential in the literature [163]. Recent studies have shown that using hesperidin in 6-hydroxydopamine Parkinson's Disease induced animal model, resulted in the downregulation of oxidative stress biomarkers such as kinases lrrk2 and gsk3β by the side of casp3, casp9 [164].

Hesperidin has demonstrated neuroprotective efficacy in other models of degenerative diseases, such as Alzheimer's, leading one to believe, based on all of the literature evidence already published on the biological processes related to hesperidin, that this promising agent is capable of protecting and even reversing the neurodegenerative syndrome that is characteristic of Parkinson's Disease [165].

Anticarcinogenic activity, on the other hand, is attributed to its ability to inhibit cancer cell metastasis and angiogenesis by inducing cell apoptosis and suppressing cell proliferation [166].

It has been shown to have antimicrobial, hypolipemic, capillary fragility correction, and capillary permeability reduction properties, as well as hypocholesterolemia, antifungal, hypoglycemic, and insulinotropic impact [167].

For the effect of hesperidin on voltage gated ion channels little is known about this property, in a study this effect of hesperidin was investigated, by conduction electrophysiological recording on human cardiac Kv1.5 channels expressed in HEK-293T cells, patch clamp technique was used to assess the fast delayed rectifier K^+ current in human trial myocytes. Results revealed a concentration-dependent inhibition of the Kv1.5 current, that moved the steady state of inactivation towards a more negative value while shifting the steady state activation curve to more positive values [168].

Hesperidin's action on human cardiac Nav1.5 channels expressed in HEK239 cells and on voltage gated Na^+ current in human atrial myocytes has also been documented, with hesperidin reversibly inhibiting Na^+ current and the voltage dependent activation and activation curves being negatively shifted, implying that hesperidin functions by blocking the active and inactive states of Na^+ channels [169].

2.7.3. CGA

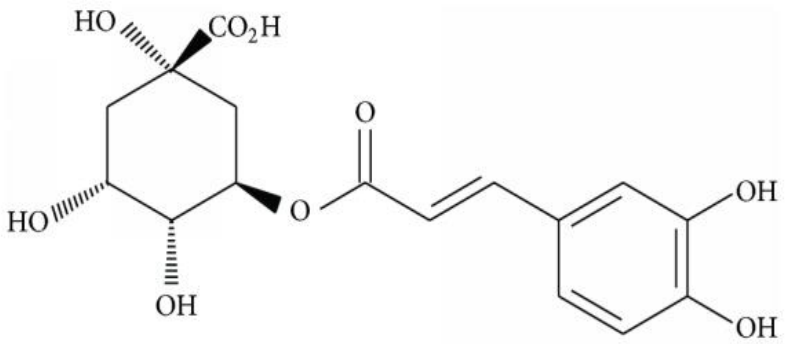

Figure 2.9. *Chemical structure of CGA (5-caffeoylquinic acid, 5CQA)* [170]

CGA belongs to the hydroxycinnamic acid family of polyphenols also known as 5-cafeolquinic acid because it has a caffeic acid and quinic acid molecule in its chemical structure.

CGA shown to have anti-oxidant, anti-inflammatory, antipyretic, analgesic properties [168, 169], anticancer [170, 171], antilipidemic and antidiabetic effects [175], antihypertensive [176], and anti-neuro degenerative activity [177].

CGA, on the other hand, can affect a wide range of bacteria, fungi, molds, viruses, and amoebas. In this regard, CGA attracted the attention of the food industry because of its antimicrobial properties and shown the possibilities of its use as a natural preservative [178].

Antioxidant and anti-inflammatory properties of CGA were related to the presence of hydroxyl (OH) groups on phenolic acids which has been shown to increase antioxidant action.

In one study [3], CGA was shown to substantially reduce interleukin-8 secretion and mRNA expression in response to oxidative stress. In a dextran sulfate Na^+-induced colitis model, caffeic and CGA were found to suppress mRNA expression of macrophage inflammatory protein 2 (a mouse homologue of interleukin-8 MIP-2) in macrophages [3].

Caffeic acid and CGA act as anti-inflammatory agent causing reduction of the intracellular reactive oxygen species via inhibition of the activation of interleukin-8 and PKD-IKKNFκB pathway [3]. This property of CGA has been linked to catechol groups, and it is believed that this functional group could help prevent inflammatory diseases.

It has been documented that CGA, which is typically present in the human diet, has protective effects in TLR4 signaling activation, modulation of adhesion molecule expression, infiltration and activation of hepatic leukocytes, and Con A-induced hepatitis triggered by the synthesis of proinflammatory cytokines [3].

There have been several studies that demonstrate the impact of CGA on different pain models. The diabetic neuropathy model and the chronic constrictive nerve injury model, which is an experimental neuropathic pain model, have both shown antipyretic and analgesic effects [176, 9].

In pain experiments using extracts from plants containing CGA, CGA was shown to be responsible for the antinociceptive effects [180]. CGA has also been found to have an antinociceptive effect in the formalin induced pain test when used in pure form [181]. However, literature on the implications and underlying mechanisms of CGA on neuropathic pain is scarce.

On trigeminal ganglion neurons, the electrophysical effect of CGA on voltage ion channels was studied. The result of whole cell patch clamp recording on two subtypes of voltage K^+ channels ($I_{K,A}$ and $I_{K,V}$ channels), revealed an analgesic effect through decreased $V_{1/2}$ values and a shift towered hyperpolarization [25]. Furthermore, CGA has been found to decrease the peak current density of $I_{K,A}$ and greatly reduce the activation and inactivation threshold of K^+ channels ($I_{K,A}$, $I_{K,V}$) in another study on acutely disassociated trigeminal ganglion neurons cells [182].

3. MATERIALS AND METHODS

3.1. Experimental Animals

Care for experimental animals and trials procedures were approved by the local ethics committee from Anadolu University (Decision no: 2021-16, Appendix I) for animal experiments.

Maximum of five animals of Sprague Dawley rats per cage of 8-12 weeks old were used for the experiments. Animals were kept in a well-ventilated laboratory environment at a temperature of (23 ± 2°C) and relative humidity (50 ± 10%) for the duration of the experiment on a 12-hour light and 12-hour dark cycle. with free access to food (standard chow) and drinking water.

3.2. Chemicals

Utilized Chemicals and providers are listed in (Table 3.1.).

Table 3.1. *List of chemicals utilized*

Name of Chemical	Supplier
Rutin	Sigma Aldrich, USA
Hesperidin	Sigma Aldrich, USA
CGA	Sigma Aldrich, USA
Phosphate buffered saline (PBS)	Sigma Aldrich, USA
Dimethyl sulfoxide (DMSO)	Sigma Aldrich, USA
Ketamine	Richter Pharma ag, Austria / Interhas A.S. Ankara, Turkey
Xylazine	Bioveta a.s., Czech Republic / Intermed Ecza Deposu, Ankara, Turkey
Penicillin- streptomycin	Sigma Aldrich, USA
Collagenase type IV	Sigma Aldrich, USA
Trypsin 0.25%	Sigma Aldrich, USA
Fetal Bovine Serum (FBS)	Sigma Aldrich, USA
Potassium chloride (KCl)	Wisent Inc. Canada
Sodium chloride (NaCl)	Wisent Inc. Canada
HEPES ACID	Wisent Inc. Canada
Mg-ATP	Wisent Inc. Canada
EGTA	Wisent Inc. Canada
D-glucose	Wisent Inc. Canada

Table 3.1. (continues) *List of chemicals utilized*

Name of Chemical	Supplier
Potassium hydroxide (KOH)	Wisent Inc. Canada
Calcium chloride ($CaCl_2$)	Wisent Inc. Canada
Magnesium chloride ($MgCl_2$)	Wisent Inc. Canada
Dulbecco's Modified Eagle's Medium (DMEM)	Sigma Aldrich, USA

3.3. Apparatus

Model and brand data of utilized Apparatus are recorded in (Table 3.2).

Table 3.2. *List of used apparatus*

Name of the Apparatus	Brand and Model
Micropipette Puller	Model: P-97. Sutter Instrument Company USA
Patch Amplifier	Model: IPA. Sutter Instrument Company USA
Glass pipettes	Model: BF150-110-10. Sutter Instrument Company USA
Anti-vibration table	Model: 9100 S. Kinetic Systems, Inc USA
Microscope	Model: Sutter BOB™. Sutter Instrument Company USA
Motorized Micromanipulator	Model: MP-285 Sutter Instrument Company USA
Multi-Micromanipulator System	Model: MPC-385 Sutter Instrument Company USA

3.4. Dissection of DRG and Primary DRG Cells Culture

An intraperitoneal injection of 1 ml/ kg of ketamine and xylazine mixture as a ratio of 1.8/1 respectively [183] was used for animal anesthetization, and a duration of 5 to 8 minutes was given for the full anesthesia to take effect.

After making sure that the animal was completely anesthetized the decapitation was performed, then by an incision of the back skin the vertebral column was exposed then removed and transferred into a 50 ml falcon tube filled with ice cold PBS for 5 minutes before starting the harvest of DRGs [184–186] .

To ensure sterility and avoid contamination, handling of vertebral column, extraction of DRGs and mechanical digestion of the ganglia was performed under a laminar flow cabinet. The vertebral column is placed in petri dish filled with DMEM solution at 4 C° then iris scissors are used to cut into two symmetrical pieces from the

centerline the vertebral column. Then, after careful removal of the spinal cord the harvest of DRGs was carried out using hairspring tweezer, and obtained individual ganglia were placed in a DMEM-Penicillin-Streptomycin filled petri dish [184, 186].

To avoid getting debris and other types of cells in the cell culture obtained DRGs were cleaned to the maximum possible from projections and attached using a surgical Lancet and iris scissor [184, 186].

The enzymatic digestion was initiated as the resulting clean ganglia were transferred into an Eppendorf tube contain 2 mg of collagenase type IV dissolved in 1 ml of DMEM-Penicillin-Streptomycin then incubated for 45 minutes at 37 °C and 5% CO_2, the Eppendorf tube was left open. Resuspension of the ganglia was performed every 10 minutes [186, 187].

After the end of the first incubation period, the supernatant was discarded and 3 washing cycles by PBS (Discard the supernatant, add 1 ml of PBS, Centrifuge for 30 s) were performed, then washed ganglia were placed into 1 ml of DMEM-Penicillin-Streptomycin containing 100 µl of 0.25% Trypsin then incubated for 6 with resuspension of DRGs after 3 minutes [184, 186, 187].

Another 3 washing cycles by DMEM (Discard the supernatant, add 1 ml of DMEM, Centrifuge for 45 to 60 s) were performed. then 1 ml of DMEM was added to the trypsin digested DRGs in Eppendorf tube then transferred to a 15 ml falcon tube contain 1 ml of DMEM to get a total volume of 2 ml of DMEM containing ganglia solution [184, 186, 187].

The mechanical digestion was performed consecutively by a gentle pipetting for 5 minutes as a rate of 4 times per minute with cut 1 ml blue tip, 5 minutes with non-cut 1 ml blue tip then a 3 times very slow passing through insulin syringe [184].

Resulted DRGs cell suspension was transferred into DMEM-Penicillin-Streptomycin + FBS as 12.5 ml for 1 ml of the cells [186, 187].

2 to 3 hours resting interval was given to the cells before performing electrophysiological recordings.

3.5. Solutions Used for Patch-Clamp Recordings

3.5.1. Current clamp recordings

Internal solution (pipette solution) used for AP recordings under current clamp mode and concentrations of its components is listed in (Table 3.3.), pH was adjusted to 7.3- 7.4 with KOH [188].

Table 3.3. *Pipette solution for AP recordings*

Components of Internal solution (313 mOsm)	Concentration (mM)
KCl	130
NaCl	10
HEPES Acid	10
Mg-ATP	4
EGTA	5
D-glucose	10

External solution (bath solution) used for AP recordings under current clamp mode and concentrations of its components is listed in (Table 3.4.), pH was adjusted to 7.4 with NaOH [188].

Table 3.4. *Bath solution for AP recordings*

Components of external solution (321 mOsm)	Concentration (mM)
NaCl	140
KCl	5
$CaCl_2$	2.5
$MgCl_2$	1.2
HEPES Acid	10
D-glucose	10

3.5.2. Voltage clamp recordings

Internal solution (pipette solution) used for current recordings under voltage clamp mode and concentrations of its components is listed in (Table 3.5.), pH was adjusted to 7.2 with KOH [188].

Table 3.5. *Pipette solution for currents recordings*

Components of Internal solution (310 mOsm)	Concentration (mM)
KCl	140
NaCl	10
$MgCl_2$	2
$CaCl_2$	0.1
HEPES Acid	10
EGTA	1.1
D-glucose	3

External solution (bath solution) used for currents recordings under voltage clamp mode and concentrations of its components is listed in (Table 3.6.), pH was adjusted to 7.3 with NaOH [188].

Table 3.6. *Pipette solution for currents recordings*

Components of external solution (320 mOsm)	Concentration (mM)
NaCl	140
KCl	3
$MgCl_2$	1
$CaCl_2$	1
D-glucose	10
HEPES Acid	10

3.6. Application of the patch-clamp technique

Patch clamp measurements were performed on primary dissociated DRG cell culture after 4 to 6 hours of cells rest. Electrophysiological experiments were performed at room temperature (18-20 °C) using the whole cell technique of the patch clamp technique. Rutin and hesperidin were dissolved in Dimethyl DMSO, with DMSO ratio not exceeding 0.3% [189, 190]. Stock solution was diluted with standard external solution to get 1 and 10 μM and 100 μM final doses of test chemicals.

The application of test substances was carried out to the extracellular solution at 50-100 μm away from the recorded cell [23, 122].

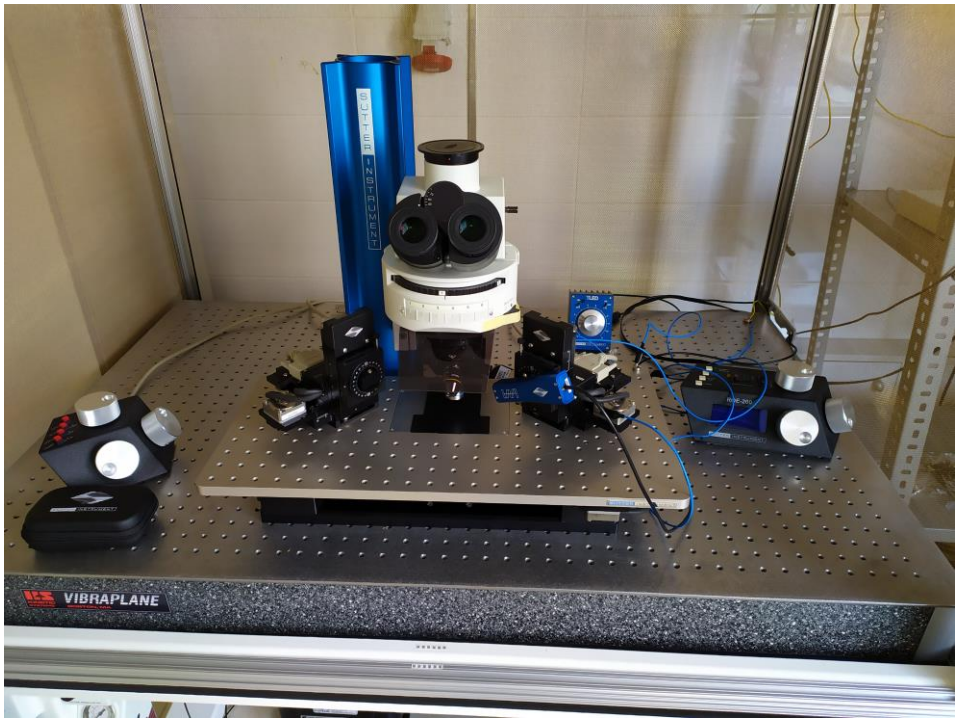

Figure 3.1. *Electrophysiology rig*

The picture of electrophysiological rig utilized in the experiments is represented in (Figure 3.1.).

3.6.1. Voltage-clamp recordings

Voltage-clamp recordings of were conducted in whole cell configuration to record ion currents from acutely dissociated DRG cells. GΩ-seals were established using Thin Wall Borosilicate Glass pipettes with filament (Sutter Instrument BF150-110-10) filled with the internal solution for Voltage-clamp recordings pulled by P-97 Micropipette Puller (Sutter Instrument) to a final pipette resistance of 2-5 MΩ. The passage to whole cell configuration was done using negative pressure applied either by mouth or by use of 1 ml syringe, the passage to whole cell is marked by a big drop in series resistance to around 10 MΩ and increase of Cm. Recordings were conducted at room temperature [122].

Depolarizing pulses to 0 mV for 300 ms were used after clamping the membrane potential to -60 mV. The current–voltage relations (IV-curve), was obtained using depolarizing steps of 10 mV increments from −60 mV to +80 mV.

The test Chemical was applied after getting a stable outward current in response multiple depolarizing steps to 0 mV [122].

Currents were recorded using a single headstage version of the Integrated Patch Amplifier (IPA) (Sutter Instrument) and SutterPatch® Data Acquisition and Analysis Software (SutterPatch 2.0.4) installed on windows®10 and used in voltage-clamp mode. Data were sampled at 25 kHz and filtered at 5kHz using the built-in filter of the IPA. electrode compensation and series resistance compensation were automatically applied using the automatic compensation option in the software.

Data were analyzed used the same software (SutterPatch 2.0.4).

3.6.2. Current-clamp recordings

Current-clamp recordings of were conducted in whole cell configuration to record variation in the voltage of acutely dissociated DRG cells. GΩ-seals were established using Thin Wall Borosilicate Glass pipettes with filament (Sutter Instrument BF150-110-10) filled with the internal solution for current-clamp recordings pulled by P-97 Micropipette Puller (Sutter Instrument) to a final pipette resistance of 4-6 MΩ. The passage to whole cell configuration was done using negative pressure applied either by mouth or by use of 1 ml syringe and marked by a big drop in series resistance to around 10 MΩ and increase of Cm. Recordings were conducted at room temperature.

Data was acquired using in current-clamp mode a single headstage version of the Integrated Patch Amplifier (IPA) (Sutter Instrument) and SutterPatch® Data Acquisition and Analysis Software (SutterPatch 2.0.4) installed on windows®10. Acquisition sampling rate was 25 kHz and filtered at 5kHz using the built-in filter of the IPA.

spontaneous firing activity were monitored for few minutes of whole-cell recording. The AP threshold was determined using depolarizing current steps of 10 pA for 10 mS from 0 pA to 300 pA and the minimum injected current amplitude that elicit an AP is chosen[122].

APs were elicited for several times using the value obtained, when a stable result is acquired the test chemical is applied and changes in signal are monitored for amplitude, half-width, fast AHP, ADP and medium AHP.

Data were analyzed used the same software (SutterPatch 2.0.4).

3.7. Statistical Analysis

Statistical analysis was done using GraphPad InStat 3 (Trial) and OriginPro 9.8.0.200 (Learning Edition).

4. RESULTS

4.1. K^+ Current Results

4.1.1. Rutin

The voltage protocol used to evaluate the effect 1 µM of rutin on K^+ current and the observed current densities are shown in (Figure 4.1.).

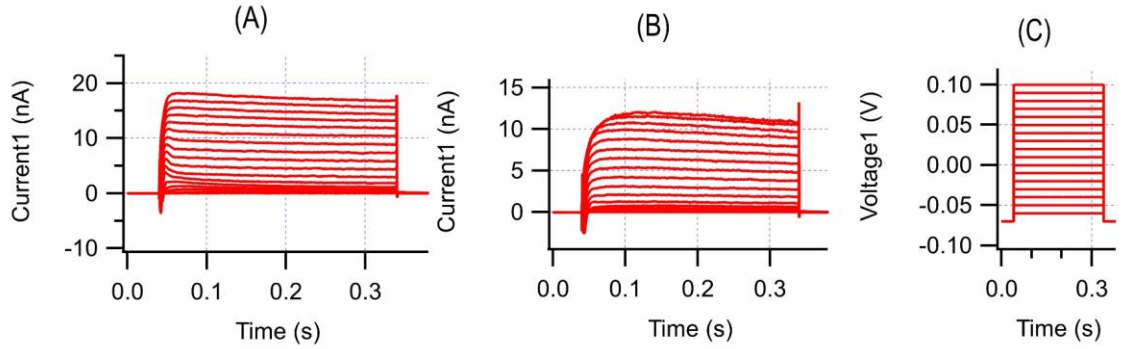

Figure 4.1. *K^+ currents densities recorded from control cell (A) after injection of incremental depolarizing voltage steps (C), and K^+ currents densities after application of 1 µM dose of rutin (B) and execution of the same voltage protocol (C).*

Control recordings of K^+ current densities, and after application of 1 µM of rutin are represented in (Figure 4.2.) as mean values ± S.E.M.

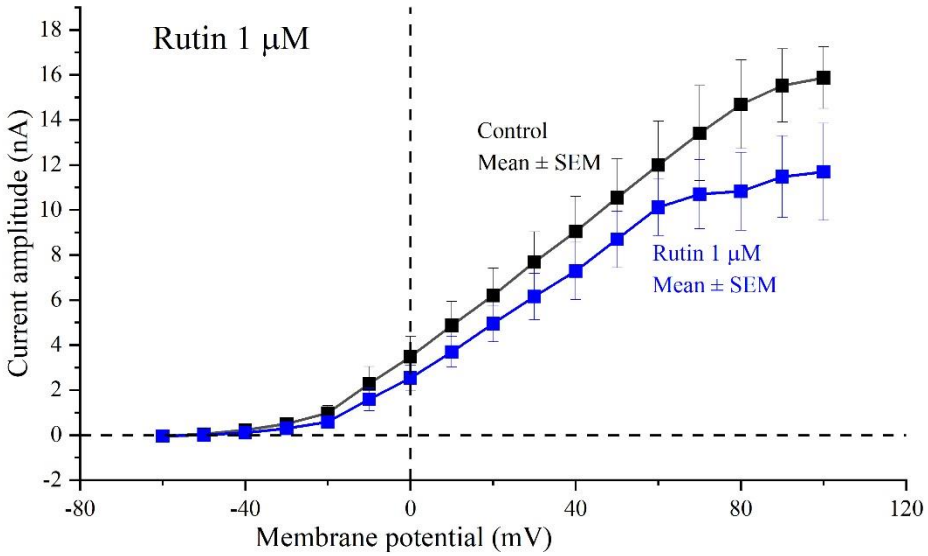

Figure 4.2. *Graphic representation of mean values ± SEM of the relation between membrane (mV) and outward K^+ current amplitudes (nA, from control cell and after application of 1 µM of rutin, with data showing 24% decrease of K^+ currents densities relatively to membrane potential, (n= 5; P<0.05).*

Conductance of K^+ channels in relation to membrane potential from control cells and after application of rutin at 1 µM dose, are shown in (Figure 4.3.), the value of potential of half activation ($V_{1/2}$) was calculated using Boltzmann equation and nonlinear curve fitting function in OriginPro.

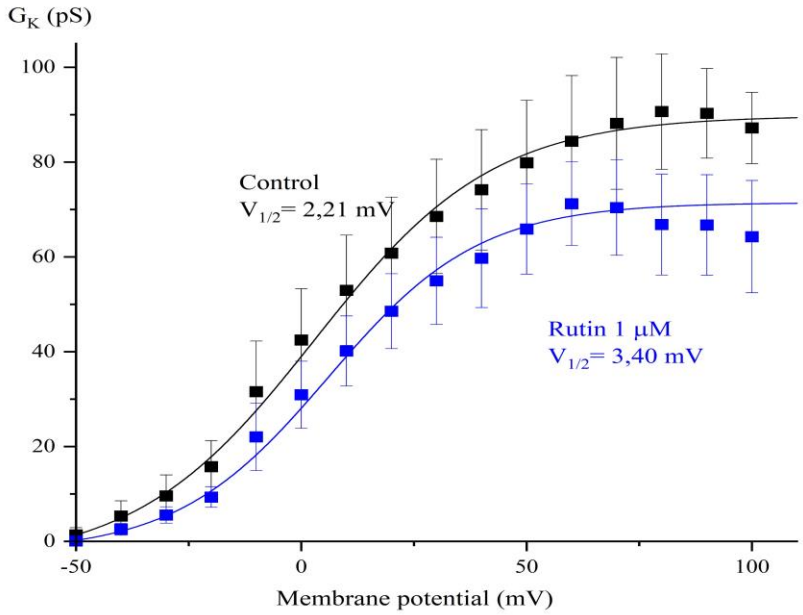

Figure 4.3. *K^+ channels conductance in relation to membrane potential and from control DRG cells and after application of 1 µM of rutin showing 23% reduction in maximum conductance and non-significant shift in the $V_{1/2}$ value (n=5; P>0.05). Data are represented as mean values ± S.E.M.*

Voltage protocol used to evaluate the effect 10 µM of rutin on K^+ current and the observed current densities are shown in (Figure 4.4.).

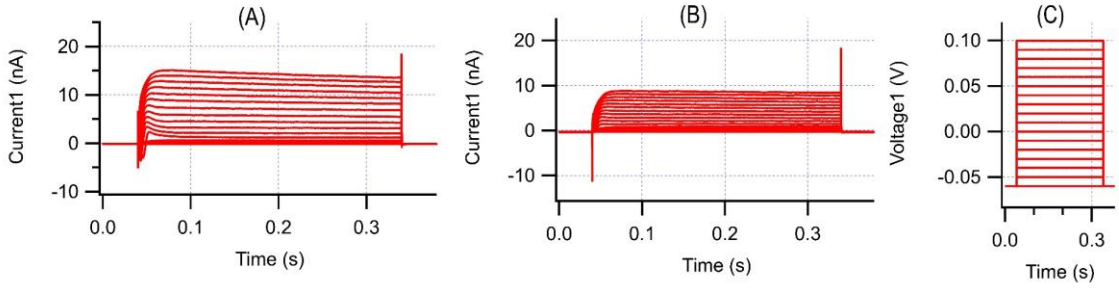

Figure 4.4. *K^+ currents densities recorded from control cell (A) after injection of incremental depolarizing voltage steps (C), and K^+ currents densities after application of 10 µM dose of rutin (B) and execution of the same voltage protocol (C).*

Control recordings of K^+ current densities, and after application of 10 µM of rutin are represented in (Figure 4.5.) as mean values ± S.E.M.

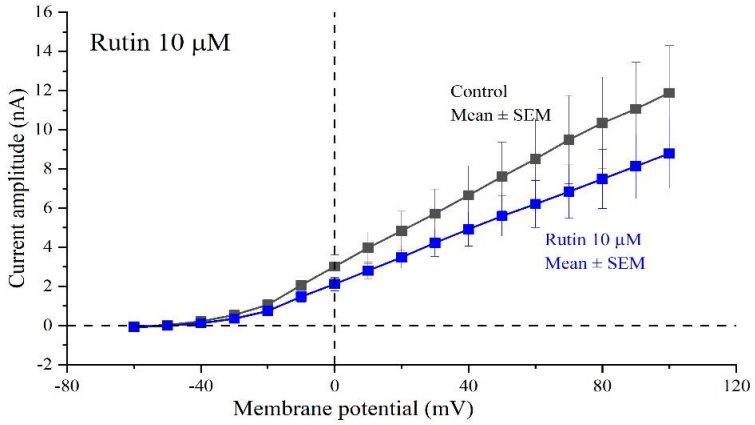

Figure 4.5. *Graphic representation of mean values ± SEM of the relation between membrane (mV) and outward K^+ current amplitudes (nA), from control cell and after application of 10 µM of rutin, with data showing 23% decrease of K^+ currents densities relatively to membrane potential, (n= 6; P<0.05).*

Conductance of K^+ channels in relation to membrane potential from control cells and after application of rutin at 10 µM dose, are shown in (Figure 4.6.), the value of potential of half activation ($V_{1/2}$) was calculated using Boltzmann equation and nonlinear curve fitting function in OriginPro.

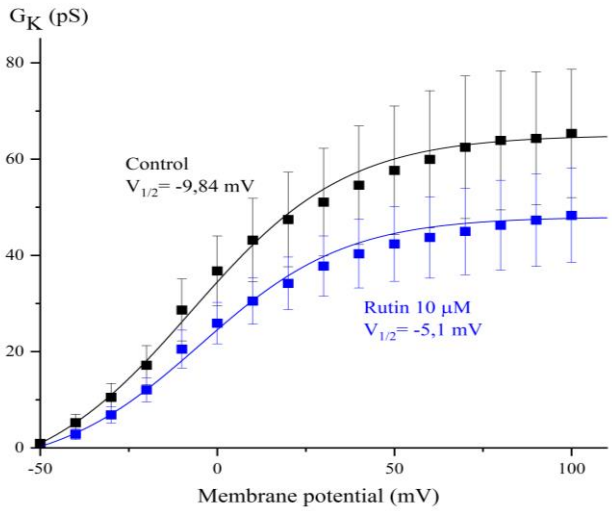

Figure 4.6. *K^+ channels conductance in relation to membrane potential and from control DRG cells and after application of 10 µM of rutin showing 25% reduction in maximum conductance. (n= 6; P<0.05). and non-significant shift in the V1/2 value (P>0.05). Data are represented as mean values ± S.E.M.*

Voltage protocol used to evaluate the effect 100 µM of rutin on K^+ current and the observed current densities are shown in (Figure 4.7.).

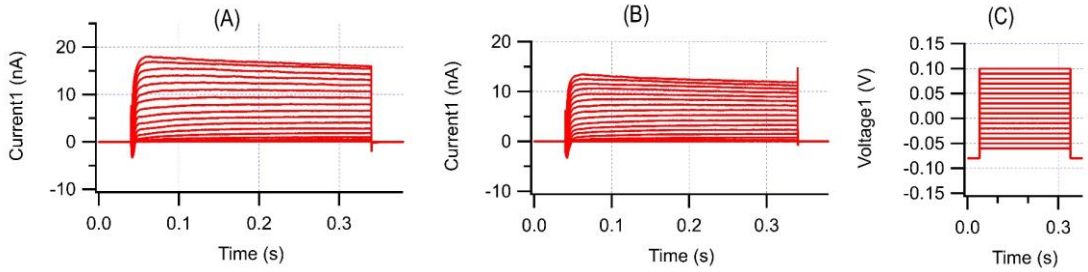

Figure 4.7. *K^+ currents densities recorded from control cell (A) after injection of incremental depolarizing voltage steps (C), and K^+ currents densities after application of 100 µM dose of rutin (B) and execution of the same voltage protocol (C).*

Control recordings of K^+ current densities, and after application of 100 µM of rutin are represented in (Figure 4.8) as mean values ± S.E.M.

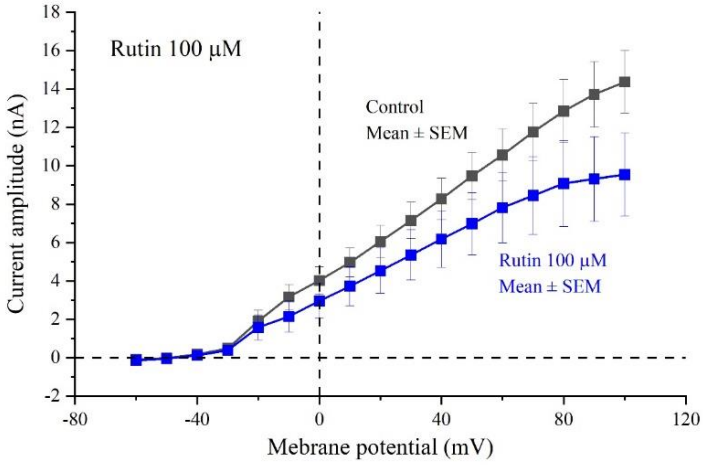

Figure 4.8. *Graphic representation of mean values ± SEM of the relation between membrane (mV) and outward K^+ current amplitudes (nA), from control cell and after application of 100 µM of rutin, with data showing 28% decrease of K^+ currents densities relatively to membrane potential, ($n = 6$; $P<0.05$).*

Conductance of K^+ channels in relation to membrane potential from control cells and after application of rutin at 100 µM dose, are shown in (Figure 4.9.), the value of potential of half activation ($V_{1/2}$) was calculated using Boltzmann equation and nonlinear curve fitting function in OriginPro.

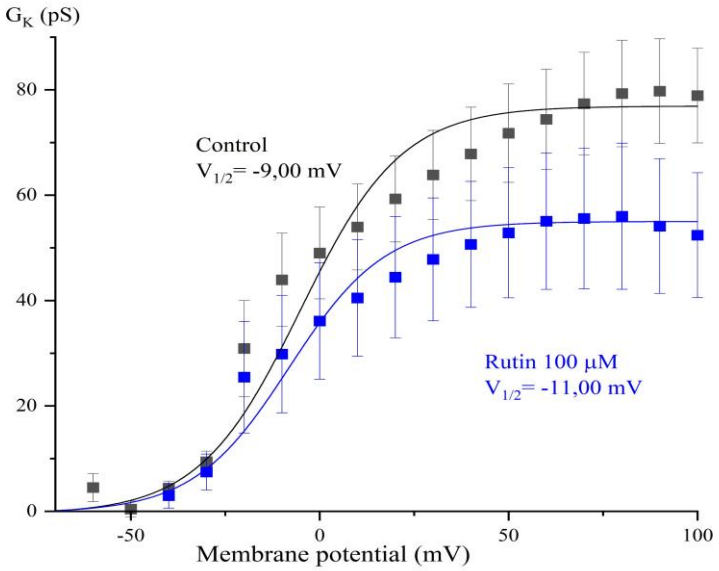

Figure 4.9. *K^+ channels conductance in relation to membrane potential and from control DRG cells and after application of 100 µM of rutin showing 30% reduction in maximum conductance (n= 6; P<0.05). and non-significant shift in the $V_{1/2}$ value (P>0.05), Data are represented as mean values ± S.E.M.*

Application of rutin at doses of 1µM, 10 µM and 100 µM induced a similar effect on the different cells tested in this study, where a resembling suppressing effect on the relative K^+ current in a dose dependent manner (Figure 4.10.).

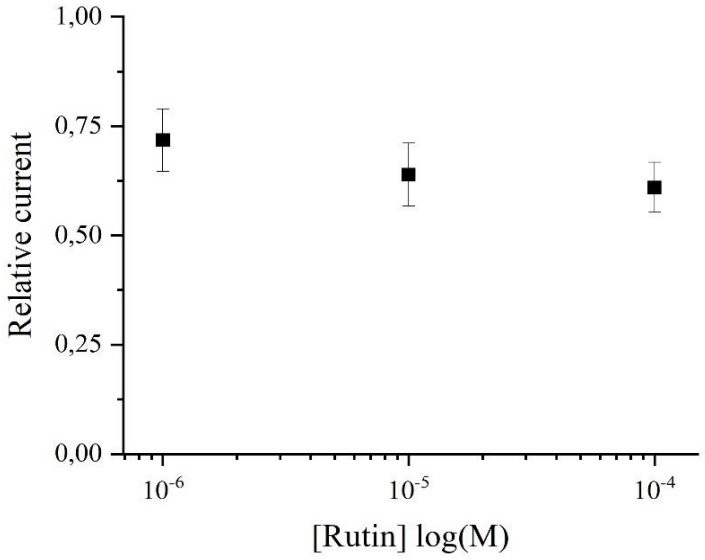

Figure 4.10. *Dose related effect of rutin on relative K^+ current showing no dose related between the 3 doses of rutin (1 µM, 10 µM, 100 µM) investigated in the study.*

4.1.2. Hesperidin

Voltage protocol used to evaluate the effect 1 µM of hesperidin on K^+ current and the observed current densities are shown in (Figure 4.11.).

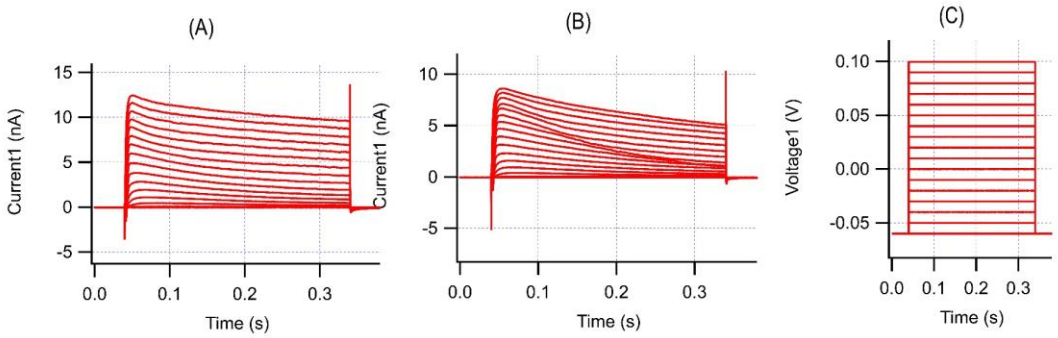

Figure 4.11. *K^+ currents densities recorded from control cell (A) after injection of incremental depolarizing voltage steps (C), and K^+ currents densities after application of 1 µM dose of hesperidin (B) and execution of the same voltage protocol (C).*

Control recordings of K^+ current densities, and after application of 1 µM of hesperidin are represented in (Figure 4.12.) as mean values ± S.E.M.

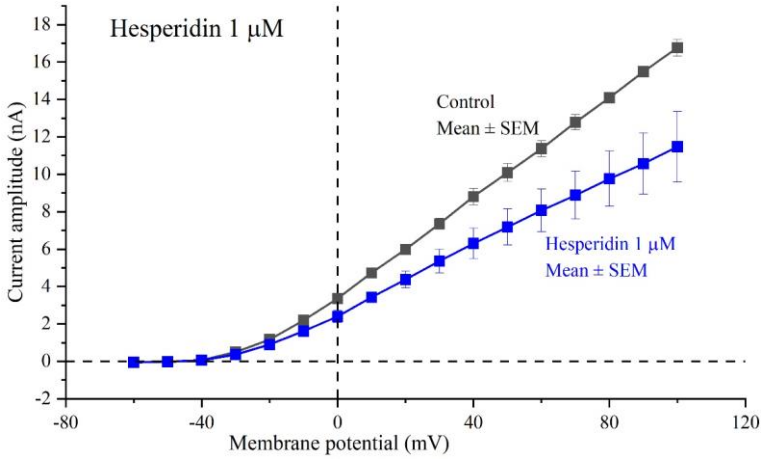

Figure 4.12. *Graphic representation of mean values ± SEM of the relation between membrane (mV) and outward K^+ current amplitudes (nA), from control cell and after application of 1µM of hesperidin, with data showing 28% decrease of K^+ currents densities relatively to membrane potential. (n= 5; P<0.05).*

Conductance of K^+ channels in relation to membrane potential from control cells and after application of hesperidin at 1 µM dose, are shown in (Figure 4.13.), the value of potential of half activation ($V_{1/2}$) was calculated using Boltzmann equation and nonlinear curve fitting function in OriginPro.

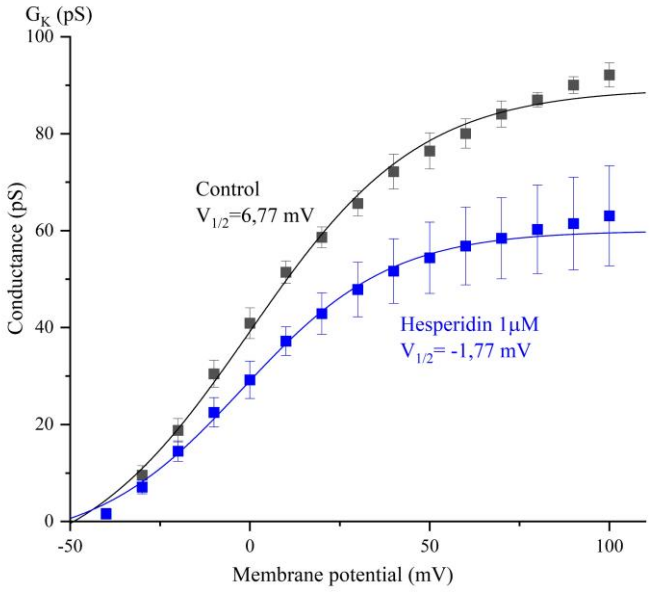

Figure 4.13. *K^+ channels conductance in relation to membrane potential and from control cells and after application of 1 µM of hesperidin showing 36% reduction in maximum conductance (n=5, P<0.05), and significant shift in the $V_{1/2}$ value (n=5; P<0.05), Data are represented as mean values ± S.E.M.*

Voltage protocol used to evaluate the effect 10 µM of hesperidin on K^+ current and the observed current densities are shown in (Figure 4.14.).

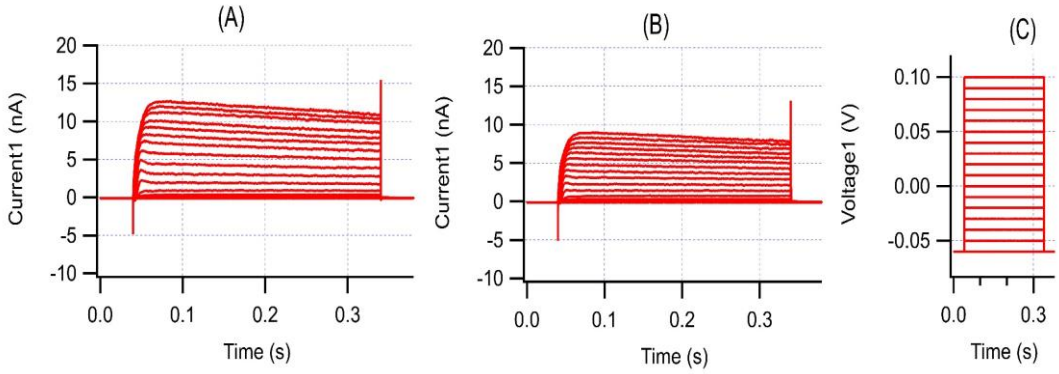

Figure 4.14. *K^+ currents densities recorded from control cell (A) after injection of incremental depolarizing voltage steps (C), and K^+ currents densities after application of 10 µM dose of hesperidin (B) and execution of the same voltage protocol (C).*

Control recordings of K^+ current densities, and after application of 10 µM of hesperidin are represented in (Figure 4.15.) as mean values ± S.E.M.

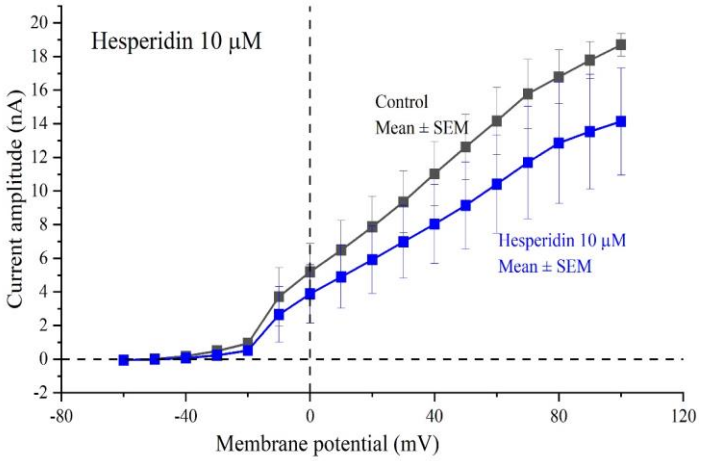

Figure 4.15. *Graphic representation of mean values ± SEM of the relation between membrane (mV) and outward K^+ current amplitudes (nA), from control cell and after application of 10 µM of hesperidin, with data showing 22% decrease of K^+ currents densities relatively to membrane potential, (n= 5; P<0.05).*

Conductance of K^+ channels in relation to membrane potential from control cells and after application of hesperidin at 10 µM dose, are shown in (Figure 4.16.), the value of potential of half activation ($V_{1/2}$) was calculated using Boltzmann equation and nonlinear curve fitting function in OriginPro.

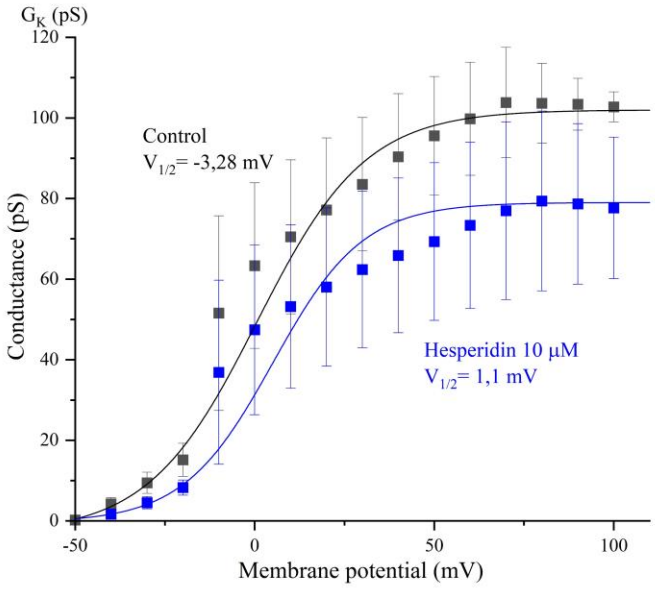

Figure 4.16. *K^+ channels conductance in relation to membrane potential and from control DRG cells and after application of 10 µM of hesperidin showing 25% reduction in maximum conductance (n= 5; P<0.05), and non-significant shift in the $V_{1/2}$ value (n= 5; P>0.05), Data are represented as mean values ± S.E.M.*

Voltage protocol used to evaluate the effect 100 µM of hesperidin on K^+ current and the observed current densities are shown in (Figure 4.17.).

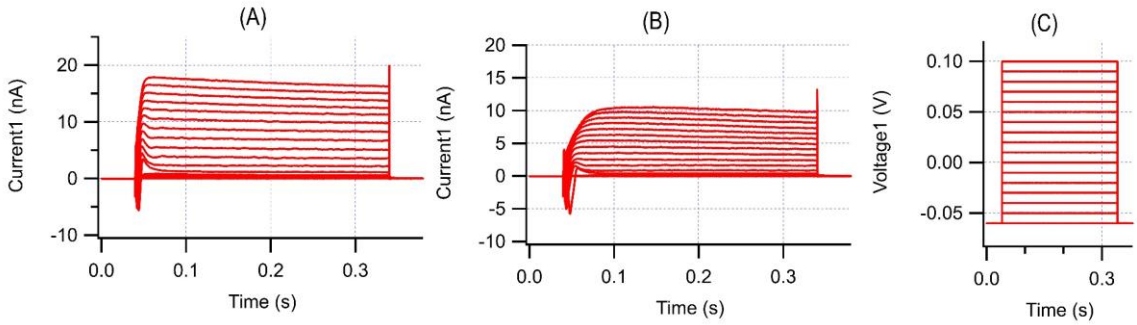

Figure 4.17. *K^+ currents densities recorded from control cell (A) after injection of incremental depolarizing voltage steps (C), and K^+ currents densities after application of 100 µM dose of hesperidin (B) and execution of the same voltage protocol (C).*

Control recordings of K^+ current densities, and after application of 10 µM of hesperidin are represented in (Figure 4.18.) as mean values ± S.E.M.

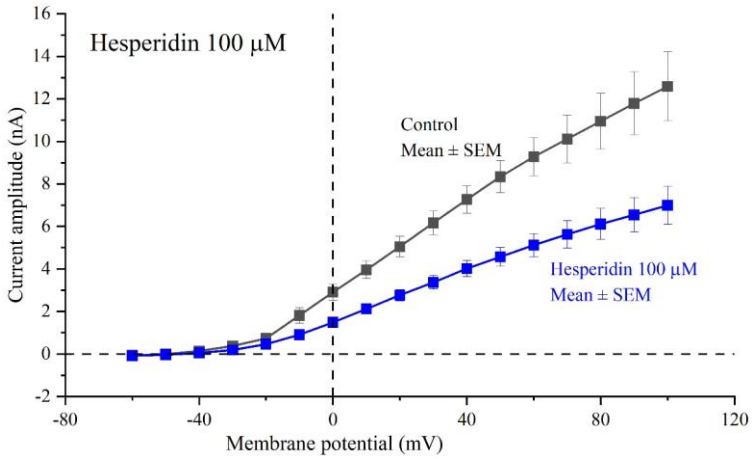

Figure 4.18. *Graphic representation of mean values ± SEM of the relation between membrane (mV) and outward K^+ current amplitudes (nA), from control cell and after application of 100 µM of hesperidin, with data showing 22% decrease of K^+ currents densities relatively to membrane potential, (n= 10; P<0.05).*

Conductance of K^+ channels in relation to membrane potential from control cells and after application of hesperidin at 10 µM dose, are shown in (Figure 4.19.), the value of potential of half activation ($V_{1/2}$) was calculated using Boltzmann equation and nonlinear curve fitting function in OriginPro.

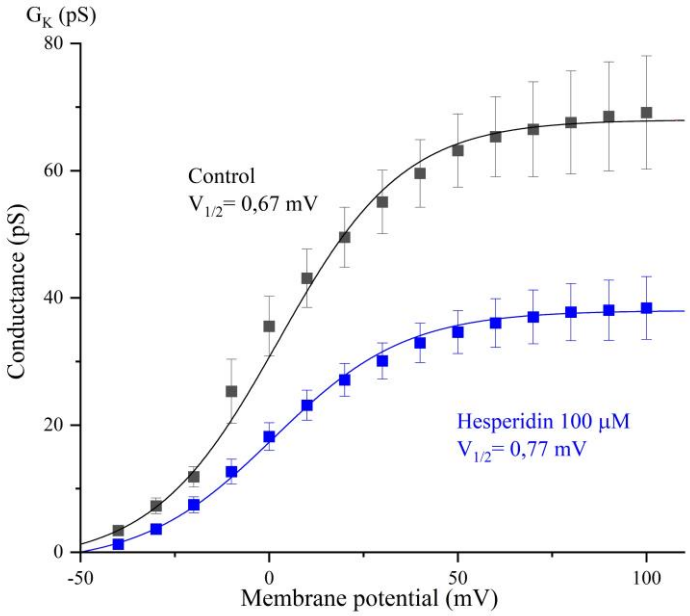

Figure 4.19. *K^+ channels conductance in relation to membrane potential and from control DRG cells and after application of 100 µM of hesperidin showing 50% reduction in maximum conductance (n= 10; P<0.05). and non-significant shift in the $V_{1/2}$ value (n= 10; P>0.05). Data are represented as mean values ± S.E.M. (n= 10; P>0.05).*

Application of hesperidin at doses of 1 µM, 10 µM and 100 µM induced a similar effect on the different cells tested in this study, where a resembling suppressing effect on the relative K current in a dose dependent manner (Figure 4.20.).

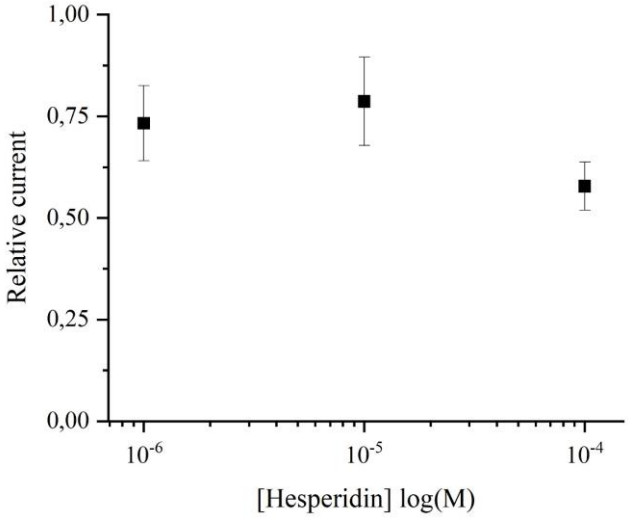

Figure 4.20. *Dose related effect of hesperidin on relative K^+ current showing no dose related effect between the 3 doses of hesperidin (1 µM, 10 µM, 100 µM) investigated in the study.*

4.1.3. CGA

Voltage protocol used to evaluate the effect 1 µM of CGA on K^+ current and the observed current densities are shown in (Figure 4.21.).

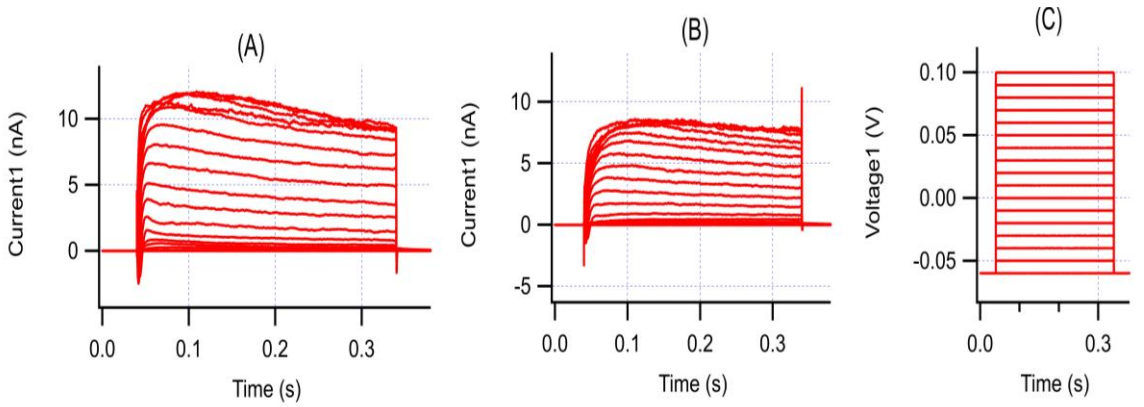

Figure 4.21. *K^+ currents densities recorded from control cell (A) after injection of incremental depolarizing voltage steps (C), and K^+ currents densities after application of 1 µM dose of CGA (B) and execution of the same voltage protocol (C).*

Control recordings of K^+ current densities, and after application of 1 µM of CGA are represented in (Figure 4.22.) as mean values ± S.E.M.

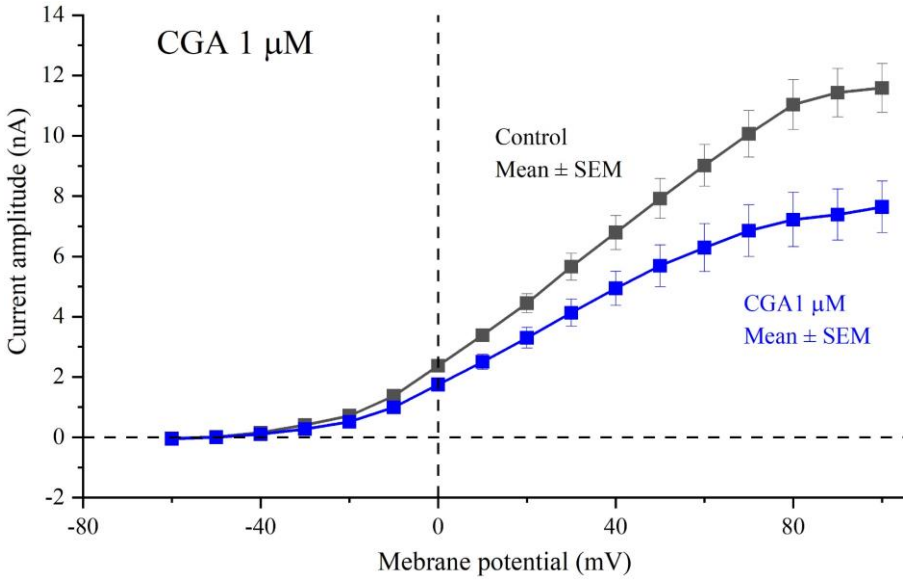

Figure 4.22. *Graphic representation of mean values ± SEM of the relation between membrane (mV) and outward K^+ current amplitudes (nA), from control cell and after application of 1 µM of CGA, with data showing 26% decrease of K^+ currents densities relatively to membrane potential. Data are represented as mean values ± S.E.M. (n= 6; P<0.05).*

Conductance of K^+ channels in relation to membrane potential from control cells and after application of CGA at 1 µM dose, are shown in (Figure 4.23.), the value of potential of half activation ($V_{1/2}$) was calculated using Boltzmann equation and nonlinear curve fitting function in OriginPro.

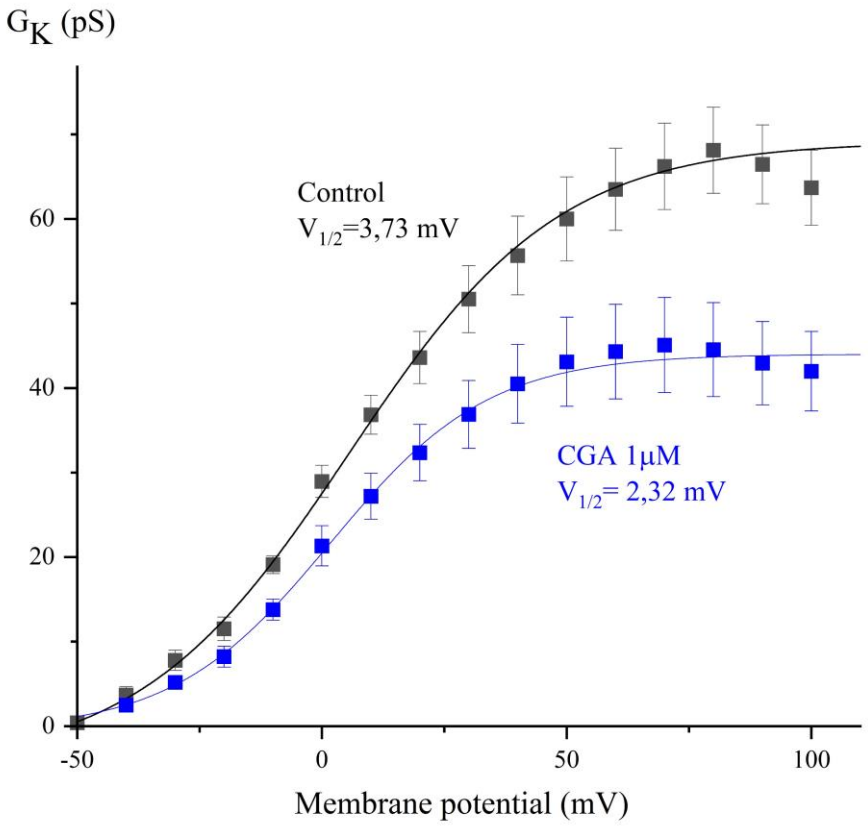

Figure 4.23. *K^+ channels conductance in relation to membrane potential and from control DRG cells and after application of 1 µM of CGA showing 30% reduction in maximum conductance (n= 6; P<0.05). and non-significant shift in the V1/2 value (n= 6; P>0.05). Data are represented as mean values ± S.E.M.*

Voltage protocol used to evaluate the effect 10 µM of CGA on K^+ current and the observed current densities are shown in (Figure 4.24.).

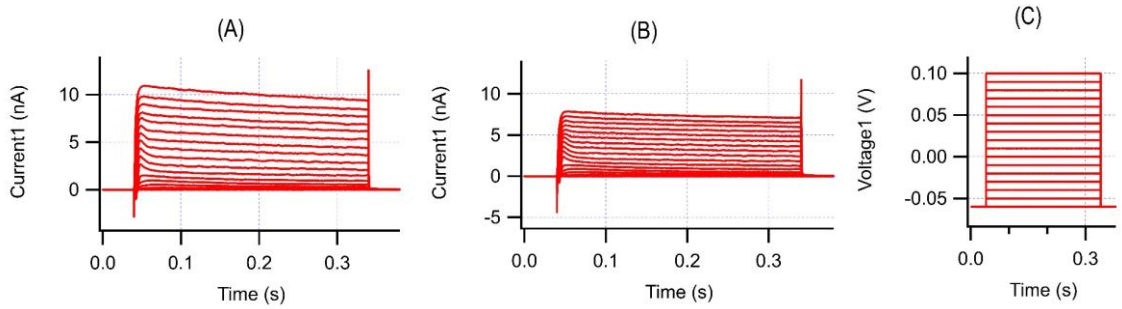

Figure 4.24. *K^+ currents densities recorded from control cell (A) after injection of incremental depolarizing voltage steps (C), and K^+ currents densities after application of 10 µM dose of CGA (B) and execution of the same voltage protocol (C).*

Control recordings of K^+ current densities, and after application of 10 µM of CGA are represented in (Figure 4.25.) as mean values ± S.E.M.

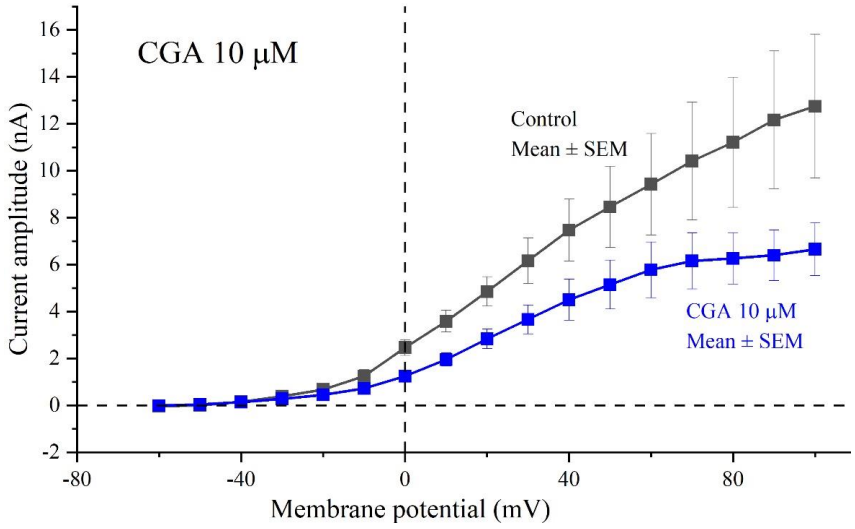

Figure 4.25. *Graphic representation of mean values ± SEM of the relation between membrane (mV) and outward K^+ current amplitudes (nA), from control cell and after application of 10 µM of CGA, with data showing 32% decrease of K^+ currents densities relatively to membrane potential, (n= 5; P<0.05).*

Conductance of K^+ channels in relation to membrane potential from control cells and after application of CGA at 10 µM dose, are shown in (Figure 4.26.), the value of potential of half activation ($V_{1/2}$) was calculated using Boltzmann equation and nonlinear curve fitting function in OriginPro.

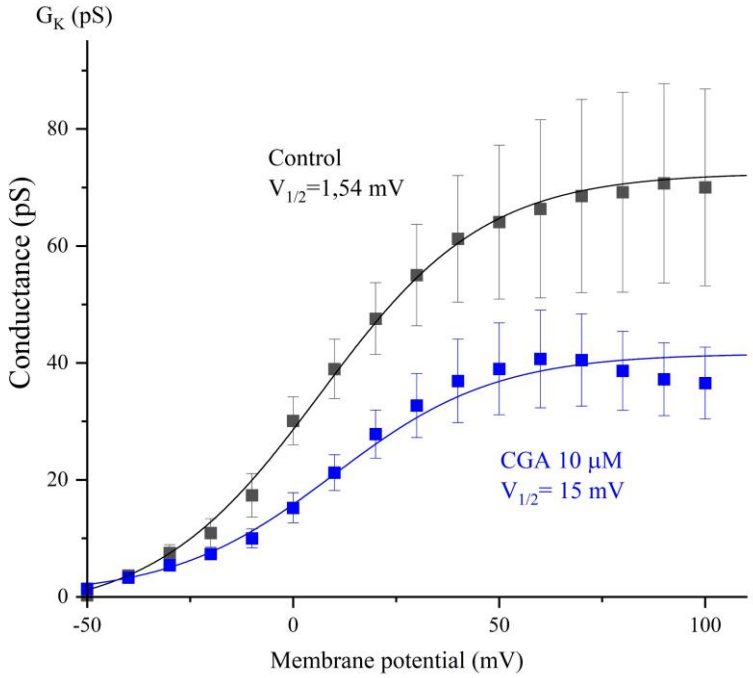

Figure 4.26. *K^+ channels conductance in relation to membrane potential and from control DRG cells and after application of 10 µM of CGA showing 25% reduction in maximum conductance (n= 5; P<0.05), and non-significant shift in the $V_{1/2}$ value (n= 5; P>0.05). Data are represented as mean values ± S.E.M.*

Voltage protocol used to evaluate the effect 100 µM of CGA on K^+ current and the observed current densities are shown in (Figure 4.27.).

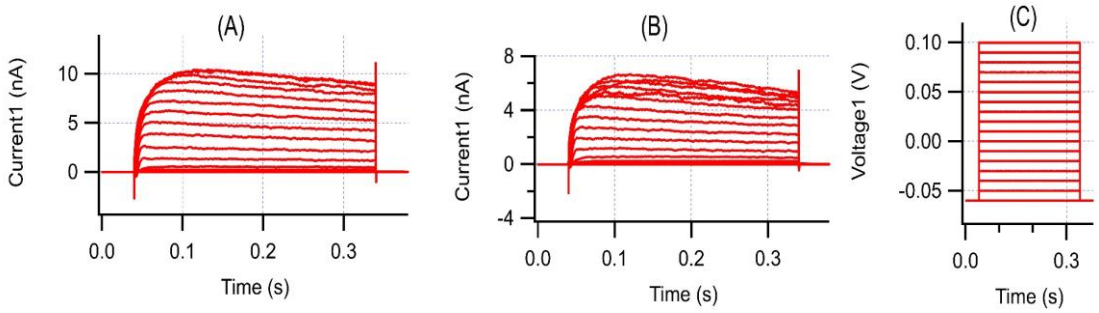

Figure 4.27. *K^+ currents densities recorded from control cell (A) after injection of incremental depolarizing voltage steps (C), and K^+ currents densities after application of 100 µM dose of CGA (B) and execution of the same voltage protocol (C).*

Control recordings of K^+ current densities, and after application of 100 µM of CGA are represented in (Figure 4.28.) as mean values ± S.E.M.

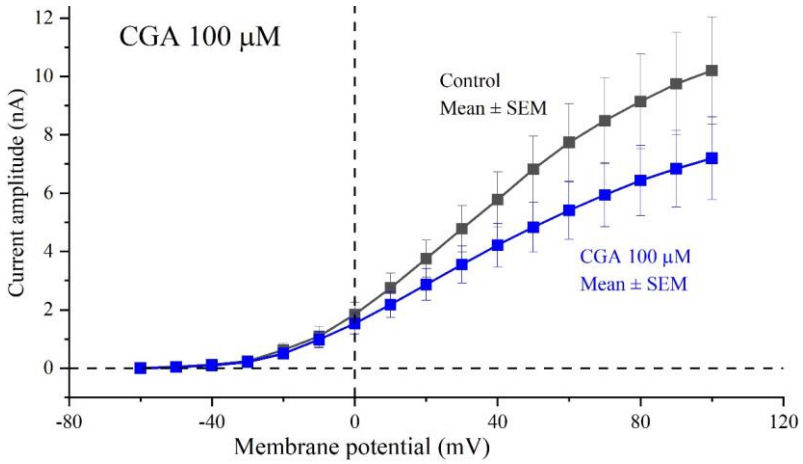

Figure 4.28. *Graphic representation of mean values ± SEM of the relation between membrane (mV) and outward K^+ current amplitudes (nA), from control cell and after application of 100 µM of CGA, with data showing 25% decrease of K^+ currents densities relatively to membrane potential, (n= 10; P<0.05).*

Conductance of K^+ channels in relation to membrane potential from control cells and after application of CGA at 100 µM dose, are shown in (Figure 4.29.), the value of potential of half activation ($V_{1/2}$) was calculated using Boltzmann equation and nonlinear curve fitting function in OriginPro.

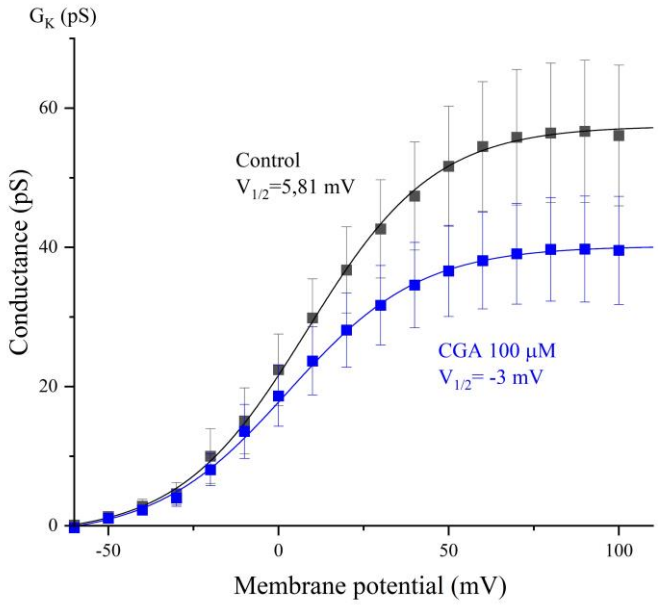

Figure 4.29. *K^+ channels conductance in relation to membrane potential and from control DRG cells and after application of 100 µM of CGA showing 33% reduction in maximum conductance (n= 10; P>0.05) and non-significant shift in the $V_{1/2}$ value (n= 10; P>0.05). Data are represented as mean values ± S.E.M.).*

Application of CGA at doses of 1 µM, 10 µM and 100 µM induced a similar effect on the different cells tested in this study, where a resembling suppressing effect on the relative K^+ current in a dose dependent manner (Figure 4.30.).

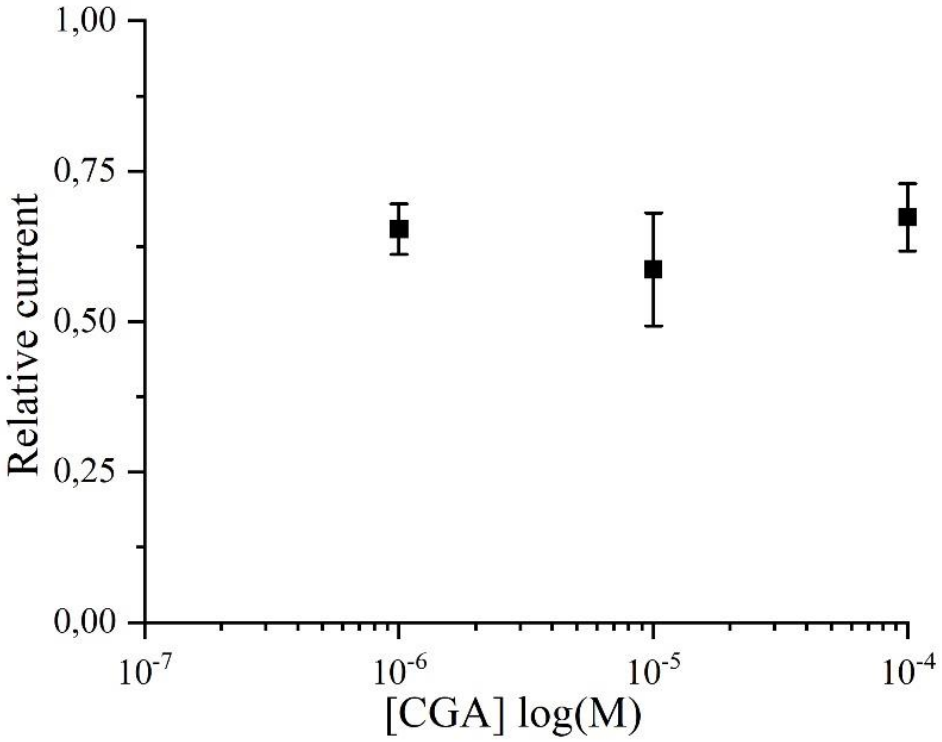

Figure 4.30. *Dose related effect of CGA on relative K^+ current showing no dose related effect between the 3 doses of CGA (1 µM, 10 µM, 100 µM) investigated in the study.*

4.2. AP Results

4.2.1. Rutin

APs were elicited by injecting the minimal depolarizing currents that induce AP firing.

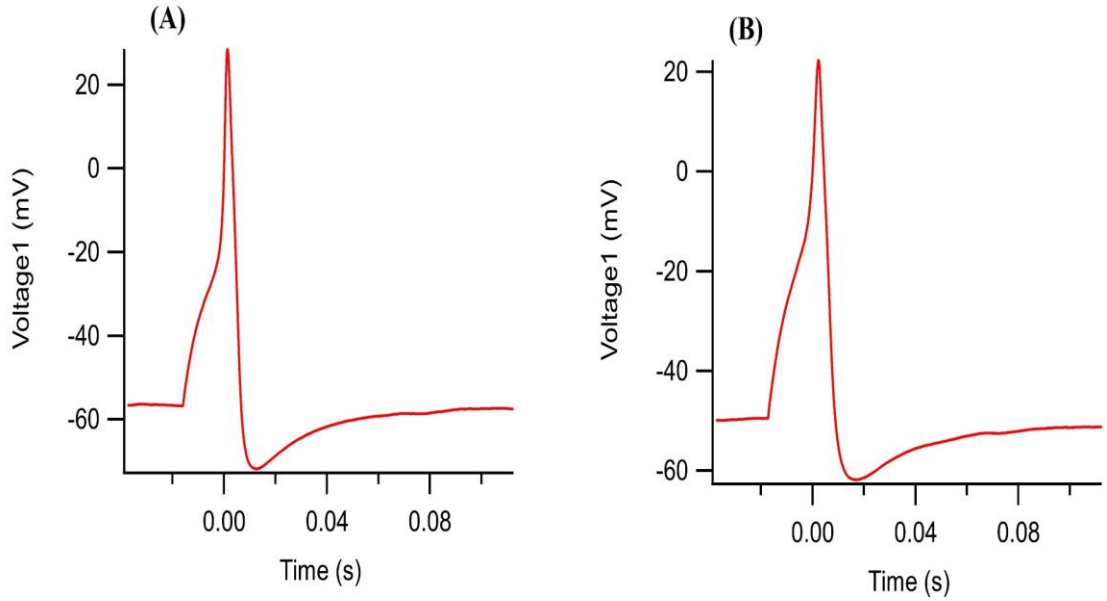

Figure 4.31. *Control recording of elicited AP before (A) and after application of rutin at 1 µM dose (B).*

Analysis results of control APs before application of 1 µM rutin are represented in (Table 4.1.).

Table 4.1. *AP parameters measured from DRG cells before application of 1 µM of rutin.*

	Threshold (mV)	Peak (mV)	AP Duration (ms) at 90%	AHP (mV)
Cell 01	-56.472	28.543	19.957	-71.649
Cell 02	-48.333	53.372	17.311	-64.849
Cell 03	-61.843	25.500	13.413	-78.268
Cell 04	-33.642	20.867	17.875	-52.734
Cell 05	-47.165	-45.871	14.423	-59.805

Analysis results of APs after application of 1 µM rutin are represented in (Table 4.2.)

Table 4.2. *AP parameters measured from DRG cells after application of 1 µM of rutin and statistical analysis of the variation observed significant effect on threshold of AP firing (P<0.05) and very significant effect on after hyperpolarization potential (P<0.05) and non-significant effect on the other parameters.*

	Threshold (mV)	Peak (mV)	AP Duration (ms) at 90%	AHP (mV)
Cell 01	-49.432	22.369	23.472	-61.456
Cell 02	-41.949	55.273	15.089	-62.478
Cell 03	-60.198	-17.077	26.054	-68.234
Cell 04	-30.581	20.263	19.096	-45.880
Cell 05	-46.168	-43.556	15.265	-52.492
P value	0.0358	0.349	0.2749	0.0066
Significance	S	NS	NS	Very S
Normality test	Passed	Passed	Passed	Passed

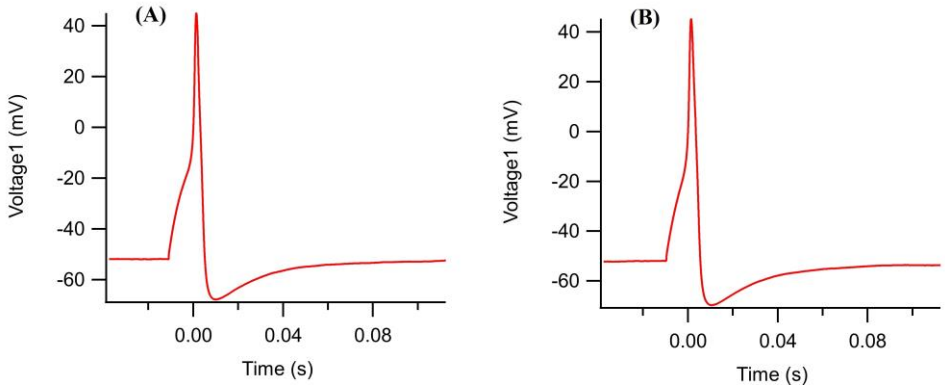

Figure 4.32. *Control recording of elicited AP before (A) and after application of rutin at 10 µM dose (B).*

Analysis results of control APs before application of 10 µM rutin are represented in (Table 4.3.).

Table 4.3. *AP parameters measured from DRG cells before application of 10 µM of rutin.*

	Threshold (mV)	Peak (mV)	AP Duration (ms) at 90%	AHP (mV)
Cell 01	-46.029	-44.766	14.076	-58.364
Cell 02	-36.422	10.540	13.119	-43.040
Cell 03	-52.148	20.736	8.463	-60.504
Cell 04	-56.549	25.787	11.565	-63.710
Cell 05	-43.115	30.499	20.989	-57.247
Cell 06	-51.596	45.037	14.185	-67.712

Analysis results of APs after application of 10 µM rutin are represented in (Table 4.4.).

Table 4.4. *AP parameters measured from DRG cells after application of 10 µM of rutin and statistical analysis of the variation observed showing non quite significant effect on threshold of AP firing (P=0.052) and non-quite significant effect on after hyperpolarization potential (P<0.05) with non-significant effect on the other parameters.*

	Threshold (mV)	**Peak (mV)**	**AP Duration (ms) at 90%**	**AHP (mV)**
Cell 01	-45.269	-42.709	14.967	-51.470
Cell 02	-34.106	10.284	15.072	-38.836
Cell 03	-49.716	10.232	10.559	-54.544
Cell 04	-53.222	24.935	10.666	-63.455
Cell 05	-35.537	23.065	17.123	-47.183
Cell 06	-51.675	45.2973	13.214	-69.595
Normality Test	Passed	Passed	Passed	Passed
P value	P=0.052	P=0.228	P=0.891	P=0.064
Significance	NQS	NS	NS	NQS

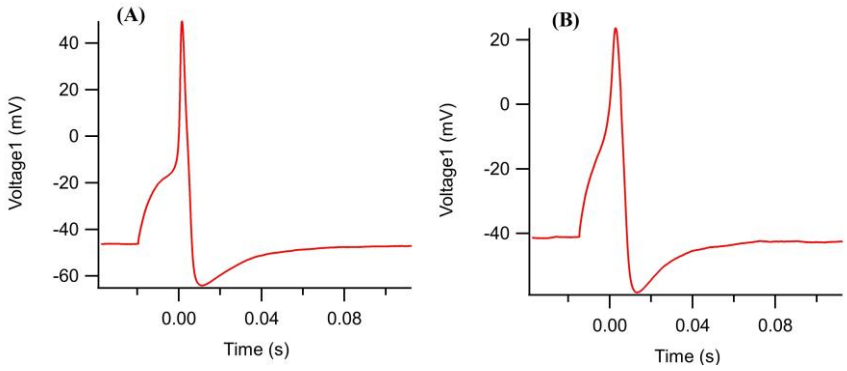

Figure 4.33. *Control recording of elicited AP before (A) and after application of 100 µM of rutin (B).*

Analysis results of control APs before application of 100 µM rutin are represented in (Table 4.5.).

Table 4.5. *AP parameters measured from DRG cells before application of 100 µM of rutin*

	Threshold (mV)	**Peak (mV)**	**AP Duration (ms) at 90%**	**AHP (mV)**
Cell 01	-45.947	49.453	23.423	-64.065
Cell 02	-56.518	49.530	14.433	-75.180
Cell 03	-65.017	37.423	12.540	-75.894
Cell 04	-48.147	48.721	17.308	-65.908
Cell 05	-55.498	26.359	11.928	-63.618

Analysis results of APs after application of 100 µM rutin are represented in (Table 4.6.).

Table 4.6. *AP parameters measured from DRG cells After application of 100 µM of rutin and statistical analysis of the variation observed showing non-significant effect on the measured AP parameters.*

	Threshold (mV)	**Peak (mV)**	**AP Duration (ms) at 90%**	**AHP (mV)**
Cell 01	-41.064	23.626	21.423	-58.255
Cell 02	-72.567	45.953	11.459	-73.193
Cell 03	-16.210	40.927	5.946	-68.267
Cell 04	-32.818	25.653	16.251	-49.746
Cell 05	-54.125	24.995	10.786	-64.007
Normality Test	Passed	Passed	Passed	Passed
P value	0.3691	0.1686	0.0542	0.0939
Significance	NS	NS	NQS	NQS

4.2.2. Hesperidin

APs were elicited by injecting the minimal depolarizing currents that induce AP firing.

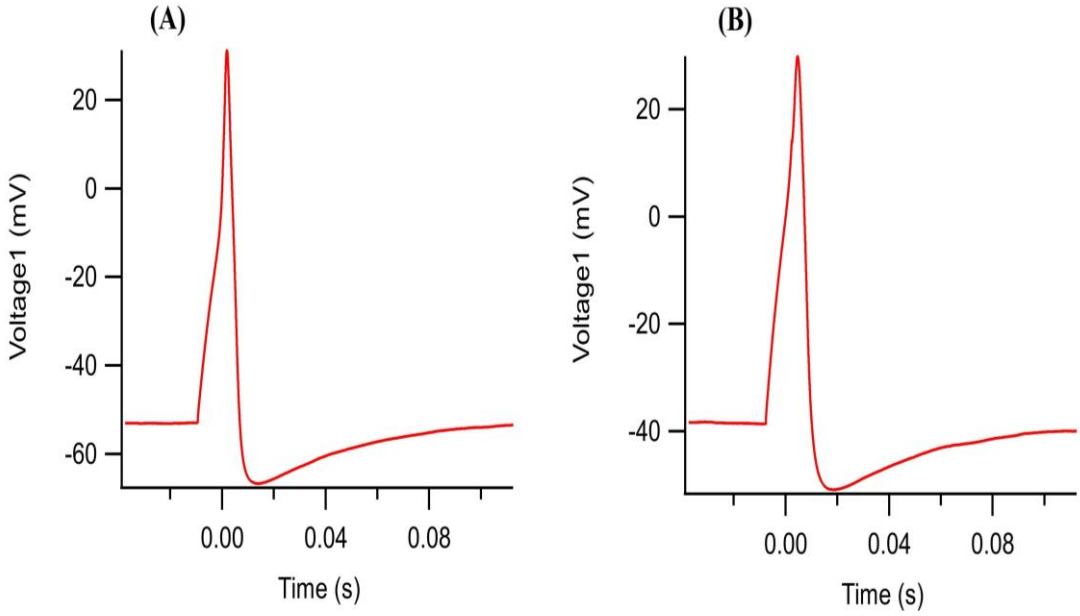

Figure 4.34. *Control recording of elicited before (A) and after application 1 µM of hesperidin (B).*

Analysis results of control APs before application of 1 µM hesperidin are represented in (Table 4.7.).

Table 4.7. *AP parameters measured from DRG cells before application of 1 µM of hesperidin*

	Threshold (mV)	**Peak (mV)**	**AP Duration (ms) at 90%**	**AHP (mV)**
Cell 01	-52.728	31.246	14.373	-66.229
Cell 02	-39.074	50.201	14.358	-51.593
Cell 03	-29.217	62.112	15.818	-47.351
Cell 04	-40.015	51.051	13.954	-52.751
Cell 05	-43.048	48.081	15.031	-52.178

Analysis results of APs after application of 1 µM hesperidin are represented in (Table 4.8.).

Table 4.8. *AP parameters measured from DRG cells after application of 1 µM of hesperidin and statistical analysis of the variation observed showing non-significant effect on the measured AP parameters.*

	Threshold (mV)	**Peak (mV)**	**AP Duration (ms) at 90%**	**AHP (mV)**
Cell 01	-38.537	14.175	16.404	-50.570
Cell 02	-37.838	54.235	12.862	-52.105
Cell 03	-27.795	14.544	22.304	-45.114
Cell 04	-38.014	55.884	12.116	-53.165
Cell 05	-32.846	18.544	13.921	-46.370
Normality Test	Passed	Passed	Passed	Passed
P value	0.0965	0.146	0.632	0.2041
Significance	NS	NS	NS	NS

Analysis results of control APs before application of 10 µM hesperidin are represented in (Table 4.9.).

Table 4.9. *AP parameters measured from DRG cells before application of 10 µM of hesperidin.*

	Threshold (mV)	**Peak (mV)**	**AP Duration (ms) at 90%**	**AHP (mV)**
Cell 01	-42.291	38.580	15.974	-54.354
Cell 02	-5.593	49.057	3.239	-71.176
Cell 03	-48.498	45.373	18.996	-64.346
Cell 04	-4.330	48.376	6.578	-65.661
Cell 05	-4.598	51.876	7.844	-61.716

Analysis results of APs after application of 10 µM hesperidin are represented in Table (4.10.).

Table 4.10. *AP parameters measured from DRG cells after application of 10 µM of hesperidin and statistical analysis of the variation observed showing non-significant effect on the measured AP parameters.*

	Threshold (mV)	**Peak (mV)**	**AP Duration (ms) at 90%**	**AHP (mV)**
Cell 01	-41.122	-38.360	15.825	-51.141
Cell 02	-56.307	52.526	14.573	-71.917
Cell 03	-43.295	48.736	17.379	-56.784
Cell 04	-2.056	50.408	6.732	-60.748
Cell 05	-3.001	49.910	7.016	-62.898
Normality Test	Passed	Passed	Passed	Passed
P value	0.496	0.239	0.501	0.174
Significance	NS	NS	NS	NS

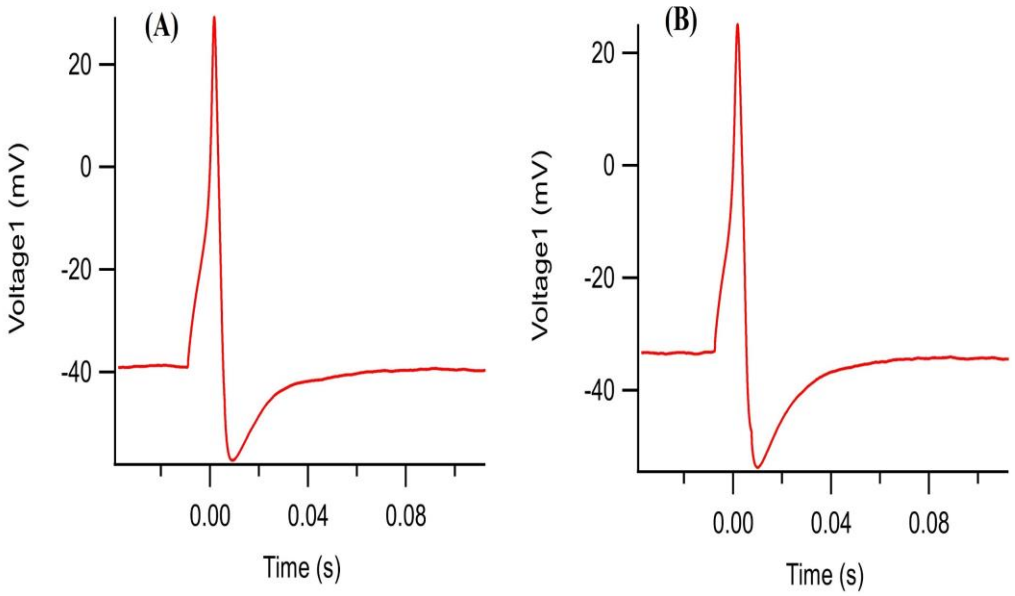

Figure 4.35. *Control recording of elicited AP before (A) and after application of hesperidin at 100 µM dose (B).*

Analysis results of control APs before application of 100 µM hesperidin are represented in (Table 4.11.).

Table 4.11. *AP parameters measured from DRG cells before application of 100 µM of hesperidin.*

	Threshold (mV)	**Peak (mV)**	**AP Duration (ms) at 90%**	**AHP (mV)**
Cell 01	-41.589	14.700	11.378	-52.951
Cell 02	-38.858	29.293	12.700	-57.159
Cell 03	-53.091	18.289	24.782	-61.257
Cell 04	-55.108	45.281	11.774	-67.883
Cell 05	-47.036	44.005	18.423	-62.406

Analysis results of APs after application of 100 µM hesperidin are represented in (Table 4.12.).

Table 4.12. *AP parameters measured from DRG cells after application of 100 µM of hesperidin and statistical analysis of the variation observed showing a very significant effect on threshold of AP firing (P<0.01) and a significant effect on after hyperpolarization potential (P<0.05) and non-significant effect on the other parameters.*

	Threshold (mV)	**Peak (mV)**	**AP Duration (ms) at 90%**	**AHP (mV)**
Cell 01	-40.291	14.241	11.023	-51.298
Cell 02	-32.980	25.131	11.625	-53.683
Cell 03	-45.666	13.281	30.813	-55.712
Cell 04	-47.216	48.941	14.145	-57.464
Cell 05	-41.99	47.267	16.855	-55.072
Normality Test	Passed	Passed	Passed	Passed
P value	0.0093	0.7791	0.4867	0.0202
Significance	VS	Ns	Ns	S

4.2.3. CGA

APs were elicited by injecting the minimal depolarizing currents that induce AP firing.

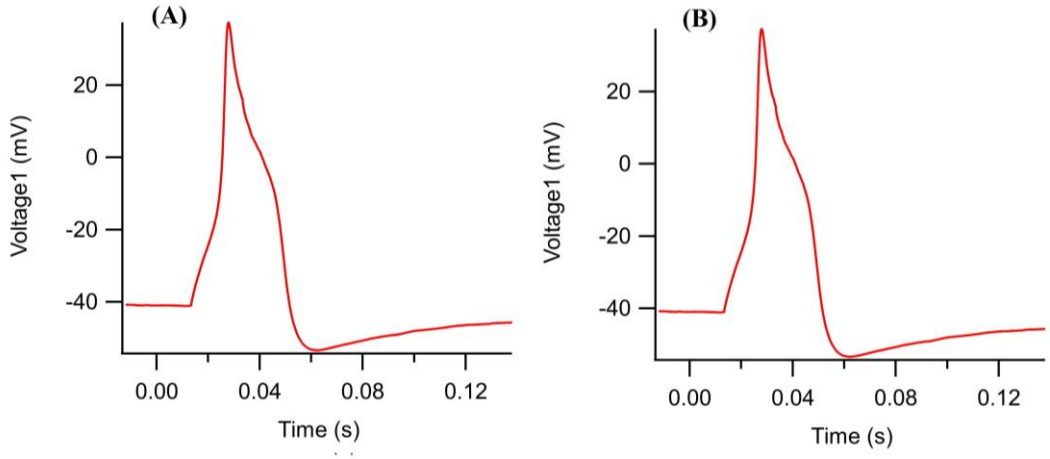

Figure 4.36. *Control recording of elicited AP before (A) and after application of CGA at 1 µM dose (B).*

Analysis results of control APs before application of 1 µM CGA are represented in (Table 4.13.).

Table 4.13. *AP parameters measured from DRG cells before application of 1 µM of CGA*

	Threshold (mV)	**Peak (mV)**	**AP Duration (ms) at 90%**	**AHP (mV)**
Cell 01	-43.664	33.978	23.341	-58.233
Cell 02	-44.589	43.948	13.368	-55.917
Cell 03	-40.563	36.495	18.980	-61.212
Cell 04	-50.509	35.382	18.465	-66.519
Cell 05	-58.520	18.008	18.391	-67.788

Analysis results of APs after application of 1 µM CGA are represented in (Table 4.14.).

Table 4.14. *AP parameters measured from DRG cells after application of 1 µM of CGA and statistical analysis of the variation observed showing a significant effect on threshold of AP firing (P<0.05) and on the afterhyperpolarization potential (P<0.05) and non-significant effect on the other parameters.*

	Threshold (mV)	**Peak (mV)**	**AP Duration (ms) at 90%**	**AHP (mV)**
Cell 01	-40.811	37.356	34.055	-52.996
Cell 02	-44.433	46.871	14.845	-55.422
Cell 03	-39.340	20.098	23.644	-56.246
Cell 04	-46.722	29.168	18.382	-62.692
Cell 05	-54.983	34.280	15.228	-61.636
Normality Test	Passed	Passed	Passed	Passed
P value	0.0299	0.9990	0.3136	0.0136
Significance	S	NS	NS	S

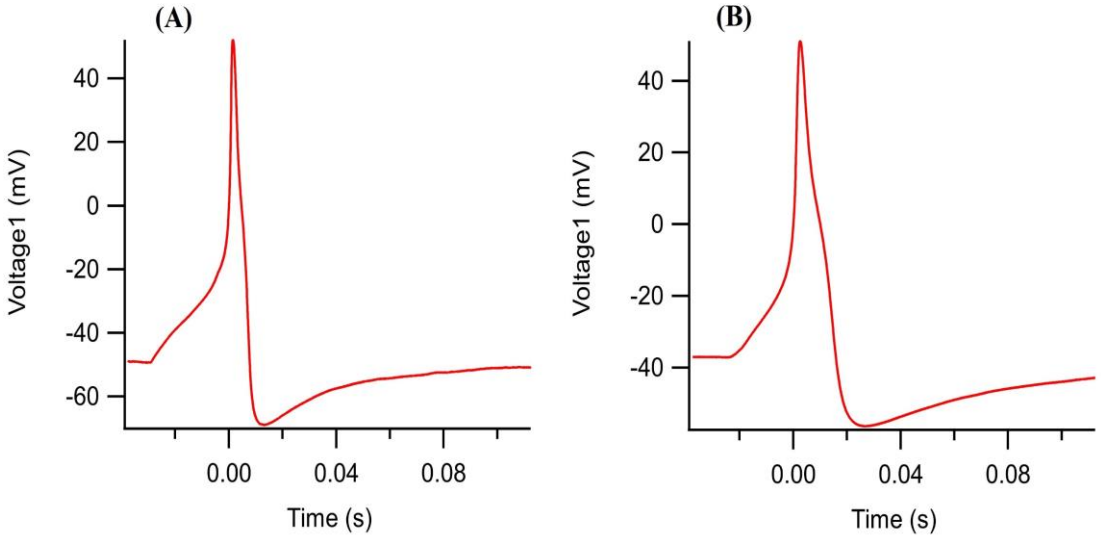

Figure 4.37. *Control recording of elicited AP before (A) and after application of CGA at 10 µM dose (B*

Analysis results of control APs before application of 10 µM CGA are represented in (Table 4.15.).

Table 4.15. *AP parameters measured from DRG cells before application of 10 µM of CGA*

	Threshold (mV)	**Peak (mV)**	**AP Duration (ms) at 90%**	**AHP (mV)**
Cell 01	-46.130	-45.269	23.255	-54.702
Cell 02	-8.609	52.130	5.045	-67.984
Cell 03	-47.860	23.770	20.117	-61.541
Cell 04	-56.811	21.264	10.962	-69.058

Analysis results of APs after application of 10 µM CGA are represented in (Table 4.16.).

Table 4.16. *AP parameters measured from DRG cells after application of 10 µM of CGA and statistical analysis of the variation observed showing non-significant effect on the measured AP parameters.*

	Threshold (mV)	**Peak (mV)**	**AP Duration (ms) at 90%**	**AHP (mV)**
Cell 01	-43.765	-42.654	31.171	-45.599
Cell 02	-36.709	-36.553	0.066	-46.691
Cell 03	-47.515	22.250	23.077	-57.934
Cell 04	-57.733	21.948	12.740	-67.016
Normality Test	Not performed	Not performed	Not performed	Not performed
P value	0.4286	0.4024	0.5223	0.1309
Significance	NS	NS	NS	NS

Analysis results of control APs before application of 100 µM CGA are represented in (Table 4.17.).

Table 4.17. *AP parameters measured from DRG cells before application of 100 µM of CGA.*

	Threshold (mV)	**Peak (mV)**	**AP Duration (ms) at 90%**	**AHP (mV)**
Cell 01	-20.043	23.925	6.637	-56.979
Cell 02	-63.558	30.865	21.245	-76.971
Cell 03	-46.838	17.764	17.994	-54.824

Analysis results of APs after application of 100 µM CGA are represented in (Table 4.18.).

Table 4.18. *AP parameters measured from DRG cells after application of 100 µM of CGA and statistical analysis of the variation observed showing non-significant effect on the measured AP parameters.*

	Threshold (mV)	**Peak (mV)**	**AP Duration (ms) at 90%**	**AHP (mV)**
Cell 01	-21.640	17.761	7.630	-57.046
Cell 02	-61.618	37.973	17.960	-75.384
Cell 03	-45.248	3.6132	20.820	-52.740
Normality Test	Not performed	Not performed	Not performed	Not performed
P value	0.6243	0.5513	0.5223	0.2060
Significance	NS	NS	NS	NS

5. GENERAL DISCUSSION, CONCLUSIONS, RECOMMENDATIONS

5.1. General Discussion

Pain management with herbal-based remedies is an area of interest and a health practice today. Comprehension of the mechanisms in which plant components studied in the scope of this thesis (rutin, hesperidin, and CGA) affect DRG cells will provide insight into the impact of these components on pain, which will be critical in their possible implementation in pain related therapeutic approaches.

DRG neurons contain nociceptors, which generate pain perception and are activated by ion channels. These ganglia are thought to be the new clinical targets of neuropathic pain [22]. Anti-hyperalgesic effects of CGA [9, 10], its anti-inflammatory, antipyretic and analgesic effects [11, 12], the antihyperalgesic effects of hesperidin on neuropathic pain [14], its anti-inflammatory and analgesic effects [15] and the amendatory effects of rutin in improvement of peripheral neuropathy [20] have been brought to the literature.

In the context of this work, it has been demonstrated that the polyphenolic compounds studied have different effects on the electrophysiological properties of primary cell culture of acutely dissociated rat DRG. These effects occur possibly via alterations of conductance of K^+ channels. This alteration might be related to a change in the probability of channel being in the open state or a modification of the number of activated channels present in the cell membrane [168] .

Within the confines of this thesis, in terms of we have found K^+ currents; rutin induced a reduction of about 25% in K^+ current densities and the K^+ channels conductance in a non-dose dependent manner (approximately the same effect was found with the 3 used doses), no significant effect on the $V_{1/2}$ with rutin also was recorded.

Hesperidin showed a dose non-related effect among the 3 doses used (1 µM, 10 µM and 100 µM) on K^+ current densities, which was found to be around reduction of 25%. On the other hand, a dose of 1 µM hesperidin induced a 36% reduction in maximum conductance of K^+ channels and significant shift to the left (towards hyperpolarization) of the $V_{1/2}$ value. Maximum conductance was reduced by 25% with 10 µM and 50% with 100 µM of hesperidin with no effect of both doses on $V_{1/2}$.

CGA also induced a dose non-related effect among the 3 used doses (1 µM, 10 µM and 100 µM) on K^+ current densities which was found to be around reduction of 30%.

Maximum conductance was reduced by the 3 doses in a dose independent manner to around 30% and no significant changes on $V_{1/2}$ were recorded.

These results introducing the suppressive effects of the test chemicals on K^+ channel conductance show that chemicals tested in this study do not affect voltage dependence in the studied channels but reduce the conductance. This reduction might be originated from a reduction in the number of active channels, or from a modification in the open state probability or from the amplitude of signal of the channel. In the scope of these findings, future analysis of the effect observed with these chemicals at the single channel level will provide more detailed and in-depth information about the observed effects.

In terms of AP, it has been found that application of rutin at 10 µM and 100 µM showed no significant effects on parameters measured. On the other hand, at a dose of 1 µM, rutin induced a significant effect on AP firing threshold ($P<0.05$) by shifting the threshold towards more depolarized potentials, and a very significant effect on after-hyperpolarization potential ($P<0.05$) by shifting the potential towards more depolarized values, with non-significant effect on the other parameters measured.

Hesperidin at doses of 1 µM and 10 µM showed no significant effects on AP related parameters measured. Even so, at a dose of 100 µM of hesperidin indicated a significant effect on threshold of AP firing ($P<0.05$) by shifting the threshold towards more depolarized potentials, and a significant effect on after hyperpolarization potential ($P<0.05$) by shifting the potential towards more depolarized values with non-significant effect on the other parameters measured.

CGA also, at 10 µM and 100 µM doses, induced no significant effect on parameters measured. But, similar to rutin, at a dose of 1 µM, CGA showed a significant effect on threshold of AP firing ($P<0.05$) by shifting the threshold towards a more depolarized potentials, and a significant effect on after hyperpolarization potential ($P<0.05$) by shifting the potential towards more depolarized values with non-significant effect on the other measured parameters.

The membrane potential at half activation or inactivation is represented by the $V_{1/2}$ value [191]. This value is related to the potential at which half of the maximal K^+ current is reached. So, when the value of $V_{1/2}$ is shifted towards more hyperpolarized potentials, it means that the cell is more prone to generate an AP, and eventually pain signaling, and vice versa. In the experiments conducted within this thesis, only one test chemical at one dosage induced a statistically significant change concerning this parameter; 1 µM

hesperidin, indicating a significant shift towards hyperpolarization, introducing another clue for its antihyperalgesic effects.

Results in the present study have showed that 1 µM hesperidin induced a major change to the left in the activation and inactivation thresholds of K_v, as well as an increased excitability, causing an inward current or membrane depolarization [191]. Other dosages of hesperidin and other substances studied, however, have no statistically significant effects on the k values of K_v, and $V_{1/2}$. As a result, we can't draw any conclusions about the speed of activation or inactivation based on these findings, and the inconsistencies in patch-clamp recordings may be due to various mechanisms & factors, such as individual differences of the experimental animals or the date the solutions were prepared, even the glass pipettes themselves, and the loss of the voltage clamp during the recording performance.

K_v channels are one of the various voltage-gated ion channels controlling neuronal excitability and frequency of APs [191]. Two types of K^+ currents with different properties and effects on neurons these currents are the A-current ($I_{K,A}$) which inactivates rapidly and the sustained K-current ($I_{K,v}$), the prevailing K^+ current being the A current or $I_{K,A}$ which constitutes the major outward current during the beginning stages of AP repolarization, controlling by that neurons repolarization AP frequency [191].

Studies on treatment of hyperalgesia and allodynia have proven that targeting K_v by substances that decrease peak current densities these channel produced an analgesic effect [192] , the chemicals testes in the scope of this thesis showed a similar effect on the Type A K^+ current where and average inhibition of 26% of the current densities was by the 3 chemicals in a dose independent manner with maximum inhibition found with 100 µM of rutin, which suggests a possible inhibitor effect on neuron excitability and indirectly a possibility of analgesia induction. The similarity of effect might be due to the similar chemical structure of the chemicals as all 3 belongs to the same family of flavones with a polyphenolic structure.

The return of membrane to resting membrane potential happens in the after-hyperpolarization phase where K^+ channels are closed and Na^+ ions enter the cells, so it plays an important role in the modulation of AP firing [193], shifting the AHP towards a less negative potential, which have shown to decrease consecutive AP firing probability and the frequency of fired APs. These effects were related to decrease of pain signals [193]. Among the studied chemicals, the most obvious effect observed with rutin,

hesperidin, and GCA on AP was a shift of threshold of AP firing and the after-hyperpolarization potential (AHP) towards less negative potentials or more depolarized values, an effect observed 1 µM with rutin, 1 µM of CGA and 100 µM of hesperidin. These findings suggest a possible beneficial effect of these plant components on peripheral painful signaling.

The shifting of threshold of AP firing towards less negative values increases the magnitude of the stimuli required for eliciting AP firing [194] which was related to improvement of painful sensation in allodynia where the opposite happens (neurons firing at more negative potential) [195]. The observed effect of the test chemicals in this thesis on threshold of AP firing suggests a possible effect of diminution AP possibility of firing and firing frequency which may be beneficial in painful signals reduction.

5.2. Conclusions

From the investigation of the effects of rutin, hesperidin and CGA on analgesia related neuronal electrophysiological parameters on primary cultured DRG cells within the scope of this master thesis it has been concluded that these chemicals at physiological doses might reduce the probability of AP firing by affecting the threshold of AP firing and after-hyperpolarization potentials, this effects might be related to the observed reduction of type A K^+ current densities and maximum conductance of K^+ found in this study, these results suggest a possible beneficial effect of these plant components on neuronal excitability and a possibility of analgesia induction. Nevertheless, the mechanisms by which these chemicals affect the channels could not be investigated and future examination of the activity of these chemicals at single channel level is required for more exhaustive understanding of the observed effects.

5.3. Recommendations

The phytochemicals tested in this thesis provided significant *in vitro* results that will attract scientists doing research in the pain management to focus on these and similar chemicals. In addition to the electrophysiological parameters investigated in this study, in consideration of the significant results obtained in this work, other pain-related channels such as Na^+, Ca^{2+} or HCN, should be studied later on. Also, future studies at the single channel level, investigating the mechanisms of action of the test chemicals tested withing the scope of this thesis, would be of a great benefit in understanding the observed

effects and assessing the possibility of use of these substances as a supplement in the management and treatment of pain.

REFERENCES

[1] Ganeshpurkar, A. and Saluja, A.K. (2017). The Pharmacological Potential of Rutin. *Saudi Pharm. J.*, 25 (2), 149–164.

[2] Zanwar, A.A., Badole, S.L., Shende, P.S., Hegde, M. V., and Bodhankar, S.L. (2013). Cardiovascular Effects of Hesperidin: A Flavanone Glycoside. in: Polyphenols Hum. Heal. Dis. (p. 989–992). Elsevier Inc.

[3] Naveed, M., Hejazi, V., Abbas, M., Kamboh, A.A., Khan, G.J., Shumzaid, M., Ahmad, F., Babazadeh, D., FangFang, X., Modarresi-Ghazani, F., WenHua, L., and XiaoHui, Z. (2018). Chlorogenic acid (CGA): A pharmacological review and call for further research. *Biomed. Pharmacother.*, 97 (2), 67–74.

[4] Raja, S.N., Carr, D.B., Cohen, M., Finnerup, N.B., Flor, H., Gibson, S., Keefe, F.J., Mogil, J.S., Ringkamp, M., Sluka, K.A., Song, X.-J., Stevens, B., Sullivan, M.D., Tutelman, P.R., Ushida, T., and Vader, K. (2020). The revised International Association for the Study of Pain definition of pain: concepts, challenges, and compromises. *Pain*, 161 (9), 1976–1982.

[5] Dekkers, W. (2017). Pain as a subjective and objective phenomenon. in: Handb. Philos. Med. (p. 169–187). Springer Netherlands.

[6] Raffaeli, W. and Arnaudo, E. (2017). Pain as a disease: An overview. *J. Pain Res.*, 10 (7), 2003–2008.

[7] Torrance, N., Smith, B.H., Bennett, M.I., and Lee, A.J. (2006). The Epidemiology of Chronic Pain of Predominantly Neuropathic Origin. Results From a General Population Survey. *J. Pain*, 7 (4), 281–289.

[8] MOUREN, P. (2009). Traitement de la douleur. *Mars. Med.*, 95 (6), 523–530.

[9] Bagdas, D., Cinkilic, N., Ozboluk, H.Y., Ozyigit, M.O., and Gurun, M.S. (2013). Antihyperalgesic activity of chlorogenic acid in experimental neuropathic pain. *J. Nat. Med.*, 67 (4), 698–704.

[10] Hara, K., Haranishi, Y., Kataoka, K., Takahashi, Y., Terada, T., Nakamura, M., and Sata, T. (2014). Chlorogenic acid administered intrathecally alleviates mechanical and cold hyperalgesia in a rat neuropathic pain model. *Eur. J. Pharmacol.*, 723 (1), 459–464.

[11] Dos Santos, M.D., Almeida, M.C., Lopes, N.P., and De Souza, G.E.P. (2006). Evaluation of the anti-inflammatory, analgesic and antipyretic activities of the natural polyphenol chlorogenic acid. *Biol. Pharm. Bull.*, 29 (11), 2236–2240.

[12] Bagdas, D., Gul, Z., Meade, J.A., Cam, B., Cinkilic, N., and Gurun, M.S. (2020) Pharmacologic Overview of Chlorogenic Acid and its Metabolites in Chronic Pain and Inflammation. *Curr. Neuropharmacol.*, 18 (3), 216–228.

[13] Carballo-Villalobos, A.I., González-Trujano, M.E., Alvarado-Vázquez, N., and López-Muñoz, F.J. (2017). Pro-inflammatory cytokines involvement in the hesperidin antihyperalgesic effects at peripheral and central levels in a neuropathic pain model. *Inflammopharmacology.*, 25 (2), 265–269.

[14] Carballo-Villalobos, A.I., González-Trujano, M.E., Pellicer, F., and López-Muñoz, F.J. (2016). Antihyperalgesic Effect of Hesperidin Improves with Diosmin in Experimental Neuropathic Pain. *Biomed Res. Int.*, 15 (3), 234–256.

[15] Pinho-Ribeiro, F.A., Hohmann, M.S.N., Borghi, S.M., Zarpelon, A.C., Guazelli, C.F.S., Manchope, M.F., Casagrande, R., and Verri, W.A. (2015). Protective effects of the flavonoid hesperidin methyl chalcone in inflammation and pain in mice: Role of TRPV1, oxidative stress, cytokines and NF-κB. *Chem. Biol. Interact.*, 228 (3), 88–99.

[16] Tao, J., Liu, L., Fan, Y., Wang, M., Li, L., Zou, L., Yuan, H., Shi, L., Yang, R., Liang, S., and Liu, S. (2019). Role of hesperidin in P2X3 receptor-mediated neuropathic pain in the dorsal root ganglia. *Int. J. Neurosci.*, 129 (8), 784–793.

[17] Al-Enazi, M. (2013). Ameliorative potential of rutin on streptozotocin-induced neuropathic pain in rat. *African J. Pharm. Pharmacol.*, 7 (41), 2743–2754.

[18] Hasanein, P., Emamjomeh, A., Chenarani, N., and Bohlooli, M. (2020). Beneficial effects of rutin in diabetes-induced deficits in acquisition learning, retention memory and pain perception in rats. *Nutr. Neurosci.*, 23 (7), 563–574.

[19] Hernandez-Leon, A., Fernández-Guasti, A., and González-Trujano, M.E. (2016). Rutin antinociception involves opioidergic mechanism and descending modulation of ventrolateral periaqueductal grey matter in rats. *Eur. J. Pain (United Kingdom)*, 20 (2), 274–283.

[20] Azevedo, M.I., Pereira, A.F., Nogueira, R.B., Rolim, F.E., Brito, G.A.C., Wong, D.V.T., Lima-Júnior, R.C.P., de Albuquerque Ribeiro, R., and Vale, M.L. (2013). The antioxidant effects of the flavonoids rutin and quercetin inhibit oxaliplatin-induced chronic painful peripheral neuropathy. *Mol. Pain*, 9 (1), 53–57.

[21] Bouhassira, D. and Attal, N. (2016). Translational neuropathic pain research: A clinical perspective. *Neuroscience*, 338 (2), 27–35.

[22] Sapunar, D., Kostic, S., Banozic, A., and Puljak, L. (2012). Dorsal root ganglion - A potential new therapeutic target for neuropathic pain. *J. Pain Res.*, 5 (1), 31–38.

[23] Ozcan, M. and Ayar, A. (2012). Modulation of action potential and calcium signaling by levetiracetam in rat sensory neurons. *J. Recept. Signal Transduct.*, 32 (3), 156–162.

[24] Qu, Z.W., Liu, T.T., Qiu, C.Y., Li, J. Da, and Hu, W.P. (2014). Inhibition of acid-sensing ion channels by chlorogenic acid in rat dorsal root ganglion neurons. *Neurosci. Lett.*, 567 (11), 35–39.

[25] Liu, F., Lu, X.W., Zhang, Y.J., Kou, L., Song, N., Wu, M.K., Wang, M., Wang, H., and Shen, J.F. (2016). Effects of chlorogenic acid on voltage-gated potassium channels of trigeminal ganglion neurons in an inflammatory environment. *Brain Res. Bull.*, 127 (1), 119–125.

[26] Henderson, L.A. and Di Pietro, F. (2016). How do neuroanatomical changes in individuals with chronic pain result in the constant perception of pain? *Pain Manag.*, 6 (2), 147–159.

[27] Lohman, D., Schleifer, R., and Amon, J.J. (2010). Access to pain treatment as a human right. *BMC Med.*, 8 (1), 8–14.

[28] Treede, R.D., Rief, W., Barke, A., Aziz, Q., Bennett, M.I., Benoliel, R., Cohen, Milton., Evers, S., Finnerup, N.B., Michael B., Giamberardino, M.A., Kaasa, S., Korwisi, B., Kosek, E., Lavand'Homme, P., Nicholas, M., Perrot, S., Scholz, J., Schug, S., Smith, B., Svensson, P., Vlaeyen, Johan W.S. Wang, Shuu Jiun. (2019). Chronic pain as a symptom or a disease: The IASP Classification of Chronic Pain for the International Classification of Diseases (ICD-11). *Pain*, 160 (1), 19–27.

[29] Ellis, A. and Bennett, D.L.H. (2013). Neuroinflammation and the generation of neuropathic pain. *Br. J. Anaesth.*, 111 (1), 26–37.

[30] Ashton, J.C. (2012). Neuropathic pain: An evolutionary hypothesis. *Med. Hypotheses*, 78 (5), 641–643.

[31] Purves, D. (2018). Neuroscience. Sixth Edit New York: Oxford University Press.

[32] Ellison, D.L. (2017). Physiology of Pain. *Crit. Care Nurs. Clin. North Am.*, 29 (4), 397–406.

[33] Baron, R., Binder, A., and Wasner, G. (2010). Neuropathic pain: Diagnosis, pathophysiological mechanisms, and treatment. *Lancet Neurol.*, 9 (8), 807–819.

[34] Purves, D. (2018). Pain. D. Purves, G.J. Augustine, D. Fitzpatrick, H. Anthony-Samuel LaMantia, H., Mooney, R.D., Platt M.L., White, L.E. (Eds.), in: Neuroscience (p. 213–230). New York: Oxford University Press.

[35] Hunt, S.P. and Mantyh, P.W. (2001). The molecular dynamics of pain control. *Nat. Rev. Neurosci.*, 2 (2), 83–91.

[36] Nickel, F.T., Seifert, F., Lanz, S., and Maihöfner, C. (2012). Mechanisms of neuropathic pain. *Eur. Neuropsychopharmacol.*, 22 (2), 81–91.

[37] Livingston, W.K. (1976). The Physiology of Pain. in: Pain Mech. (p. 44–61). Boston, MA: Springer US.

[38] Derderian, C. and Tadi, P. (2019). Physiology, Withdrawal Response (p. 67–72). Florida: StatPearls Publishing.

[39] Meacham, K., Shepherd, A., Mohapatra, D.P., and Haroutounian, S. (2017). Neuropathic Pain: Central vs. Peripheral Mechanisms. *Curr. Pain Headache Rep.*, 21 (12), 132–143.

[40] St. John Smith, E. (2018). Advances in understanding nociception and neuropathic pain. *J. Neurol.*, 265 (2), 231–238.

[41] Jensen, T.S. (2002). An improved understanding of neuropathic pain. *Eur. J. Pain*, 6 (6), 3–11.

[42] Widerström-Noga, E. (2017). Neuropathic Pain and Spinal Cord Injury: Phenotypes and Pharmacological Management. *Drugs*, 77 (9), 967–984.

[43] Patrick, N., Emanski, E., and Knaub, M.A. (2016). Acute and Chronic Low Back Pain. *Med. Clin. North Am.*, 100 (1), 169–181.

[44] Brandow, A.M. and DeBaun, M.R. (2018). Key Components of Pain Management for Children and Adults with Sickle Cell Disease. *Hematol. Oncol. Clin. North Am.*, 32 (3), 535–550.

[45] Magee, D., Bachtold, S., Brown, M., and Farquhar-Smith, P. (2019). Cancer pain: where are we now? *Pain Manag.*, 9 (1), 63–79.

[46] Fink, R.M. and Gallagher, E. (2019). Cancer Pain Assessment and Measurement. *Semin. Oncol. Nurs.*, 35 (3), 229–234.

[47] Sen, D. and Christie, D. (2006). Chronic idiopathic pain syndromes. *Best Pract. Res. Clin. Rheumatol.*, 20 (2), 369–386.

[48] Watson, J.C. and Sandroni, P. (2016). Central Neuropathic Pain Syndromes. *Mayo Clin. Proc.*, 91 (3), 372–385.

[49] Grass, G.W. and GW, G. (2011). Neuropathic Pain. *Essentials Pain Manag.*, 110 (3), 515–544.

[50] Abdulla, F.A. and Smith, P.A. (2001). Axotomy- and autotomy-induced changes in the excitability of rat dorsal root ganglion neurons. *J. Neurophysiol.*, 85 (2), 630–643.

[51] Talbot, W.H., Darian-Smith, I., Kornhuber, H.H., and Mountcastle, V.B. (1968). The sense of flutter-vibration: comparison of the human capacity with response patterns of mechanoreceptive afferents from the monkey hand. *J. Neurophysiol.*, 31 (2), 301–334.

[52] Petruska, J.C., Napaporn, J., Johnson, R.D., Gu, J.G., and Cooper, B.Y. (2000). Subclassified acutely dissociated cells of rat DRG: Histochemistry and patterns of capsaicin-, proton-, and ATP-activated currents. *J. Neurophysiol.*, 84 (5), 2365–2379.

[53] Burgess, P.R. and Perl, E.R. (1967). Myelinated afferent fibres responding specifically to noxious stimulation of the skin. *J. Physiol.*, 190 (3), 541–562.

[54] Boada, M.D. and Woodbury, C.J. (2007). Physiological properties of mouse skin sensory neurons recorded intracellularly in vivo: Temperature effects on somal membrane properties. *J. Neurophysiol.*, 98 (2), 668–680.

[55] Rosenbaum, T. and Simon, S.A. (2007). TRPV1 Receptors and Signal Transduction. CRC Press/Taylor & Francis.

[56] O'Neill, J., Brock, C., Olesen, A.E., Andresen, T., Nilsson, M., and Dickenson, A.H. (2012). Unravelling the mystery of capsaicin: A tool to understand and treat pain. *Pharmacol. Rev.*, 64 (4), 939–971.

[57] Dray, A., Bettaney, J., and Forster, P. (1990). Actions of capsaicin on peripheral nociceptors of the neonatal rat spinal cord-tail in vitro: Dependence of extracellular ions and independence of second messengers. *Br. J. Pharmacol.*, 101 (3), 727–733.

[58] Caterina, M.J., Schumacher, M.A., Tominaga, M., Rosen, T.A., Levine, J.D., and Julius, D. (1997). The capsaicin receptor: A heat-activated ion channel in the pain pathway. *Nature*, 389 (6653), 816–824.

[59] Montell, C. (2005). The TRP superfamily of cation channels. *Sci. S.T.K.E*, 6 (272), 227–232.

[60] Scholz, J. and Woolf, C.J. (2002). Can we conquer pain? *Nat. Neurosci.*, 5 (11s),

1062–1067.

[61] Cesare, P. and Mcnaughton, P. (1996). A novel heat-activated current in nociceptive neurons and its sensitization by bradykinin. *Proc. Natl. Acad. Sci. U. S. A.*, 93 (26), 15435–15439.

[62] Caterina, M.J., Leffler, A., Malmberg, A.B., Martin, W.J., Trafton, J., Petersen-Zeitz, K.R., Koltzenburg, M., Basbaum, A.I., and Julius, D. (2000). Impaired nociception and pain sensation in mice lacking the capsaicin receptor. *Science*, 288 (5464), 306–313.

[63] Vyklický, L., Vlachová, V., Vitásková, Z., Dittert, I., Kabát, M., and Orkand, R.K. (1999). Temperature coefficient of membrane currents induced by noxious heat in sensory neurones in the rat. *J. Physiol.*, 517 (1), 181–192.

[64] Tominaga, M. and Calerina, M.J. (2004). Thermosensation and pain. *J. Neurobiol.*, 61 (1), 3–12.

[65] Sugiura, T., Tominaga, M., and Mizumura, H.K.K. (2002). Bradykinin lowers the threshold temperature for heat activation of vanilloid receptor 1. *J. Neurophysiol.*, 88 (1), 544–548.

[66] Tominaga, M., Wada, M., and Masu, M. (2001). Potentiation of capsaicin receptor activity by metabotropic ATP receptors as a possible mechanism for ATP-evoked pain and hyperalgesia. *Proc. Natl. Acad. Sci. U. S. A.*, 98 (12), 6951–6956.

[67] Cortright, D.W. and Szallasi, A. (2004). Biochemical pharmacology of the vanilloid receptor TRPV1: An update. *Eur. J. Biochem.*, 271 (10), 1814–1819.

[68] Szolcsanyi, J., Anton, F., Reeh, P.W., and Handwerker, H.O. (1988). Selective excitation by capsaicin of mechano-heat sensitive nociceptors in rat skin. *Brain Res.*, 446 (2), 262–268.

[69] Belmonte, C. and Giraldez, F. (1981). Responses of cat corneal sensory receptors to mechanical and thermal stimulation. *J. Physiol.*, 321 (1), 355–368.

[70] Maljevic, S. and Lerche, H. (2013). Potassium channels: A review of broadening therapeutic possibilities for neurological diseases. *J. Neurol.*, 260 (9), 2201–2211.

[71] Mannuzzu, L.M., Moronne, M.M., and Isacoff, E.Y. (1996). Direct physical measure of conformational rearrangement underlying potassium channel gating. *Science.*, 271 (5246), 213–216.

[72] Jiang, Q.-X., Wang, D.-N., and MacKinnon, R. (2004). Electron microscopic analysis of KvAP voltage-dependent K^+ channels in an open conformation. *Nature*,

430 (7001), 806–810.

[73] Franks, N.P. and Lieb, W.R. (1991). An anaesthetic-activated potassium channel. *Alcohol Alcohol. (Oxford, Oxfordshire). Suppl.*, 1 (2), 197–202.

[74] Zemel, B.M., Ritter, D.M., Covarrubias, M., and Muqeem, T. (2018). A-Type KV Channels in Dorsal Root Ganglion Neurons: Diversity, Function, and Dysfunction. *Front. Mol. Neurosci.*, 11 (5), 253–255.

[75] Kawano, T., Zoga, V., McCallum, J.B., Wu, H.E., Gemes, G., Liang, M.Y., Abram, S., Kwok, W.M., Hogan, Q.H., and Sarantopoulos, C.D. (2009). ATP-sensitive potassium currents in rat primary afferent neurons: biophysical, pharmacological properties, and alterations by painful nerve injury. *Neuroscience*, 162 (2), 431–443.

[76] Kim, D.S., Choi, J.O., Rim, H.D., and Cho, H.J. (2002). Downregulation of voltage-gated potassium channel α gene expression in dorsal root ganglia following chronic constriction injury of the rat sciatic nerve. *Mol. Brain Res.*, 105 (1–2), 146–152.

[77] Li, W., Gao, S.-B., Lv, C.-X., Wu, Y., Guo, Z.-H., Ding, J.-P., and Xu, T. (2007). Characterization of voltage-and Ca^{2+}-activated K^+ channels in rat dorsal root ganglion neurons. *J. Cell. Physiol.*, 212 (2), 348–357.

[78] Mongan, L.C., Hill, M.J., Chen, M.X., Tate, S.N., Collins, S.D., Buckby, L., and Grubb, B.D. (2005). The distribution of small and intermediate conductance calcium-activated potassium channels in the rat sensory nervous system. *Neuroscience*, 131 (1), 161–175.

[79] Park, S.Y., Choi, J.Y., Kim, R.U., Lee, Y.S., Cho, H.J., and Kim, D.S. (2003). Downregulation of voltage-gated potassium channel α gene expression by axotomy and neurotrophins in rat dorsal root ganglia. *Mol. Cells*, 16 (2), 256–259.

[80] Passmore, G.M., Selyanko, A.A., Mistry, M., Al-Qatari, M., Marsh, S.J., Matthews, E.A., Dickenson, A.H., Brown, T.A., Burbidge, S.A., Main, M., and Brown, D.A. (2003). KCNQ/M currents in sensory neurons: Significance for pain therapy. *J. Neurosci.*, 23 (18), 7227–7236.

[81] Vydyanathan, A., Wu, Z.Z., Chen, S.R., and Pan, H.L. (2005). A-type voltage-gated K^+ currents influence firing properties of isolectin B4-positive but not isolectin B4-negative primary sensory neurons. *J. Neurophysiol.*, 93 (6), 3401–3409.

[82] Yang, E.K., Takimoto, K., Hayashi, Y., De Groat, W.C., and Yoshimura, N. (2004). Altered expression of potassium channel subunit mRNA and α-dendrotoxin sensitivity of potassium currents in rat dorsal root ganglion neurons after axotomy. *Neuroscience*, 123 (4), 867–874.

[83] Robbins, J. (2001). KCNQ potassium channels: Physiology, pathophysiology, and pharmacology. *Pharmacol. Ther.*, 90 (1), 1–19.

[84] Brown, D.A. and Adams, P.R. (1980). Muscarinic suppression of a novel voltage-sensitive K^+ current in a vertebrate neurone [18]. *Nature*, 283 (5748), 673–676.

[85] Ishikawa, K., Tanaka, M., Black, J.A., and Waxman, S.G. (1999). Changes in expression of voltage-gated potassium channels in dorsal root ganglion neurons following axotomy. *Muscle Nerve*, 22 (4), 502–507.

[86] Roeper, J., Lorra, C., and Pongs, O. (1997). Frequency-dependent inactivation of mammalian A-type K^+ channel K(v)1.4 regulated by Ca2+/calmodulin-dependent protein kinase. *J. Neurosci.*, 17 (10), 3379–3391.

[87] Zemel, B.M., Muqeem, T., Brown, E. V., Goulão, M., Urban, M.W., Tymanskyj, S.R., Lepore, A.C., and Covarrubias, M. (2017). Calcineurin dysregulation underlies spinal cord injury-induced K^+ channel dysfunction in DRG neurons. *J. Neurosci.*, 37 (34), 8256–8272.

[88] Chien, L.Y., Cheng, J.K., Chu, D., Cheng, C.F., and Tsaur, M.L. (2007). Reduced expression of A-type potassium channels in primary sensory neurons induces mechanical hypersensitivity. *J. Neurosci.*, 27 (37), 9855–9865.

[89] Ritter, D.M., Ho, C., O'Leary, M.E., and Covarrubias, M. (2012). Modulation of Kv3.4 channel N-type inactivation by protein kinase C shapes the action potential in dorsal root ganglion neurons. *J. Physiol.*, 590 (1), 145–161.

[90] Covarrubias, M., Wei, A., Salkoff, L., and Vyas, T.B. (1994). Elimination of rapid potassium channel inactivation by phosphorylation of the inactivation gate. *Neuron*, 13 (6), 1403–1412.

[91] Liu, P.W., Blair, N.T., and Bean, B.P. (2017). Action potential broadening in capsaicin-sensitive DRG neurons from frequency-dependent reduction of Kv3 current. *J. Neurosci.*, 37 (40), 9705–9714.

[92] Grabauskas, G., Heldsinger, A., Wu, X., Xu, D., Zhou, S.Y., and Owyang, C. (2011). Diabetic visceral hypersensitivity is associated with activation of mitogen-activated kinase in rat dorsal root ganglia. *Diabetes*, 60 (6), 1743–1751.

[93] Furuta, S., Watanabe, L., Doi, S., Horiuchi, H., Matsumoto, K., Kuzumaki, N., Suzuki, T., and Narita, M. (2012). Subdiaphragmatic vagotomy increases the sensitivity of lumbar Aδ primary afferent neurons along with voltage-dependent potassium channels in rats. *Synapse*, 66 (2), 95–105.

[94] Cao, X.H., Byun, H.S., Chen, S.R., Cai, Y.Q., and Pan, H.L. (2010). Reduction in voltage-gated K^+ channel activity in primary sensory neurons in painful diabetic neuropathy: Role of brain-derived neurotrophic factor. *J. Neurochem.*, 114 (5), 1460–1475.

[95] Duan, K.-Z., Xu, Q., Zhang, X.-M., Zhao, Z.-Q., Mei, Y.-A., and Zhang, Y.-Q. (2012). Targeting A-type K^+ channels in primary sensory neurons for bone cancer pain in a rat model. *Pain*, 153 (3), 562–574.

[96] Davila, H.M. (1999). Molecular and functional diversity of voltage-gated calcium channels. in: Ann. N. Y. Acad. Sci. (p. 102–117). New York: Academy of Sciences.

[97] Scroggs, R.S. and Fox, A.P. (1992). Calcium current variation between acutely isolated adult rat dorsal root ganglion neurons of different size. *J. Physiol.*, 445 (1), 639–658.

[98] Kim, D.S., Yoon, C.H., Lee, S.J., Park, S.Y., Yoo, H.J., and Cho, H.J. (2001). Changes in voltage-gated calcium channel α1 gene expression in rat dorsal root ganglia following peripheral nerve injury. *Mol. Brain Res.*, 96 (1–2), 151–156.

[99] Zamponi, G.W., Lewis, R.J., Todorovic, S.M., Arneric, S.P., and Snutch, T.P. (2009). Role of voltage-gated calcium channels in ascending pain pathways. *Brain Res. Rev.*, 60 (1), 84–89.

[100] Heblich, F., Van Minh, A.T., Hendrich, J., Watschinger, K., and Dolphin, A.C. (2008). Time course and specificity of the pharmacological disruption of the trafficking of voltage-gated calcium channels by gabapentin. *Channels*, 2 (1), 4–9.

[101] McGivern, J.G. (2007). Ziconotide: A review of its pharmacology and use in the treatment of pain. *Neuropsychiatr. Dis. Treat.*, 3 (1), 69–85.

[102] Catterall, W.A. (2012). Voltage-gated sodium channels at 60: Structure, function and pathophysiology. *J. Physiol.*, 590 (11), 2577–2589.

[103] Catterall, W.A. (2000). From ionic currents to molecular mechanisms: The structure and function of voltage-gated sodium channels. *Neuron*, 26 (1), 13–25.

[104] Yu, F.H. and Catterall, W.A. (2003). Overview of the voltage-gated sodium

channel family. *Genome Biol.*, 4 (3), 207-219.

[105] Watanabe, E., Fujikawa, A., Matsunaga, H., Yasoshima, Y., Sako, N., Yamamoto, T., Saegusa, C., and Noda, M. (2000). Na(v)2/NaG channel is involved in control of salt-intake behavior in the CNS. *J. Neurosci.*, 20 (20), 7743–7751.

[106] Zhang, X.F., Zhu, C.Z., Thimmapaya, R., Choi, W.S., Honore, P., Scott, V.E., Kroeger, P.E., Sullivan, J.P., Faltynek, C.R., Gopalakrishnan, M., and Shieh, C.C. (2004). Differential action potentials and firing patterns in injured and uninjured small dorsal root ganglion neurons after nerve injury. *Brain Res.*, 1009 (1–2), 147–158.

[107] Huang, Z.J. and Song, X.J. (2008). Differing alterations of sodium currents in small dorsal root ganglion neurons after ganglion compression and peripheral nerve injury. *Mol. Pain*, 4 (2), 20-23.

[108] Renganathan, M., Cummins, T.R., and Waxman, S.G. (2001). Contribution of Nav 1.8 sodium channels to action potential electrogenesis in DRG neurons. *J. Neurophysiol.*, 86 (2), 629–640.

[109] Dunlop, J., Vasilyev, D., Lu, P., Cummons, T., and Bowlby, M. (2009). Hyperpolarization-Activated Cyclic Nucleotide-Gated (HCN) Channels and Pain. *Curr. Pharm. Des.*, 15 (15), 1767–1772.

[110] Santoro, B., Liu, D.T., Yao, H., Bartsch, D., Kandel, E.R., Siegelbaum, S.A., and Tibbs, G.R. (1998). Identification of a gene encoding a hyperpolarization-activated pacemaker channel of brain. *Cell*, 93 (5), 717–729.

[111] Biel, M., Schneider, A., and Wahl, C. (2002). Cardiac HCN channels: Structure, function, and modulation. *Trends Cardiovasc. Med.*, 12 (5), 206–213.

[112] Mayer, M.L. and Westbrook, G.L. (1983). A voltage-clamp analysis of inward (anomalous) rectification in mouse spinal sensory ganglion neurones. *J. Physiol.*, 340 (1), 19–45.

[113] Jiang, Y.Q., Sun, Q., Tu, H.Y., and Wan, Y. (2008). Characteristics of HCN channels and their participation in neuropathic pain. *Neurochem. Res.*, 33 (10), 1979–1989.

[114] Kouranova, E. V., Strassle, B.W., Ring, R.H., Bowlby, M.R., and Vasilyev, D. V. (2008). Hyperpolarization-activated cyclic nucleotide-gated channel mRNA and protein expression in large versus small diameter dorsal root ganglion neurons: Correlation with hyperpolarization-activated current gating. *Neuroscience*, 153

(4), 1008–1019.

[115] Chaplan, S.R., Guo, H.Q., Lee, D.H., Luo, L., Liu, C., Kuei, C., Velumian, A.A., Butler, M.P., Brown, S.M., and Dubin, A.E. (2003). Neuronal hyperpolarization-activated pacemaker channels drive neuropathic pain. *J. Neurosci.*, 23 (4), 1169–1178.

[116] Luo, L., Chang, L., Brown, S.M., Ao, H., Lee, D.H., Higuera, E.S., Dubin, A.E., and Chaplan, S.R. (2007). Role of peripheral hyperpolarization-activated cyclic nucleotide-modulated channel pacemaker channels in acute and chronic pain models in the rat. *Neuroscience*, 144 (4), 1477–1485.

[117] Sherman-Gold, R. (2008). The axon guide for electrophysiology and biophysics laboratory techniques 3rd Edition., Foster City, CA: Axon Instruments

[118] Molleman, A. (2003). Basic Theoretical Principles. in: Patch Clamping An Introd. Guid. To Patch Clamp Electrophysiol. (p. 5–42). Chichester, UK: John Wiley & Sons, Ltd.

[119] Walz, W. (2016). Advanced Patch-Clamp Analysis for Neuroscientists. Saskatoon: Humana Press .

[120] Neher, E. and Sakmann, B. (1976). Single-channel currents recorded from membrane of denervated frog muscle fibres. *Nature*, 260 (5554), 799–802.

[121] Molleman, A. (2003). The Practice of Patch Clamping. in: Patch Clamping An Introd. Guid. To Patch Clamp Electrophysiol. (p. 95–114). Chichester, UK: John Wiley & Sons, Ltd.

[122] Molleman, A. (2003). Whole-Cell Protocols and Data Analysis. in: Patch Clamping An Introd. Guid. To Patch Clamp Electrophysiol. (p. 115–139). Chichester, UK: John Wiley & Sons, Ltd.

[123] Erlund, I. (2004). Review of the flavonoids quercetin, hesperetin, and naringenin. Dietary sources, bioactivities, bioavailability, and epidemiology. *Nutr. Res.*, 24 (10), 851–874.

[124] Formica, J. V. and Regelson, W. (1995). Review of the biology of quercetin and related bioflavonoids. *Food Chem. Toxicol.*, 33 (12), 1061–1080.

[125] Wach, A., Pyrzyńska, K., and Biesaga, M. (2007). Quercetin content in some food and herbal samples. *Food Chem.*, 100 (2), 699–704.

[126] Kumar, S. and Pandey, A.K. (2013). Chemistry and biological activities of flavonoids: An overview. *Sci. World J.*, 6 (3), 78–119.

[127] Sharma, S., Sahni, J., Ali, J., and Baboota, S. (2013). Patent Perspective for Potential Antioxidant Compounds-Rutin and Quercetin. *Recent Patents Nanomed.*, 3 (1), 62–68.

[128] Chua, L.S. (2013). A review on plant-based rutin extraction methods and its pharmacological activities. *J. Ethnopharmacol.*, 150 (3), 805–817.

[129] Yang, J., Guo, J., and Yuan, J. (2008). In vitro antioxidant properties of rutin. *LWT - Food Sci. Technol.*, 41 (6), 1060–1066.

[130] Soni, H., Malik, J., Singhai, A.K., and Sharma, S. (2013). Antimicrobial and antiinflammatory activity of the hydrogels containing rutin delivery. *Asian J. Chem.*, 25 (15), 8371–8373.

[131] Singh, M., Govindarajan, R., Rawat, A.K.S., and Khare, P.B. (2008). Antimicrobial flavonoid rutin from Pteris vittata L. against pathogenic gastrointestinal microflora. *Am. Fern. J.*, 98 (2), 98–103.

[132] Gullón, B., Lú-Chau, T.A., Moreira, M.T., Lema, J.M., and Eibes, G. (2017). Rutin: A review on extraction, identification and purification methods, biological activities and approaches to enhance its bioavailability. *Trends Food Sci. Technol.*, 67 (5), 220–235.

[133] Orhan, D.D., Özçelik, B., Özgen, S., and Ergun, F. (2010). Antibacterial, antifungal, and antiviral activities of some flavonoids. *Microbiol. Res.*, 165 (6), 496–504.

[134] Rabišková, M., Bautzová, T., Gajdziok, J., Dvořáčková, K., Lamprecht, A., Pellequer, Y., and Spilková, J. (2012). Coated chitosan pellets containing rutin intended for the treatment of inflammatory bowel disease: In vitro characteristics and in vivo evaluation. *Int. J. Pharm.*, 422 (1–2), 151–159.

[135] Torres-Rêgo, M., Furtado, A.A., Bitencourt, M.A.O., Lima, M.C.J. de S., Andrade, R.C.L.C. de, Azevedo, E.P. de, Soares, T. da C., Tomaz, J.C., Lopes, N.P., da Silva-Júnior, A.A., Zucolotto, S.M., and Fernandes-Pedrosa, M. de F. (2016). Anti-inflammatory activity of aqueous extract and bioactive compounds identified from the fruits of Hancornia speciosa Gomes (Apocynaceae). *BMC Complement. Altern. Med.*, 16 (1),15-36.

[136] Nafees, S., Rashid, S., Ali, N., Hasan, S.K., and Sultana, S. (2015). Rutin ameliorates cyclophosphamide induced oxidative stress and inflammation in Wistar rats: Role of NFκB/MAPK pathway. *Chem. Biol. Interact.*, 231 (3), 98–

107.

[137] Hao, G., Dong, Y., Huo, R., Wen, K., Zhang, Y., and Liang, G. (2016). Rutin Inhibits Neuroinflammation and Provides Neuroprotection in an Experimental Rat Model of Subarachnoid Hemorrhage, Possibly Through Suppressing the RAGE–NF-κB Inflammatory Signaling Pathway. *Neurochem. Res.*, 41 (6), 1496–1504.

[138] Yoo, H., Ku, S.K., Baek, Y.D., and Bae, J.S. (2014). Anti-inflammatory effects of rutin on HMGB1-induced inflammatory responses in vitro and in vivo. *Inflamm. Res.*, 63 (3), 197–206.

[139] Perk, A.A., Shatynska-mytsyk, I., Gerçek, Y.C., Boztas, K., Yazgan, M., Fayyaz, S., and Farooqi, A.A. (2014). Rutin mediated targeting of signaling machinery in cancer cells. *Cancer Cell Int.*, 14 (1), 253–265.

[140] Karakurt, S. (2016). Modulatory effects of rutin on the expression of cytochrome P450s and antioxidant enzymes in human hepatoma cells. *Acta Pharm.*, 66 (4), 491–502.

[141] Alonso-Castro, A.J., Domínguez, F., and García-Carrancá, A. (2013). Rutin exerts antitumor effects on nude mice bearing SW480 tumor. *Arch. Med. Res.*, 44 (5), 346–351.

[142] Chen, H.C., Chang, T.C., Lin, Y.T., Cheng, H.Y., and Chang, T.L. (2013). Application of DMAIC process to enhance health effects in caring institution. *Qual. Quant.*, 47 (4), 2065–2080.

[143] ben Sghaier, M., Pagano, A., Mousslim, M., Ammari, Y., Kovacic, H., and Luis, J. (2016). Rutin inhibits proliferation, attenuates superoxide production and decreases adhesion and migration of human cancerous cells. *Biomed. Pharmacother.*, 84 1972–1978.

[144] Lee, Y.J. and Jeune, K.H. (2013). The Effect of Rutin on Antioxidant and Anti-inflammation in Streptozotocin-induced Diabetic Rats. *Appl. Microsc.*, 43 (2), 54–64.

[145] Saklani, R., Gupta, S.K., Mohanty, I.R., Kumar, B., Srivastava, S., and Mathur, R. (2016). Cardioprotective effects of rutin via alteration in TNF-α, CRP, and BNP levels coupled with antioxidant effect in STZ-induced diabetic rats. *Mol. Cell. Biochem.*, 420 (1–2), 65–72.

[146] Chen, S.S., Gong, J., F-T, L., and Mohammed, U. (2000). Naturally occurring polyphenolic antioxidants modulate IgE-mediated mast cell activation.

Immunology, 100 (4), 471–480.

[147] Kim, H.Y., Nam, S.Y., Hong, S.W., Kim, M.J., Jeong, H.J., and Kim, H.M. (2015). Protective effects of rutin through regulation of vascular endothelial growth factor in allergic rhinitis. *Am. J. Rhinol. Allergy*, 29 (3), e87–e94.

[148] Choi, J.K. and Kim, S.H. (2013). Rutin suppresses atopic dermatitis and allergic contact dermatitis. *Exp. Biol. Med.*, 238 (4), 410–417.

[149] Choi, J.Y., Lee, J.M., Lee, D.G., Cho, S., Yoon, Y.H., Cho, E.J., and Lee, S. (2015). The n-butanol fraction and rutin from tartary buckwheat improve cognition and memory in an in vivo model of amyloid-β-induced Alzheimer's disease. *J. Med. Food*, 18 (6), 631–641.

[150] Bhandary, B., Piao, C.S., Kim, D.S., Lee, G.H., Chae, S.W., Kim, H.R., and Chae, H.J. (2012). The protective effect of rutin against ischemia/reperfusion-associated hemodynamic alteration through antioxidant activity. *Arch. Pharm. Res.*, 35 (6), 1091–1097.

[151] Islam, F., Khan, M.M., Raza, S.S., Javed, H., Ahmad, A., Khan, A., Islam, F., and Safhi, M.M. (2012). Rutin protects dopaminergic neurons from oxidative stress in an animal model of parkinson's disease. *Neurotox. Res.*, 22 (1), 1–15.

[152] Garg, A., Garg, S., Zaneveld, L.J.D., and Singla, A.K. (2001). Chemistry and pharmacology of the Citrus bioflavonoid hesperidin. *Phyther. Res.*, 15 (8), 655–669.

[153] Tejada, S., Pinya, S., Martorell, M., Capó, X., Tur, J.A., Pons, A., and Sureda, A. (2017). Potential Anti-inflammatory Effects of Hesperidin from the Genus Citrus. *Curr. Med. Chem.*, 25 (37), 4929–4945.

[154] Li, Y.S., Zhang, J., Tian, G.H., Shang, H.C., and Tang, H. Bin (2021). Kirenol, darutoside and hesperidin contribute to the anti-inflammatory and analgesic activities of Siegesbeckia pubescens makino by inhibiting COX-2 expression and inflammatory cell infiltration. *J. Ethnopharmacol.*, 268 (10), 113-137.

[155] Hirata, A., Murakami, Y., Shoji, M., Kadoma, Y., and Fujisawa, S. (2005). Kinetics of radical-scavenging activity of hesperetin and hesperidin and their inhibitory activity on COX-2 expression. *Anticancer Res.*, 25 (5), 3367–3374.

[156] Tao, J., Liu, L., Fan, Y., Wang, M., Li, L., Zou, L., Yuan, H., Shi, L., Yang, R., Liang, S., and Liu, S. (2019). Role of hesperidin in P2X3 receptor-mediated neuropathic pain in the dorsal root ganglia. *Int. J. Neurosci.*, 129 (8), 784–793.

[157] Aswar, M., Kute, P., Mahajan, S., Mahajan, U., Nerurkar, G., and Aswar, U. (2014). Protective effect of hesperetin in rat model of partial sciatic nerve ligation induced painful neuropathic pain: An evidence of anti-inflammatory and anti-oxidative activity. *Pharmacol. Biochem. Behav.*, 124 (5), 101–107.

[158] Yurtal, Z., Altug, M.E., Unsaldi, E., Secinti, I.E., and Kucukgul, A. (2020). Investigation of Neuroprotective and Therapeutic Effects of Hesperidin in Experimental Spinal Cord Injury. *Turk. Neurosurg.*, 30 (6), 899–906.

[159] Kalpana, K.B., Devipriya, N., Srinivasan, M., and Menon, V.P. (2009). Investigation of the radioprotective efficacy of hesperidin against gamma-radiation induced cellular damage in cultured human peripheral blood lymphocytes. *Mutat. Res. - Genet. Toxicol. Environ. Mutagen.*, 676 (1), 54–61.

[160] Park, S.H., Pradeep, K., and Ko, K.C. (2009). Protective effect of hesperidin against γ-radiation induced oxidative stress in Sprague-Dawley rats. *Pharm. Biol.*, 47 (10), 940–947.

[161] Tamilselvam, K., Braidy, N., Manivasagam, T., Essa, M.M., Prasad, N.R., Karthikeyan, S., Thenmozhi, A.J., Selvaraju, S., and Guillemin, G.J. (2013). Neuroprotective effects of hesperidin, a plant flavanone, on rotenone-induced oxidative stress and apoptosis in a cellular model for Parkinson's disease. *Oxid. Med. Cell. Longev.*, 7 (1), 345–367.

[162] Antunes, M.S., Goes, A.T.R., Boeira, S.P., Prigol, M., and Jesse, C.R. (2014). Protective effect of hesperidin in a model of Parkinson's disease induced by 6-hydroxydopamine in aged mice. *Nutrition*, 30 (11–12), 1415–1422.

[163] Kiasalari, Z., Khalili, M., Baluchnejadmojarad, T., and Roghani, M. (2016). Protective Effect of Oral Hesperetin Against Unilateral Striatal 6-Hydroxydopamine Damage in the Rat. *Neurochem. Res.*, 41 (5), 1065–1072.

[164] Kesh, S., Kannan, R.R., Sivaji, K., and Balakrishnan, A. (2021). Hesperidin downregulates kinases lrrk2 and gsk3β in a 6-OHDA induced Parkinson's disease model. *Neurosci. Lett.*, 740 (2), 135–426.

[165] Hajialyani, M., Farzaei, M.H., Echeverría, J., Nabavi, S.M., Uriarte, E., and Eduardo, S.S. (2019). Hesperidin as a neuroprotective agent: A review of animal and clinical evidence. *Molecules*, 24 (3), 224–279.

[166] Aggarwal, V., Tuli, H.S., Thakral, F., Singhal, P., Aggarwal, D., Srivastava, S., Pandey, A., Sak, K., Varol, M., Khan, M.A., and Sethi, G. (2020). Molecular

mechanisms of action of hesperidin in cancer: Recent trends and advancements. *Exp. Biol. Med.*, 245 (5), 486–497.

[167] Mas-Capdevila, A., Teichenne, J., Domenech-Coca, C., Caimari, A., Bas, J.M.D., Escoté, X., and Crescenti, A. (2020). Effect of hesperidin on cardiovascular disease risk factors: The role of intestinal microbiota on hesperidin bioavailability. *Nutrients*, 12 (5), 170–219.

[168] Wang, H., Wang, H. fei, Wang, C., Chen, Y. fang, Ma, R., Xiang, J. zhou, Du, X. ling, and Tang, Q. (2016). Inhibitory effects of hesperetin on Kv1.5 potassium channels stably expressed in HEK 293 cells and ultra-rapid delayed rectifier K^+ current in human atrial myocytes. *Eur. J. Pharmacol.*, 789 (10), 98–108.

[169] Wang, H., Wang, H.F., Zhang, H., Wang, C., Chen, Y.F., Ma, R., Xiang, J.Z., Du, X.L., and Tang, Q. (2016). Inhibitory effects of hesperetin on Nav1.5 channels stably expressed in HEK 293 cells and on the voltage-gated cardiac sodium current in human atrial myocytes. *Acta Pharmacol. Sin.*, 37 (12), 1563–1573.

[170] Toyama, D.O., Ferreira, M.J.P., Romoff, P., Fávero, O.A., Gaeta, H.H., and Toyama, M.H. (2014). Effect of Chlorogenic Acid (5-Caffeoylquinic Acid) Isolated from Baccharis oxyodonta on the Structure and Pharmacological Activities of Secretory Phospholipase A2 from Crotalus durissus terrificus. *Biomed Res. Int.*, 3 (5), 115–167.

[171] Bagdas, D., Gul, Z., Meade, J.A., Cam, B., Cinkilic, N., and Gurun, M.S. (2019). Pharmacologic Overview of Chlorogenic Acid and its Metabolites in Chronic Pain and Inflammation. *Curr. Neuropharmacol.*, 18 (3), 216–228.

[172] Liang, N. and Kitts, D.D. (2015). Role of chlorogenic acids in controlling oxidative and inflammatory stress conditions. *Nutrients*, 8 (1), 1–20.

[173] Belkaid, A., Currie, J.C., Desgagnés, J., and Annabi, B. (2006). The chemopreventive properties of chlorogenic acid reveal a potential new role for the microsomal glucose-6-phosphate translocase in brain tumor progression. *Cancer Cell Int.*, 6 (1), 1–12.

[174] Kozuki, Y., Miura, Y., and Yagasaki, K. (2000). Inhibitory effects of carotenoids on the invasion of rat ascites hepatoma cells in culture. *Cancer Lett.*, 151 (1), 111–115.

[175] Meng, S., Cao, J., Feng, Q., Peng, J., and Hu, Y. (2013). Roles of chlorogenic acid on regulating glucose and lipids metabolism: A review. *Evidence-Based*

Complement. Altern. Med., 23 (1), 11–26.

[176] Zhao, Y., Wang, J., Ballevre, O., Luo, H., and Zhang, W. (2012). Antihypertensive effects and mechanisms of chlorogenic acids. *Hypertens. Res.*, 35 (4), 370–374.

[177] Aseervatham, G.S.B., Suryakala, U., Doulethunisha, Sundaram, S., Bose, P.C., and Sivasudha, T. (2016). Expression pattern of NMDA receptors reveals antiepileptic potential of apigenin 8-C-glucoside and chlorogenic acid in pilocarpine induced epileptic mice. *Biomed. Pharmacother.*, 82 (2), 54–64.

[178] Santana-Gálvez, J., Cisneros-Zevallos, L., and Jacobo-Velázquez, D.A. (2017). Chlorogenic Acid: Recent advances on its dual role as a food additive and a nutraceutical against metabolic syndrome. *Molecules*, 22 (3), 7–9.

[179] Bagdas, D., Ozboluk, H.Y., Cinkilic, N., and Gurun, M.S. (2014). Antinociceptive effect of chlorogenic acid in rats with painful diabetic neuropathy. *J. Med. Food*, 17 (6), 730–732.

[180] Gorzalczany, S., Marrassini, C., Miño, J., Acevedo, C., and Ferraro, G. (2011). Antinociceptive activity of ethanolic extract and isolated compounds of Urtica circularis. *J. Ethnopharmacol.*, 134 (3), 733–738.

[181] Dos Santos, M.D., Almeida, M.C., Lopes, N.P., and De Souza, G.E.P. (2006). Evaluation of the anti-inflammatory, analgesic and antipyretic activities of the natural polyphenol chlorogenic acid. *Biol. Pharm. Bull.*, 29 (11), 2236–2240.

[182] Zhang, Y.J., Lu, X.W., Song, N., Kou, L., Wu, M.K., Liu, F., Wang, H., and Shen, J.F. (2014). Chlorogenic acid alters the voltage-gated potassium channel currents of trigeminal ganglion neurons. *Int. J. Oral Sci.*, 6 (4), 233–240.

[183] Duque, A.P. do N., Pinto, N. de C.C., Mendes, R. de F., da Silva, J.M., Aragão, D.M. de O., Castañon, M.C.M.N., and Scio, E. (2016). In vivo wound healing activity of gels containing *Cecropia pachystachya* leaves. *J. Pharm. Pharmacol.*, 68 (1), 128–138.

[184] Lin, Y.T. and Chen, J.C. (2018). Dorsal root ganglia isolation and primary culture to study neurotransmitter release. *J. Vis. Exp.*, 1 (140), 57-76.

[185] Sleigh, J.N., West, S.J., and Schiavo, G. (2020). A video protocol for rapid dissection of mouse dorsal root ganglia from defined spinal levels. *BMC Res. Notes*, 13 (1), 302-311.

[186] De Luca, A.C., Faroni, A., and Reid, A.J. (2015). Dorsal root ganglia neurons and differentiated adipose-derived stem cells: An in vitro co-culture model to study

peripheral nerve regeneration. *J. Vis. Exp.*, 96 (96), 525–543.

[187] Heinrich, T., Hübner, C., and Kurth, I. (2016). Isolation and Primary Cell Culture of Mouse Dorsal Root Ganglion Neurons. *Bio. Protoc.*, 6 (7), 36–50.

[188] Cummins, T.R., Rush, A.M., Estacion, M., Dib-Hajj, S.D., and Waxman, S.G. (2009). Voltage-clamp and current-clamp recordings from mammalian DRG neurons. *Nat. Protoc.*, 4 (8), 1103–1112.

[189] Hyun, S.W., Kim, B.R., Hyun, S.A., and Seo, J.W. (2017). The assessment of electrophysiological activity in human-induced pluripotent stem cell-derived cardiomyocytes exposed to dimethyl sulfoxide and ethanol by manual patch clamp and multi-electrode array system. *J. Pharmacol. Toxicol. Methods*, 87 (3), 93–98.

[190] Du, X., Lu, D., Daharsh, E.D., Yao, A., Dewoody, R., and Yao, J.A. (2006). Dimethyl sulfoxide effects on hERG channels expressed in HEK293 cells. *J. Pharmacol. Toxicol. Methods*, 54 (2), 164–172.

[191] Liu, F., Lu, X.W., Zhang, Y.J., Kou, L., Song, N., Wu, M.K., Wang, M., Wang, H., and Shen, J.F. (2016). Effects of chlorogenic acid on voltage-gated potassium channels of trigeminal ganglion neurons in an inflammatory environment. *Brain Res. Bull.*, 127 (1), 119–125.

[192] Takeda, M., Tsuboi, Y., Kitagawa, J., Nakagawa, K., Iwata, K., and Matsumoto, S. (2011). Potassium channels as a potential therapeutic target for trigeminal neuropathic and inflammatory pain. *Mol. Pain*, 7 (2), 5–19.

[193] Duménieu, M., Fourcaud-Trocmé, N., Garcia, S., and Kuczewski, N. (2015). Afterhyperpolarization (AHP) regulates the frequency and timing of action potentials in the mitral cells of the olfactory bulb: Role of olfactory experience. *Physiol. Rep.*, 3 (5), 78–93.

[194] Obata, H. (2017). Analgesic mechanisms of antidepressants for neuropathic pain. *Int. J. Mol. Sci.*, 18 (11), 206–213.

[195] Garcia-Larrea, L. and Hagiwara, K. (2019). Electrophysiology in diagnosis and management of neuropathic pain. *Rev. Neurol. (Paris).*, 175 (1–2), 26–37.